

Maren Sandvold

# Small scale changes superimposed on larger scale sea level-induced changes in cores from the Nordkapp Basin.

Master's thesis in Geology  
Supervisor: Maarten Felix  
June 2022



Maren Sandvold

# **Small scale changes superimposed on larger scale sea level-induced changes in cores from the Nordkapp Basin.**

Master's thesis in Geology  
Supervisor: Maarten Felix  
June 2022

Norwegian University of Science and Technology  
Faculty of Engineering  
Department of Geoscience and Petroleum





## Abstract

This work looked at different types of small scale cyclicity within different depositional environments in eight cores from the Mesozoic succession of the Nordkapp Basin and tried to determine the duration and possible causes of the cyclicity. The shallow stratigraphic cores looked at in this project were taken from the central part of the basin. Previously Bugge et al. (2002) described and interpreted six different depositional environments and reported that the changes in depositional environments was caused by large scale sea level changes of over 10 to several tens of metres. In this work the aim is to study small scale changes within the different environments by thoroughly describing the cores.

Overview logs were made for all eight cores and included descriptions of lithology and sedimentary structures, with special focus on bioturbation intensity, heterolithics, and mottling. Based on the observations the cores were divided into 17 main facies which were described and interpreted. The facies were used to interpret the depositional environments of the deposits.

Sedimentary graphical logs combined with graphs of bioturbation intensity, heterolithics, mottling, facies and depositional environments show that there are cyclic small scale changes, with thicknesses ranging from 0.4 to 10 meters, superimposed on the larger scale changes in most of the cores. The cycles are not continuous and the deposits contain many single cycles or intervals with a few cycles. Durations of the changes were calculated based on the biostratigraphy from Bugge et al. (2002) and the calculations show that some of the cycles found in bioturbation intensity, heterolithics and mottling in the coastal, shoreface and inner shelf may be the result of precession, obliquity or eccentricity cycles.

## Sammendrag

Dette arbeidet har sett på ulike typer småskala sykliske endringer innenfor forskjellige avsetningsmiljøer i åtte borekjerner fra den mesozoiske lagrekken i Nordkappbassenget og har forsøkt å bestemme varigheten og mulige årsaker til de sykliske endringene. De grunne stratigrafiske borekjernene, som ble sett på i dette prosjektet, ble hentet opp fra den sentrale delen av bassenget. Bugge et al. (2002) har tidligere beskrevet og tolket seks ulike avsetningsmiljøer og rapporterte at endringene i avsetningsmiljø var forårsaket av store havnivåendringer på over ti til flere titalls meter. I dette arbeidet er målet å studere småskalaendringer innenfor de ulike miljøene ved grundig beskrivelse av borekjernene.

Oversiktslogger ble laget for alle de åtte kjernene og inkluderer beskrivelse av litologi og sedimentære strukturer, med særlig vekt på bioturbasjonsintensitet, heterolittiske sedimenter og «mottling». Kjernene ble delt inn i 17 hovedfacies som ble beskrevet og tolket og deretter brukt til å tolke avsetningsmiljøene til avsetningene.

Sedimentære grafiske logger kombinert med grafer over bioturbasjonsintensitet, heterolittiske sedimenter, «mottling», «facies», og avsetningsmiljø viser at det er sykliske småskala endringer, med tykkelser fra 0.4 til 10 meter, lagt over endringer av en større skala i de fleste kjernene. Syklusene er ikke kontinuerlige, og det er ofte mange enkeltsykluser eller intervaller med noen få sykluser. Varigheten på endringene ble beregnet på bakgrunn av biostratigrafien fra Bugge et al. (2002) og beregningene viser at noen av syklusene, som er funnet i bioturbasjonsintensiteten, de heterolittiske sedimentene og «mottling» i kyst, strandskråning og på indre sokkel, kan være et resultat av «precession»-, «obliquity»-, eller «eccentricity» sykluser.

## Acknowledgement

I would like to thank my supervisor Maarten Felix for his guidance and patience with me which made it possible for me to get to where I am today. Thank you for always being available and for all constructive feedback. I would also like to thank you for helping me participate in my first ever conference, EGU 2022.

Atle Mørk, thank you for bringing out cores for me at Dora.

I would also like to thank my family and friends for their support and for seeing the light at the end of the tunnel for me the days when I could not.

Finally, I would like to thank my good friend Kine for being there for me and keeping me sane while I have been working on this master thesis. You are a true friend.

# Table of contents

1. Introduction.....	9
2. Background.....	11
2.1 Regional geology .....	11
2.2 Previous work on the cores .....	15
2.3 Theory.....	19
3. Methodology.....	20
4. Results .....	21
4.1 Facies .....	21
4.2 Microstructures in mudstone.....	56
4.3 Graphical sedimentary logs, descriptions, and interpretations of all cores.....	65
5. Discussion .....	90
5.1 Duration of the small scale variations.....	90
5.2 Causes of the small scale variations.....	95
5.3 Furter work.....	96
6. Conclusion .....	97
References.....	98

# List of tables

**Table 1:** The durations of sedimentation, sedimentation rates and duration of changes for each core or part of core. .... 94

## List of figures

<b>Figure 1:</b> Overview of the Nordkapp Basin showing where the shallow stratigraphic cores used in this research were drilled. From Bugge et al. (2002). .....	10
<b>Figure 2:</b> The regional Mesozoic stratigraphy of the Barents shelf and Spitsbergen. From Bugge et al. (2002). .....	10
<b>Figure 3:</b> An overview of the major structural elements in the Barents Sea. From Worsley (2008). ...	11
<b>Figure 4:</b> Paleogeographic reconstruction of the SW Barents Sea in the Middle Anisian. From Glørstad-Clark et al. (2011). .....	13
<b>Figure 5:</b> Overview logs of all the cores. From Bugge et al. (2002). .....	18
<b>Figure 6:</b> Orbital cycles. From de Boer and Smith (1994). .....	19
<b>Figure 7:</b> Core photos showing massive sandstone. (a) Massive sandstone overlying a claystone. (b) massive sandstone with pieces of coal. ....	23
<b>Figure 8:</b> Core photos showing laminated sandstone. (a) Laminated sandstone with coal laminae. (b) Laminated sandstone with a water escape structure indicated by the arrow. ....	24
<b>Figure 9:</b> Core photos showing cross bedded sandstone. (a) Trough cross bedded sandstone with dark grey mud (green arrow) and black coal (blue arrows). (b) cross bedded sandstone with coal laminae. ....	25
<b>Figure 10:</b> Core photos showing coarsening upwards sandstone. (a) Coarsening upwards sandstone with some mud clasts. (b) A thinner coarsening upwards sandstone layer with some coal above the lower boundary. ....	27
<b>Figure 11:</b> Core photos showing fining upwards sandstone. (a) Fining upwards sandstone with rootlets. (b) fining upwards sandstone with lamination.....	29
<b>Figure 12:</b> Core photos showing planar laminated sandstone. (a) Planar laminated sandstone overlain by rippled sandstone. (b) Laminated sandstone overlying mudstone.....	31
<b>Figure 13:</b> Core photos showing rippled sandstone indicated by the arrows. (a) Rippled sandstone overlying a thin layer of parallel laminated sandstone and underlying laminated sandstone. (b) Rippled sandstone overlying a thicker layer of parallel laminated sandstone and underlying mudstone. ....	33
<b>Figure 14:</b> Core photos showing heterolithics. (a) Alternating layers of sand and mud, possible flute cast (blue arrows). (b) Two cycles of upward grading from mudstone to flaser bedding. ....	35
<b>Figure 15:</b> Core photos showing distorted heterolithics. (a) Muddy distorted heterolithic bed. (b) Sandy distorted heterolithic bed.....	37
<b>Figure 16:</b> Core photos showing chaotic facies. (a) Sub angular mud clasts floating in a sandstone matrix. (b) Chaotic facies overlying a massive sandstone.....	39
<b>Figure 17:</b> Core photo showing heavily bioturbated muddy sandstone.....	40
<b>Figure 18:</b> Core photos showing laminated mudstone. (a) Laminated mudstone with silt laminae. (b) Laminated mudstone with red pyrite or siderite laminae. ....	42
<b>Figure 19:</b> core photos showing slightly bioturbated clayey mudstone. (a) Slightly bioturbated clayey mudstone. (b) Gradual upwards transition from bioturbated silty mudstone to slightly bioturbated clayey mudstone. ....	44
<b>Figure 20:</b> Core photos showing bioturbated silty mudstone. (a) Bioturbated silty mudstone with a gradual upper boundary transitioning to slightly bioturbated clayey mudstone. (b) Bioturbated silty mudstone. ....	46
<b>Figure 21:</b> Core photos showing shales. (a) Shale. (b) Black shale with cone in cone structures (blue arrow) and fossil fragments (green arrows).....	48
<b>Figure 22:</b> Core photos showing mottled claystone. (a) Red and white coloured mottled claystone. (b) Multi coloured mottled claystone, possible rootlet indicated by arrow. ....	50

<b>Figure 23:</b> Core photo showing interlaminated sandstone and mudstone. ....	51
<b>Figure 24:</b> Core photos showing shell beds. (a) Large shells in a greenish grey sand matrix. (b) large shells in a mottled and bioturbated muddy sandstone matrix. ....	53
<b>Figure 25:</b> Core photos showing carbonates. (a) Mudstone gradually transitioning to wackestone. (b) Packstone. ....	55
<b>Figure 26:</b> Laminated mudstone with siderite or pyrite laminae (a) core photo of the interval from which the thin section was taken, (b) full scan of the thin section (5x magnification),.....	57
<b>Figure 27:</b> Slightly bioturbated clayey mudstone (a) core photo of the interval from which the thin section was taken, (b) full scan of the thin section (5x magnification), (c) photomicrograph showing dark discontinuous patches of mud in a slightly lighter coloured mudstone (5x magnification). ....	59
<b>Figure 28:</b> Bioturbated silty mudstone (a) core photo of the interval from which the thin section was taken, (b) full scan of the thin section (5x magnification), (c) photomicrograph showing a dark clay rich burrow in a light grey coloured siltstone (5x magnification). ....	61
<b>Figure 29:</b> Black shale (a) core photo of the interval from which the thin section was taken, (b) full scan of the thin section (5x magnification), (c) scan showing a fossil fragment (blue arrow) and some red pieces of mineral (green arrows) in the black shale (5x magnification). ....	63
<b>Figure 30:</b> Black shale (a) core photo of the interval from which the thin section was taken, (b) full scan of the thin section (5x magnification), (c) scan showing silt enriched lamina (5x magnification). ....	64
<b>Figure 31:</b> Legend (Lithology).....	65
<b>Figure 32:</b> Legend (structures) .....	66
<b>Figure 33:</b> Legend (facies) .....	66
<b>Figure 34:</b> Core 7230/05-U-06. (a) overview log, (b) variations in bioturbation intensity, (c) heterolithics, (d) mottling, (e) facies and (f) depositional environments. Cycles are indicated by the green arrows; increase or decrease of bioturbation intensity in (b) and increase or decrease in amount of mud in (c). ....	69
<b>Figure 35:</b> Core 7230/05-U-05. (a) overview log, (b) variations in bioturbation intensity, (c) heterolithics, (d) facies and (e) depositional environments. Cycles are indicated by the green arrows; increase or decrease in bioturbation intensity in (b) and increase or decrease in amount of mud in (c). ....	71
<b>Figure 36:</b> Core 7230/05-U-04. (a) overview log, (b) variations in bioturbation intensity, (c) heterolithics, (d) mottling, (e) facies and (f) depositional environments. Cycles are indicated by the green arrows; increase or decrease in bioturbation intensity in (b) and increase or decrease in amount of mud in (c). The red boxes indicate cycles that are too small to indicate with green arrows. ....	74
<b>Figure 37:</b> Core 7230/05-U-03. (a) overview log, (b) variations in bioturbation intensity, (c) heterolithics, (d) mottling, (e) facies and (f) depositional environments. Cycles in the bioturbation intensity are indicated by green arrows. The red boxes indicate cycles in the heterolithics which are too small to indicate with arrows. ....	77
<b>Figure 38:</b> Core 7230/05-U-02. (a) overview log, (b) variations in bioturbation intensity, (c) heterolithics, (d) facies and (e) depositional environments. Cycles are indicated by the green arrows; increase or decrease in bioturbation intensity in (b) and increase or decrease in amount of mud in (c). ....	80
<b>Figure 39:</b> Core 7231/01-U-01. (a) overview log, (b) variations in bioturbation intensity, (c) facies and (d) depositional environments. ....	83
<b>Figure 40:</b> Core 7231/04-U-01. (a) overview log, (b) variations in bioturbation intensity, (c) facies and (d) depositional environments. The green arrows indicate a 200ka cycle, the yellow arrows indicate a 400ka cycle and the orange arrows indicate tree 260ka cycles. ....	86

**Figure 41:** Core 7230/05-U-09. (a) overview log, (b) variations in bioturbation intensity, (c) heterolithics, (d) mottling, (e) facies and (f) depositional environments. Cycles are indicated by the green arrows; increase or decrease in bioturbation intensity in (b) and increase or decrease in amount of mud in (c). The red box indicates cycles that are too small to be indicated by arrows.

..... 89

**Figure 42:** Examples of small scale changes in (a) bioturbation intensity, (b) mottling and (c) heterolithics..... 92

**Figure 43:** Chronogram of the cores. From Bugge et al. (2002)..... 93



## 1. Introduction

Sedimentary deposits are not uniform, but show changes at different depths and thus changes through time. Changes can be caused by many different processes such as tectonics, the movement of lithospheric plates, and climate changes. These changes can be long-term and result in changes over large thicknesses. Other processes vary rapidly and result in changes over smaller thicknesses.

Large scale changes with thicknesses from several metres to several tens of metres can be seen in many different ways such as changes in depositional environments (Bugge et al., 2002), changes in lithology for example variations between sandstone and mudstone (Marshall et al., 2017), variations in the thickness of the beds (Tucker et al., 2009), and cycles of coarsening upwards sediments (Steel et al., 1977).

Small scale changes with thicknesses from centimetres to several metres can be seen in many different ways such as changes in lithology for example variation between carbonates and clastics (Tucker et al., 2009), variations in chemical components (Kochhann et al., 2020), variations in the amount of dropstones and foraminifera in the sediments (Heinrich, 1988), variation in grain size (Liu et al., 2016) and cycles of fining upwards sediments (Liu et al., 2016).

Small scale changes are of interest because they are often caused Milankovitch cycles and that is something that will be looked for in this work.

This research used eight shallow stratigraphic cores from the Nordkapp Basin to study smaller scale changes within the environments that had been recognised but not described extensively by Bugge et al. (2002). The aim of this work is to look at the smaller scale changes across the different environments encountered in the cores and try to determine their durations and possible causes.

Shallow stratigraphic cores were drilled in the central and SW Nordkapp basin in the Barents Sea just offshore Finnmark in the 1980s. The cores used in this research were drilled in the central segment of the Nordkapp Basin (Figure 1). The cored intervals are part of the Mesozoic succession (Figure 2).

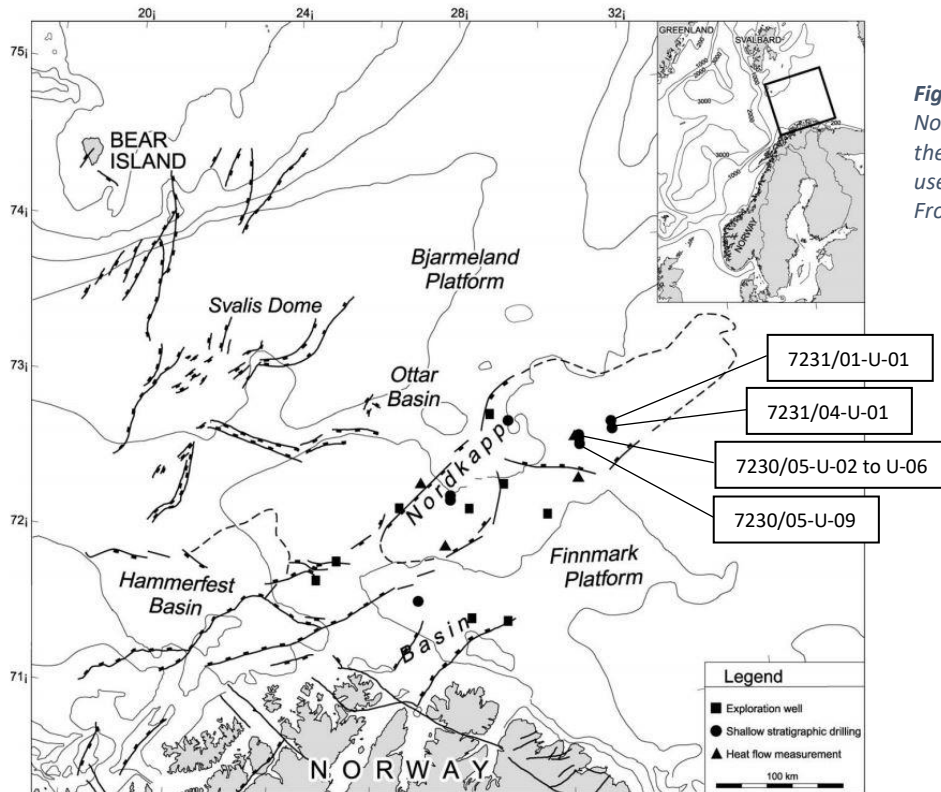


Figure 1: Overview of the Nordkapp Basin showing where the shallow stratigraphic cores used in this research were drilled. From Bugge et al. (2002).

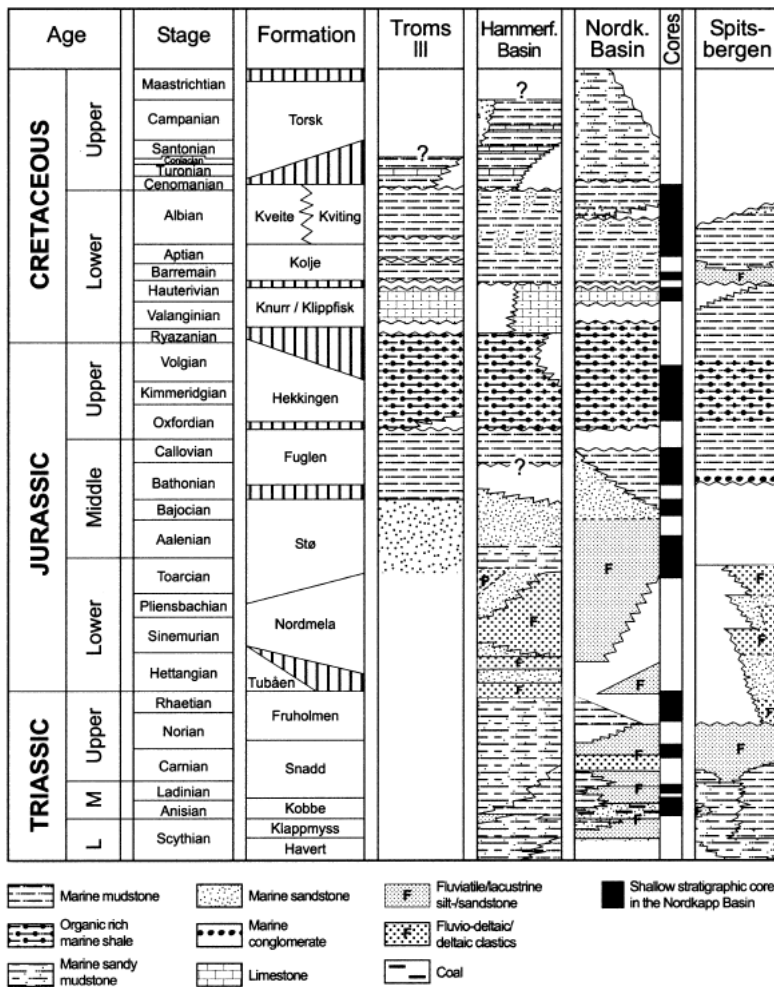
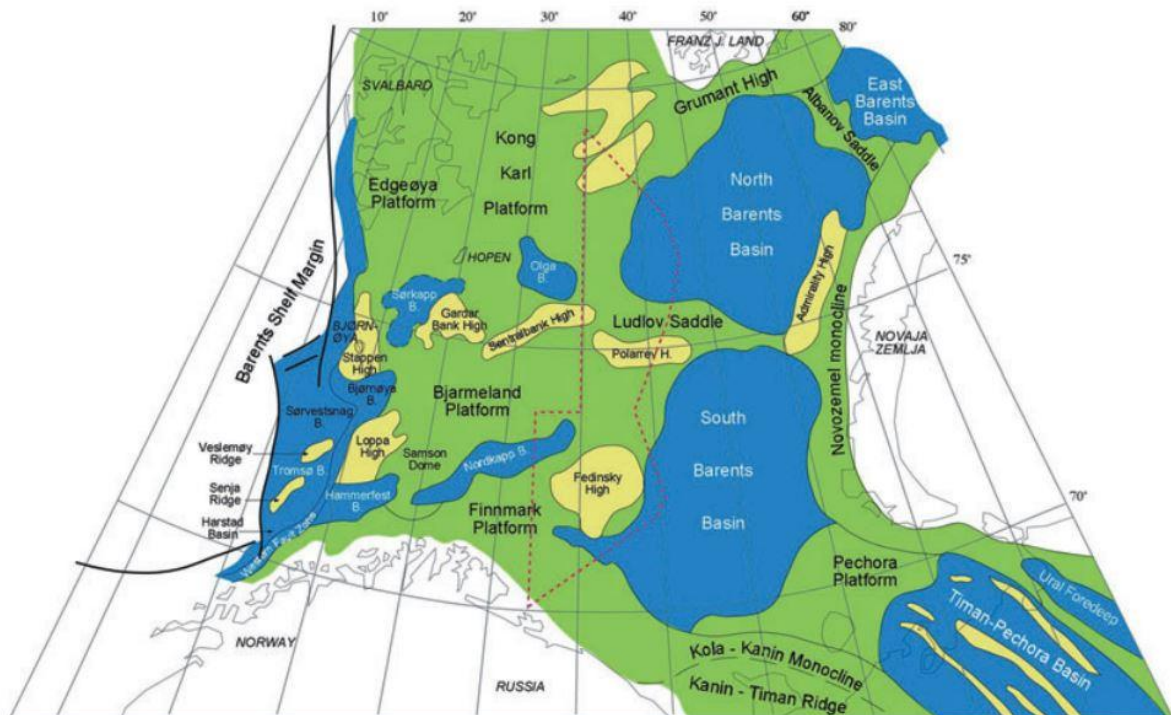


Figure 2: The regional Mesozoic stratigraphy of the Barents shelf and Spitsbergen. From Bugge et al. (2002).

## 2. Background

### 2.1 Regional geology

The Nordkapp Basin is a 300 km long and 30 to 80 km wide NE-SW trending basin situated in the southwest Barents Sea (Figure 3). The basin is a fault related Late Palaeozoic rift basin and it is delimited by the Nysleppen, Måsøy and Thor Iversen Fault complexes. The Barents Sea – Svalbard margin is mostly a sheared margin. The margin can be divided into three sections, of which the northernmost and southernmost sections of the margins are sheared while the central section is rifted (Faleide et al., 2008). The basin consists of a half graben in the SW part and symmetrical grabens in the central and NE parts (Gabrielsen and Norge, 1990). The basin was probably initially formed by extension in the Late Devonian-Early Carboniferous and was initially filled with coal-rich alluvial siliciclastics of the Billefjorden Group. This was followed by renewed regional rifting in the mid Carboniferous (Bugge et al., 2002).



*Figure 3: An overview of the major structural elements in the Barents Sea. From Worsley (2008).*

The geology in the areas surrounding the Barents Sea varies widely. In the areas to the south the rocks are older than the rocks in the east and northeast. Analysis of the age and the mineralogic composition of the grains in the sandstones deposited in the Barents Sea was used to determine the source of the sediments. Analysis of Triassic sandstones shows that during this time the sediments was supplied from the south and east but mostly east and that the main sediment sources was the Urals (Mørk, 1999).

## Devonian to Permian

There were several rifting episodes over a large area of the Barents Sea platform in the Late Palaeozoic which lead to the formation of several rift basins in the Barents Sea including the Nordkapp Basin (Faleide et al., 2008).

In the Carboniferous the Barents Sea was dominated by shallow marine carbonate deposits (Brekke et al., 2001). In the Permian there was a transgression and the ocean in the NE closed during the Uralian orogeny. During this time, the continents moved north from the equatorial zone to about 30-35°N which caused the climate to change from warm and arid to temperate and humid (Worsley, 2008).

Worsley (2008) explained that there was widespread rifting in the Barents Sea from the Devonian. A post rift carbonate platform developed in the Carboniferous on top of coal-rich alluvial sediments. In some of the basins including the Nordkapp Basin several km thick evaporites were deposited. When the temperature in the sea decreased the carbonates shifted from warm-water carbonates to cool-water carbonates. This shift happened in the early Permian. The warm-water carbonates mainly consisted of extensively dolomitized in situ carbonates like coral reefs. The cool-water carbonates were mainly limestones. In the Permian, the subsidence and sedimentation rates increased, and in the late Permian the platform shifted from a carbonate to a clastic platform. Initially mostly non-silicate mud was deposited on top of the carbonate platform.

## Triassic

Extension lasted from the Devonian until complete continental separation between NW Europe and Greenland in the early Cenozoic but the Triassic was a tectonically quiet period (Faleide et al., 2008). Glørstad-Clark et al. (2011) show that there were several transgression/regression cycles in the Triassic. Since the platform was wide and gently sloping there was rapid flooding and emergence of land during rise and fall in sea level. A rise in sea level could cause a landward displacement of the shoreline up to several hundred km from the platform margin. During sea-level low stand the sediments bypassed most of the platform and were deposited at the edge as large platform margin deltas.

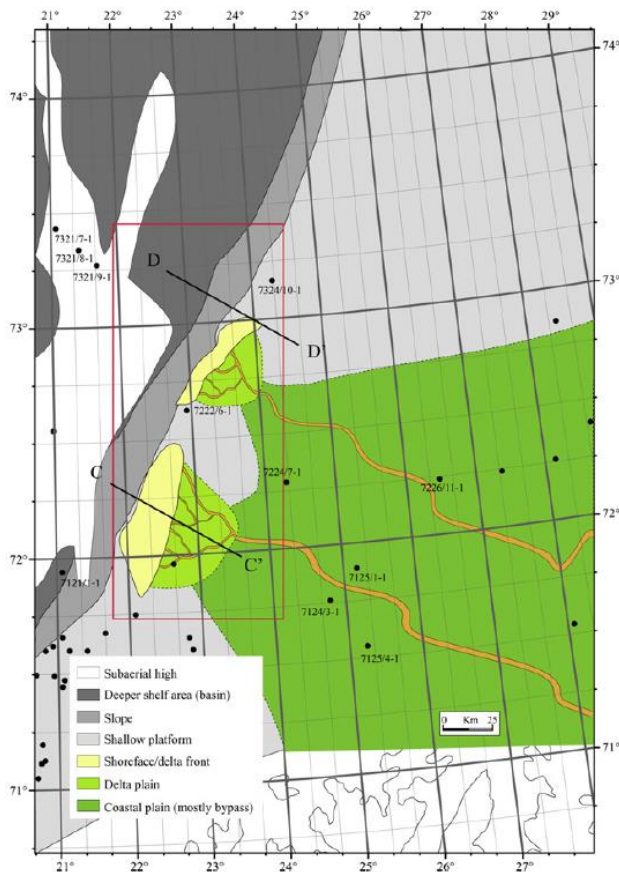
Between the palaeo – Loppa High and the platform margin there was a narrow basin as shown in Figure 4. During low stand the margin prograded towards the palaeo – Loppa High which caused a narrowing of the basin in between. This narrowing of the basin lead to an increased marine reworking of the sediments by alongshore and tidal currents which in turn lead to straightened platform edges (Glørstad-Clark et al., 2011).

As shown in Bugge et al. (2002) the coastline prograded in the early – middle Triassic and because of the change in the coastline and the changing sea level during this time the depositional environment in the Nordkapp basin varied. It varied from near coast environments on land like coastal plains to shelf environments. In the Anisian the sea level was at relative high stand and the depositional environment in the Nordkapp Basin was



anoxic middle shelf. In the Late Norian – Early Rhaetian the sea level had fallen, and the coastline had prograded westward. The sedimentary environments in the Nordkapp Basin during this time included inner shelf with offshore bars, lagoons and deltas.

The rates of subsidence and sedimentation on the Barents Shelf decreased greatly in the late Triassic resulting in the Uralian-sourced progradational system no longer dominating and shallow marine and coastal environments were established (Worsley, 2008)



**Figure 4:** Paleogeographic reconstruction of the SW Barents Sea in the Middle Anisian. From Glørstad-Clark et al. (2011).

### Jurassic to Present

Shallow marine conditions were established in the Barents Sea in the early Jurassic due to a global sea level rise in the Toarcian (Smelror et al., 2009). According to Johannessen and Nøttvedt (2006) large areas were flooded in the Early Jurassic before the coastline prograded westwards again. There was a balance between sediment supply and subsidence throughout the early Jurassic which meant that after a rapid progradation the coastline stood still for a long time.

An extensive sea level rise in the Middle Jurassic led to flooding of the Nordkapp Basin and the deposition of tidal and shallow marine sediments (Johannessen and Nøttvedt, 2006). After this there was a large regression which reached its maximum in the Bajocian exposing large areas of the Barents Shelf. In the Nordkapp Basin the environment was shallow marine at this time (Smelror et al., 2009).

After a tectonically quiet period in the Triassic the tectonic activity increased in the Late Jurassic. Rifting in the Norwegian Sea spread to the north and reached the south-west Barents Sea in the late Jurassic (Nøttvedt and Johannessen, 2006). Rifting and relative sea level rise in the Jurassic caused a permanent seaway between the northern and southern oceans to form (Brekke et al., 2001).

In the Late Jurassic there was a period of regression followed by a transgression which led to the establishment of a large shallow ocean and deposition of marine mud (Nøttvedt and Johannessen, 2006). The Late Jurassic sea-level reached its maximum in the Tithonian and this resulted in a shallow to deep marine environment (Smelror et al., 2009). This was followed by a sea-level fall which changed the depositional environment at the end of the

Jurassic and Early Cretaceous. In general the environment became more open with better circulation of the bottom water except in restricted basins where the circulation remained poor (Worsley, 2008). In the Early Cretaceous the deposition of fine clastics dominated. Mud was deposited over large areas, and shales up to 700- m -thick with intervals rich in organic matter were deposited in some basins (Worsley, 2008).

The Nordkapp Basin was uplifted and deeply eroded in the Pliocene – Pleistocene. This erosion removed almost all Cenozoic sediments except some early Cenozoic sediments in the SW part of the basin. After this the basin was overlain by a thin layer of Quaternary sediments. The Nordkapp Basin floor is today located about 300-400 m below sea level (Bugge et al., 2002).

## 2.2 Previous work on the cores

To better understand the geology of the Nordkapp Basin Bugge et al. (2002) described the lithology of the cores (Figure 5). The results that were reported are on a large scale. Six different depositional environments were interpreted in the cored Mesozoic succession: coastal plain/delta plain, shallow subtidal/tidal channels/tidal flat, shoreface environment, inner-outer shelf, open marine shelf and restricted marine basin.

According to Bugge et al. (2002) the coastal plain/delta plain deposits are made up of mottled claystone and fining upwards to fine to very fine laminated sandstone. Coal, rootlets and concretions are common.

The shallow subtidal/tidal channels/tidal flat deposits consist mostly of bioturbated sandstone and heterolithics. Wave and current ripples are common and the beds often coarsen upwards with an upwards grading from lenticular to flaser bedding. Fining upwards beds with rootlets at the top are also common.

The shoreface environment shows a high energy, regressive development. Deposits from the shoreface environment are made up of fine to coarse sandstones that have in some places been bioturbated but mostly are rippled, trough cross bedded or planar laminated. The deposits often contain plant debris.

The inner-outer shelf deposits are mostly heterolithics and mudstones. The mudstone is quite silty on the inner shelf and becomes more clay rich further out. Fine-grained sandstone beds have been interpreted as turbidite beds. This facies also contains wave ripples and hummocky cross stratification.

The open marine shelf deposits consist of light grey bioturbated carbonate. The carbonate is a greenish grey glauconitic mudstone overlain by wackestone and packstone. Fragmented bivalves, cephalopods, crinoids, bryozoa and foraminifers are very common.

The restricted marine basin deposits consist mostly of black to dark brownish grey shales. Fossils, concretions and cone in cone structures occur occasionally throughout these deposits.

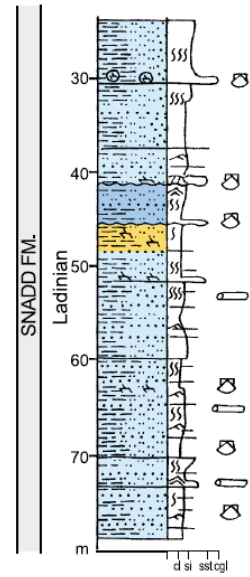
**Legend**

- |  |                       |  |                      |
|--|-----------------------|--|----------------------|
|  | Shale                 |  | Trough cross bedding |
|  | Siltstone             |  | Bioturbation         |
|  | Sandstone             |  | Cross bedding        |
|  | Limestone             |  | Roots                |
|  | Conglomerate          |  | Bivalve              |
|  | Coal                  |  | Ammonite             |
|  | Clast                 |  | Cephalopod hook      |
|  | Pyrite                |  | Fish remains         |
|  | Glauconite            |  | Belemnite            |
|  | Mud clast             |  | Wood fragment        |
|  | Volcanic ash          |  | Plant fragment       |
|  | Siderite              |  | Coquina bed          |
|  | Siderite cement       |  | Oolite               |
|  | Calcite cement        |  | Echinoderm           |
|  | Erosion               |  | Bryozoan             |
|  | Ripple lamination     |  | Algae                |
|  | Flaser bedding        |  | Foraminifera         |
|  | Wave ripples          |  | Macro fossil         |
|  | Horizontal lamination |  |                      |

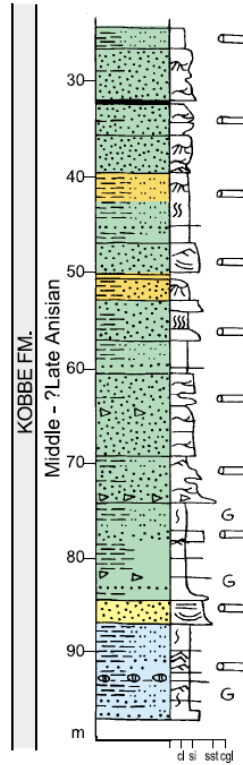
**Sedimentary facies**

- |  |                                 |
|--|---------------------------------|
|  | Coastal plain / delta plain     |
|  | Lagoon / tidal flat / embayment |
|  | Shoreface / delta front         |
|  | Inner shelf                     |
|  | Middle shelf                    |
|  | Outer shelf                     |
|  | Anoxic / dysoxic basin          |

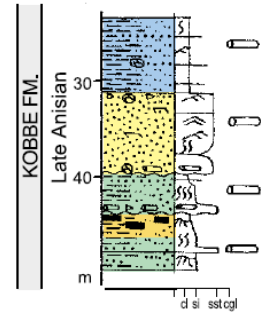
**7230/05-U-04**



**7230/05-U-06**



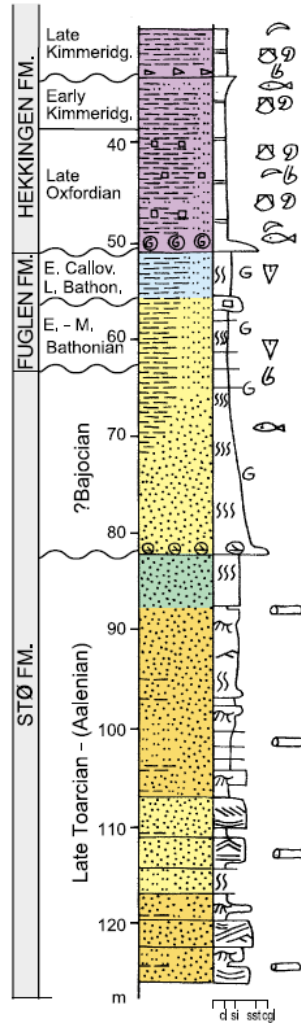
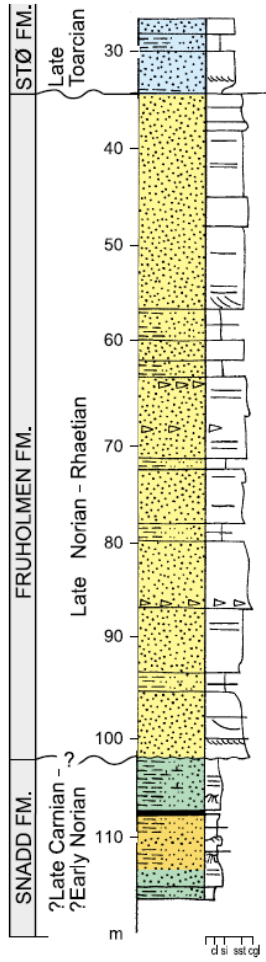
**7230/05-U-05**





7230/05-U-02

7230/05-U-03



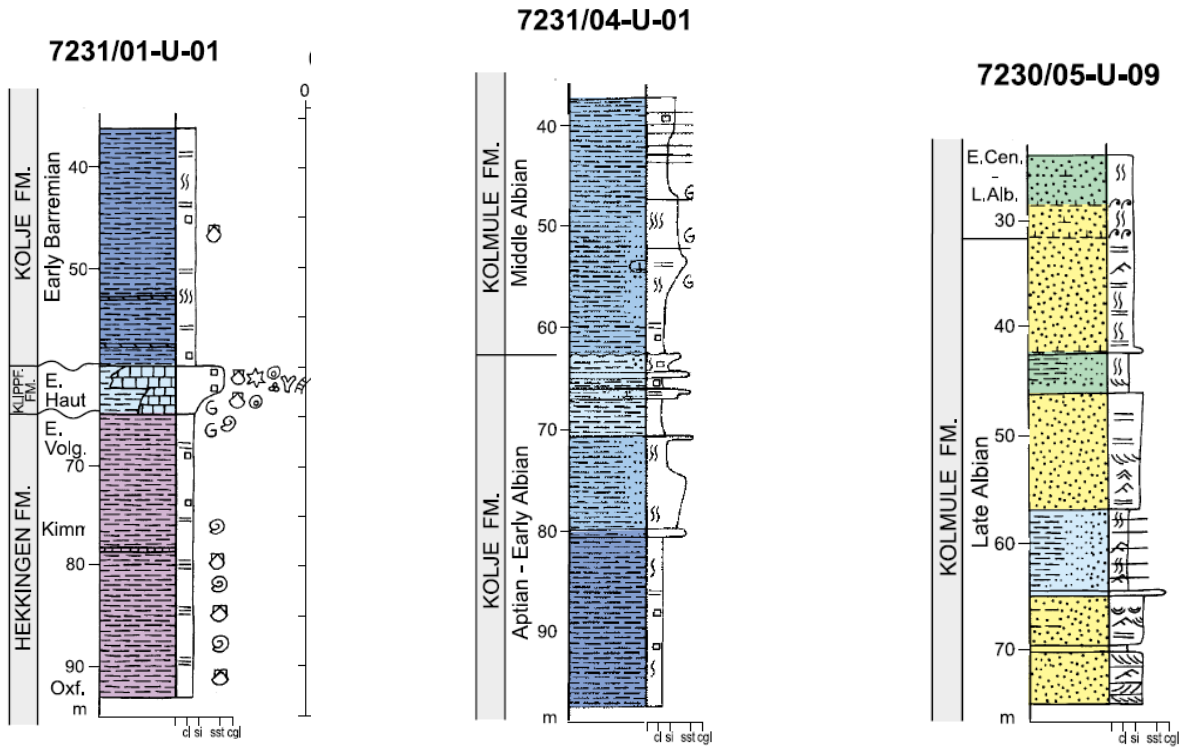


Figure 5: Overview logs of all the cores. From Bugge et al. (2002).

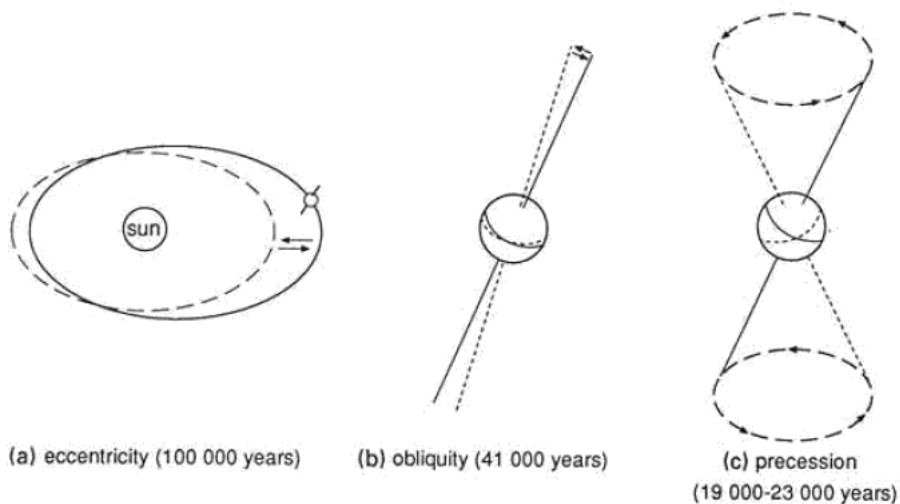
### 2.3 Milankovitch cycles

The amount of solar radiation received by the earth varies on short and long terms influencing the climate. The longer term variations in insolation are caused by variations in the distance between the earth and the sun which depend on the obliquity, eccentricity and precession of the earth (de Boer and Smith, 1994; Schwarzacher, 1993).

Obliquity is the variation in the tilt of the earth's axis which varies between  $22^{\circ}$  and  $24.5^{\circ}$  with 41ka cycles. Currently the axis is at a  $23.5^{\circ}$  angle (de Boer and Smith, 1994).

Eccentricity is the shape of the earth's orbit around the sun which varies from almost circular to slightly elliptic. The elliptic shape of earth's orbit is caused by the gravitational pull from other planets. The changes in eccentricity take place in cycles with duration of 100ka, 400ka 1300 ka and 2Ma (de Boer and Smith, 1994).

Precession is the variation in the direction of the axis of the earth tilt which is caused by the gravitational pull of the sun and the moon. The precession cycles have a duration of 23ka and 19ka (de Boer and Smith, 1994; Schwarzacher, 1993).



*Figure 6: Orbital cycles. From de Boer and Smith (1994).*

### 3. Methodology

The cores were observed and the detailed observations were recorded on logging paper with a 1:20 scale. To determine the grainsizes a hand lens or a microscope was used together with a grain size comparator. The cores were stored in one-metre-long sections and the depth was measured downwards from the top. The cores that were logged are:

- 7230/05-U-06
- 7230/05-U-05
- 7230/05-U-04
- 7230/05-U-03
- 7230/05-U-02
- 7231/01-U-01
- 7231/04-U-01
- 7230/05-U-09

Based on the observations facies analyses were carried out, and variations in depositional environments, bioturbation intensity, heterolithics, mottling and facies were plotted against core depth. This was then used to compare small scale changes across different environments. The duration of sedimentation, that was used to calculate the sedimentation rates for each core or part of core, was found using Figure 6 in Bugge et al. (2002). The sedimentation rates were used to calculate the durations of the small scale changes by translating thickness of change to duration of change.

Thin sections were used to look at microstructures in selected intervals of the cores where it was hard to see any structures with the naked eye or with a hand lens. The thin sections were taken from core(s):

- 7230/05-U-02, depth 46.57m – Black shale
- 7231/01-U-01, depth 72.85m – Black shale
- 7231/01-U-01, depth 42.96m – Laminated mudstone
- 7231/04-U-01, depth 74.59m – Bioturbated silty mudstone
- 7231/04-U-01, depth 70.59m – Slightly bioturbated clayey mudstone

## 4. Results

### 4.1 Facies

Intervals within the cores which show similar sedimentological parameters define a facies. The cores have been divided into 17 different facies which have been described and their depositional mechanisms have been interpreted.

## **Sandstone facies**

### *Description*

Massive, laminated and trough cross bedded sandstone are included in the same facies because they largely consist of the same sand size. There is no sharp boundary between the different types of sandy deposits in these cores. Since there are quite large intervals with each of the three sub facies and the sandstone is not mainly massive sandstone with a ripple here and some lamination here, the sandstone facies is subdivided in to massive, laminated and trough cross bedding. The sandstone beds can be several metres thick and are often overlying and underlying heterolithics or mudstones.

### Massive

The massive sandstone subfacies consists of fine to medium sand. The colour is mostly light grey but sometimes there is a green tint to it due to the presence of glauconite and sometimes there is a red tint to the colour due to oxidation. This is a structureless facies (Figure 7). It contains small pieces of coal, mud clasts and concretions.

### Laminated

This subfacies is very similar to the massive sandstone but it shows parallel planar lamination and in one place a water escape structure (Figure 8). Parts of this facies contain coal and mud which make the lamination clearer.

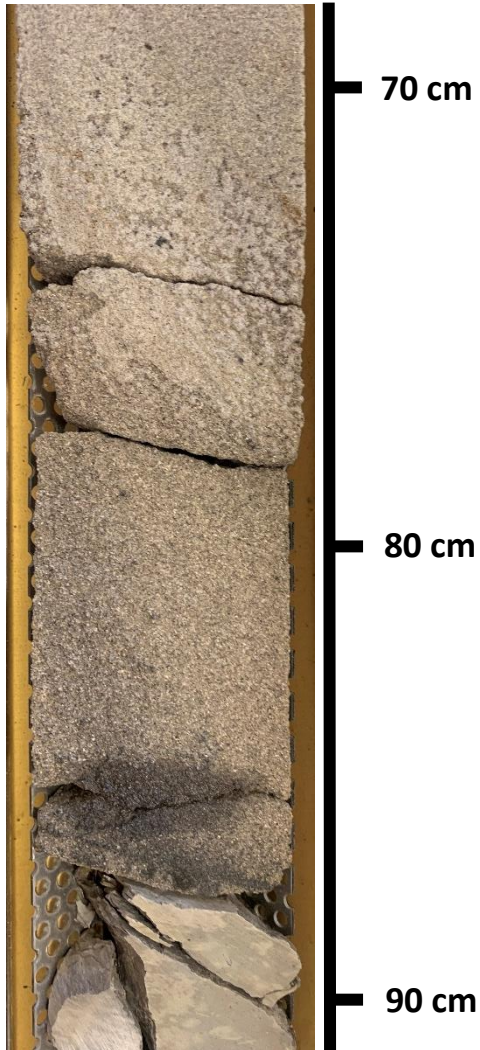
### Trough cross bedded

This subfacies is very similar to the massive and planar laminated sand but it shows trough cross bedding (Figure 9). Parts of this facies contain streaks of coal and mud which make the trough cross bedding in the sandstone clearer.

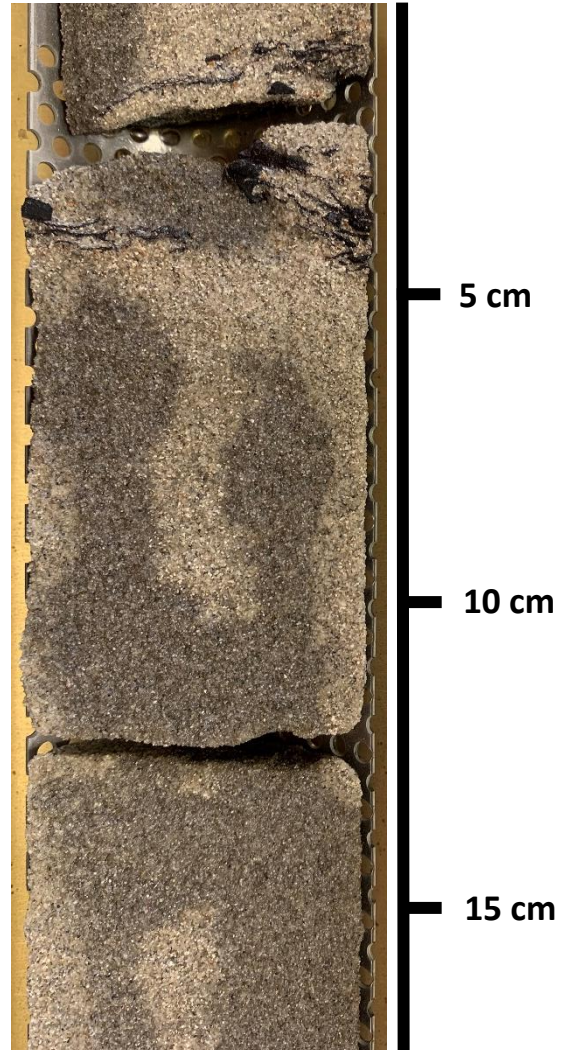
### *Interpretation*

This facies is typical of shoreface deposits (Nichols, 2009d).

(a) 7230/05-U-03  
101-102m



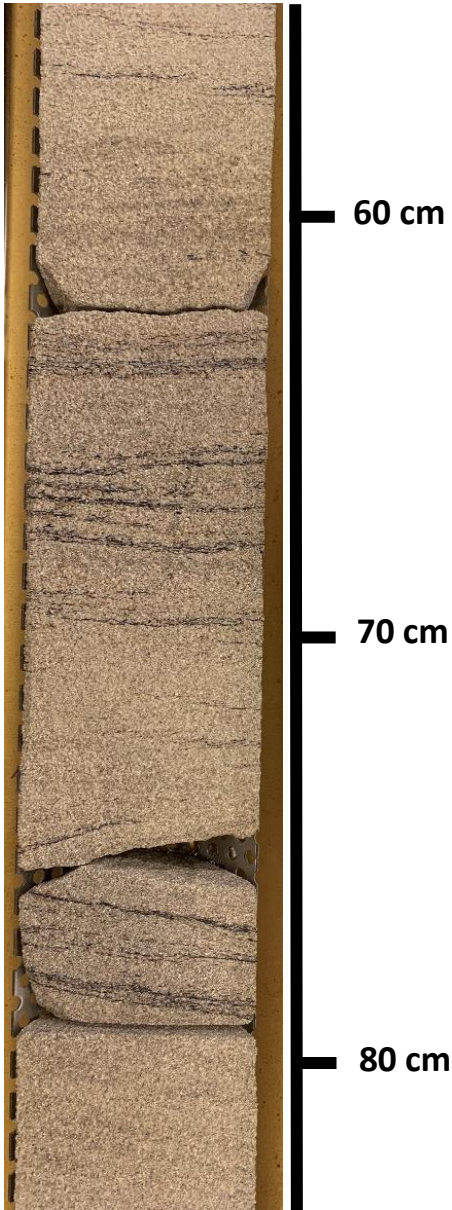
(a) 7230/05-U-03  
98-99m



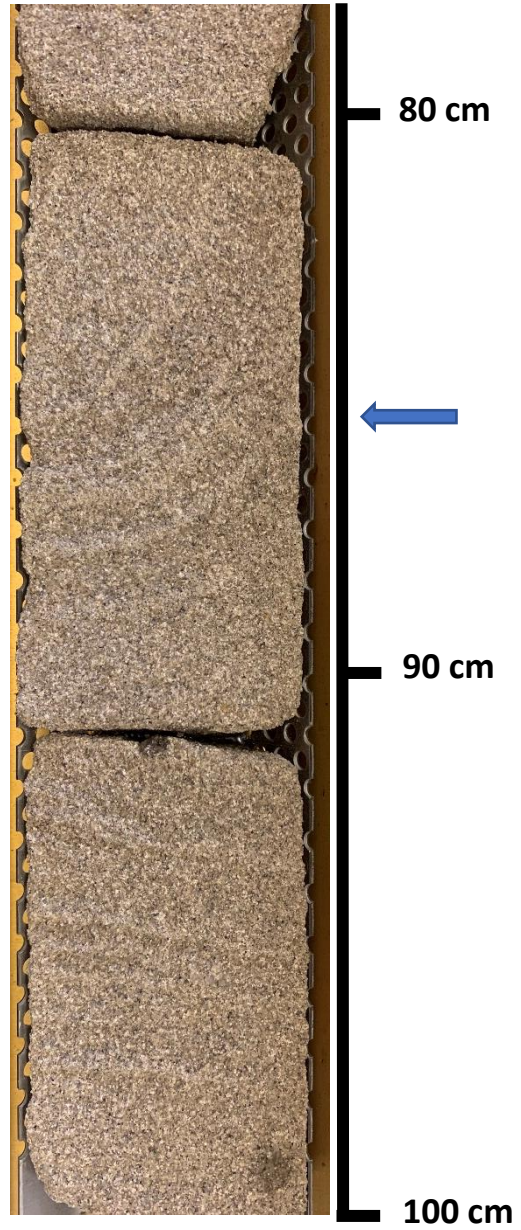
**Figure 7:** Core photos showing massive sandstone. (a) Massive sandstone overlying a claystone. (b) massive sandstone with pieces of coal.



(a) 7230/05-U-03  
74-75 m

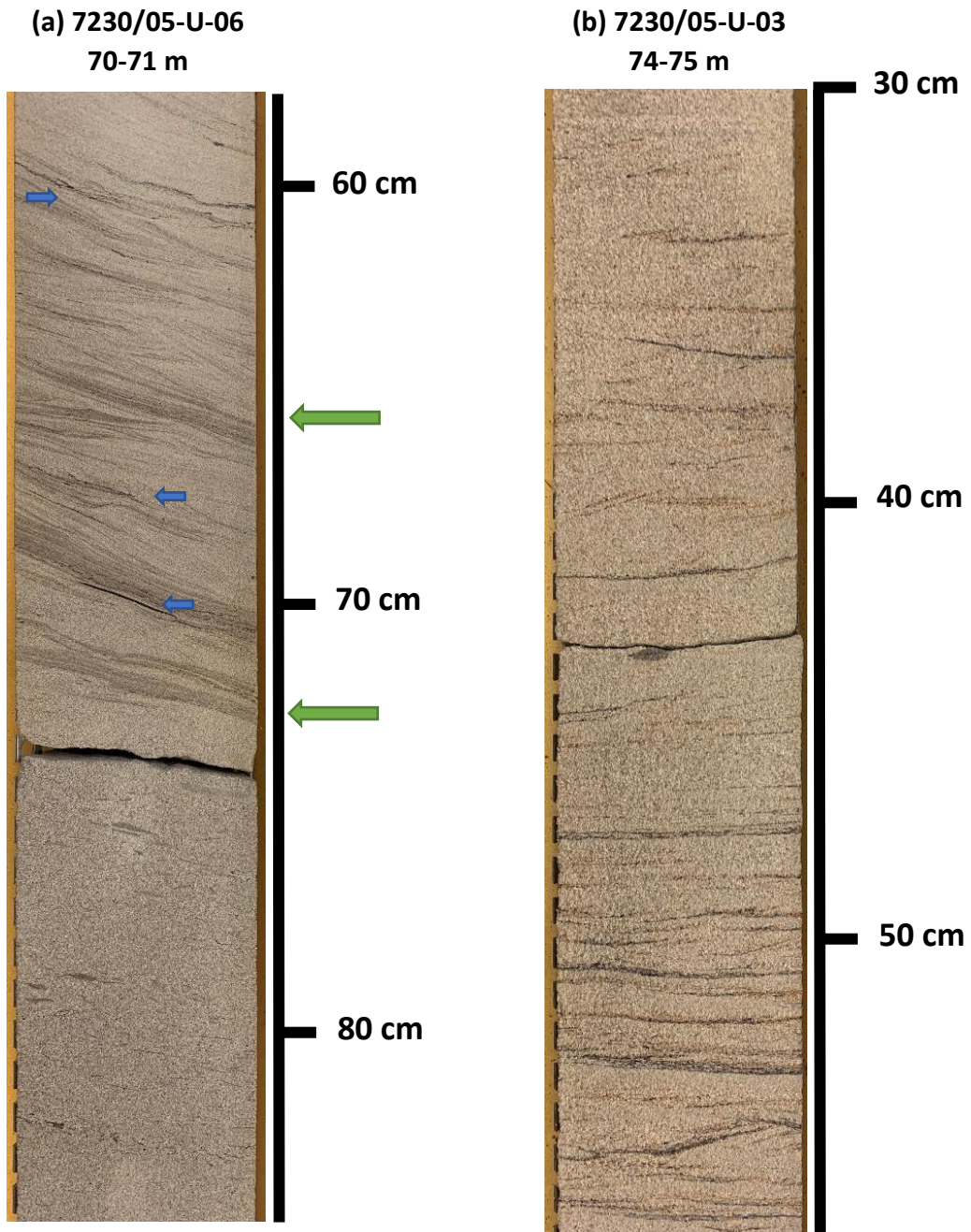


(b) 7230/05-U-03  
40-41 m



**Figure 8:** Core photos showing laminated sandstone. (a) Laminated sandstone with coal laminae. (b) Laminated sandstone with a water escape structure indicated by the arrow.





*Figure 9: Core photos showing cross bedded sandstone. (a) Trough cross bedded sandstone with dark grey mud (green arrow) and black coal (blue arrows). (b) cross bedded sandstone with coal laminae.*

## **Coarsening upwards sandstone facies**

### *Description*

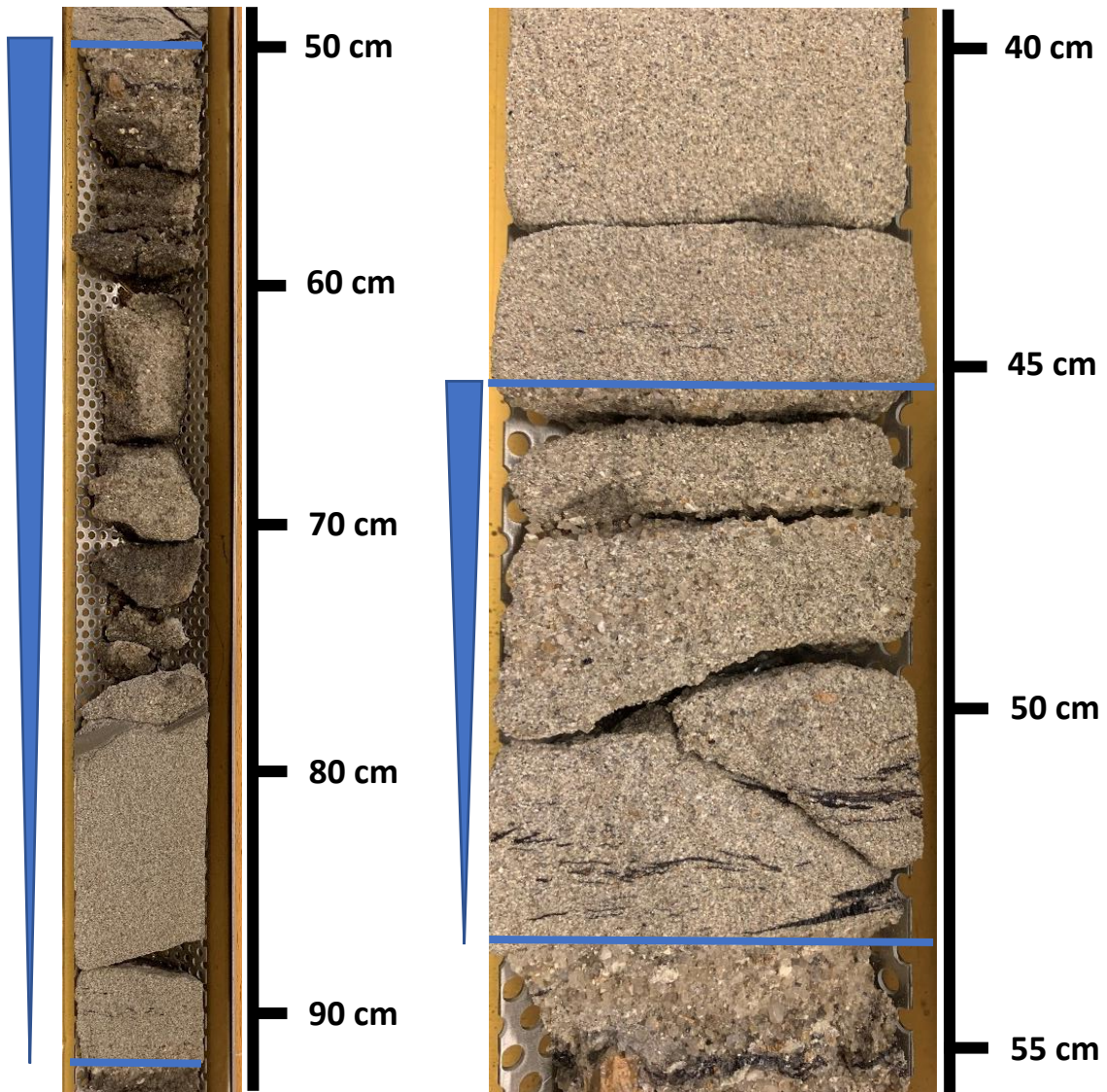
This facies has a light grey colour. The grain sizes vary from fine sand to very coarse sand and the facies is reverse graded (Figure 10). The beds are a few centimetres to a metre thick. This facies does not contain many sedimentary structures, but planar lamination does sometimes occur. The upper boundary is often sharp, and the lower boundary is sharp or gradual. This facies is often overlain and underlain by massive sandstone or coarsening upwards sandstone. There can also be several cycles of coarsening upwards sandstone stacked on top of each other.

### *Interpretation*

This facies is associated with mouth bar deposits (Nichols, 2009a). When the river meets the ocean the flow velocity is reduced abruptly leading to the deposition of sediments transported in bedload. The coarsest sediments are deposited most proximally, and progressively finer sediments are deposited further away from the mouth of the river. This results in a coarsening upwards sequence as the delta progrades.

(a) 7230/05-U-03  
99-100 m

(b) 7230/05-U-03  
99-100 m



*Figure 10: Core photos showing coarsening upwards sandstone. (a) Coarsening upwards sandstone with some mud clasts. (b) A thinner coarsening upwards sandstone layer with some coal above the lower boundary.*

## **Fining upwards sandstone facies**

### *Description*

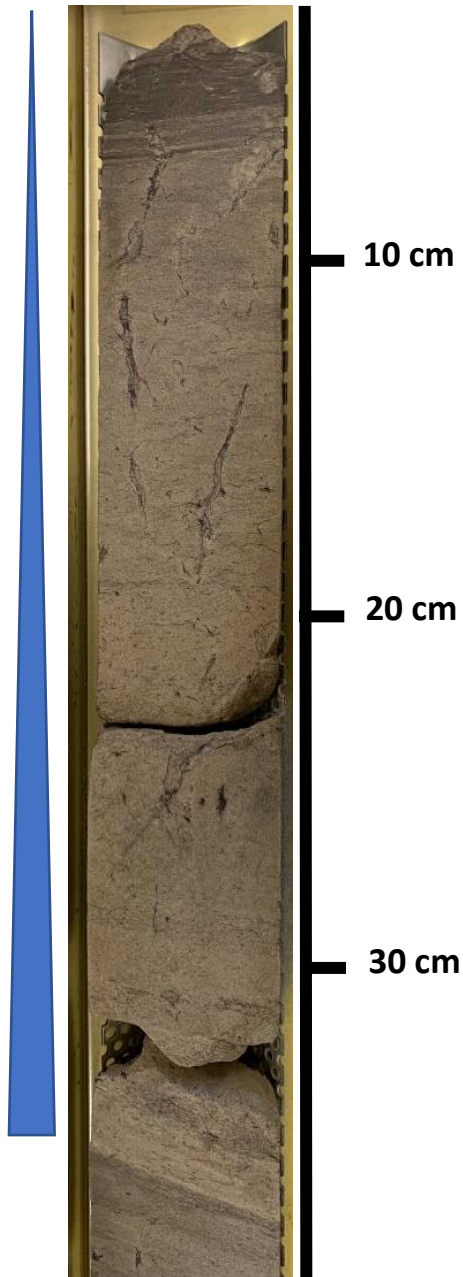
This facies consists of light grey coloured sand. The sandstone is graded, and the dominant grainsizes are very fine to medium sand. In some places this facies is laminated, and rootlets occur occasionally (Figure 11). The beds are several centimetres to a metre thick. The lower boundary is sharp or gradual. If the sandstone is underlain by a massive sandstone, it often has a gradual lower boundary. The upper boundary is often sharp but in some places the sandstone transitions gradually to mudstone as it fines upwards.

### *Interpretation*

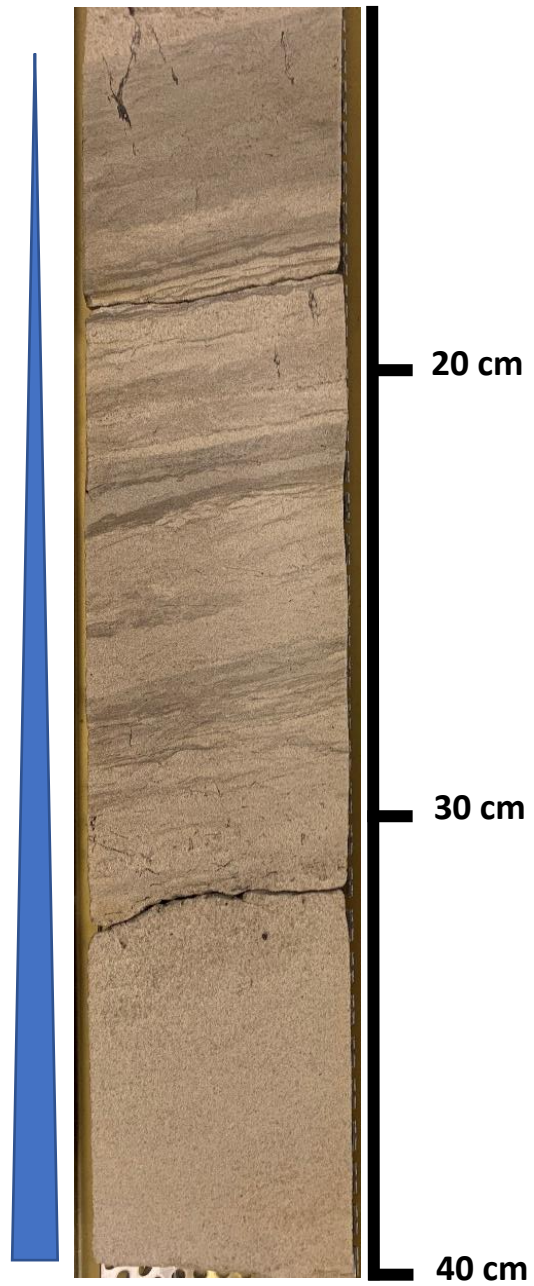
This facies is commonly associated with distributary channel deposits (Nichols, 2009a). When a channel is abandoned, the flow decelerates and its strength and therefore ability to carry sediments decreases. This results in the deposition of progressively smaller grains through time. The rootlets are a result of plant growing next to the channel on the delta plains and on the channel infill after the channel has been abandoned. The mud laminae could be the result of flocculation causing mud to settle out of suspension at higher energy than the grain size would indicate (Schieber et al., 2007). It could also be due to processes similar to the those that form the heterolithics, where the conditions vary between calm and energetic because of tides which allow for the deposition of mud at times and sand at other times.



(a) 7230/05-U-02  
104-105 m



(b) 7230/05-U-02  
100-101 m



**Figure 11:** Core photos showing fining upwards sandstone. (a) Fining upwards sandstone with rootlets. (b) fining upwards sandstone with lamination

## **Laminated sandstone facies**

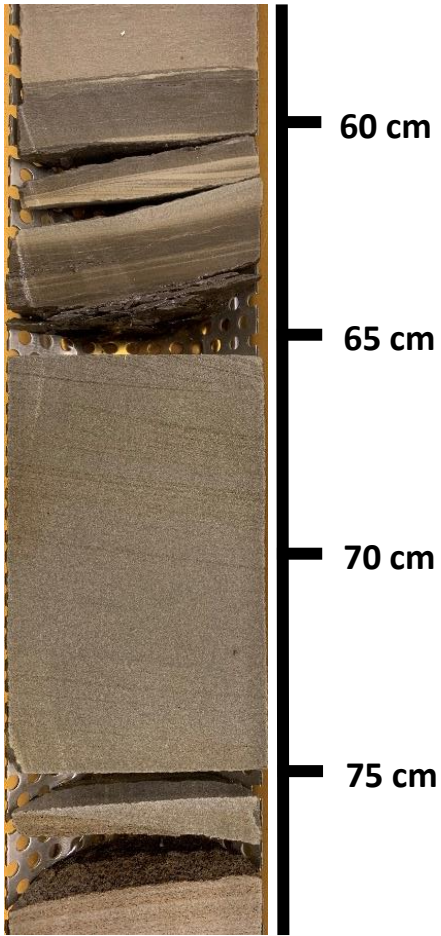
### *Description*

This facies consists mostly of very fine sand, and it has a grey colour. It shows planar lamination (Figure 12). The thickness of this facies is about 2-40cm. The lower boundary is often sharp and erosional. It is often overlain by rippled sandstone and often underlain by mudstones.

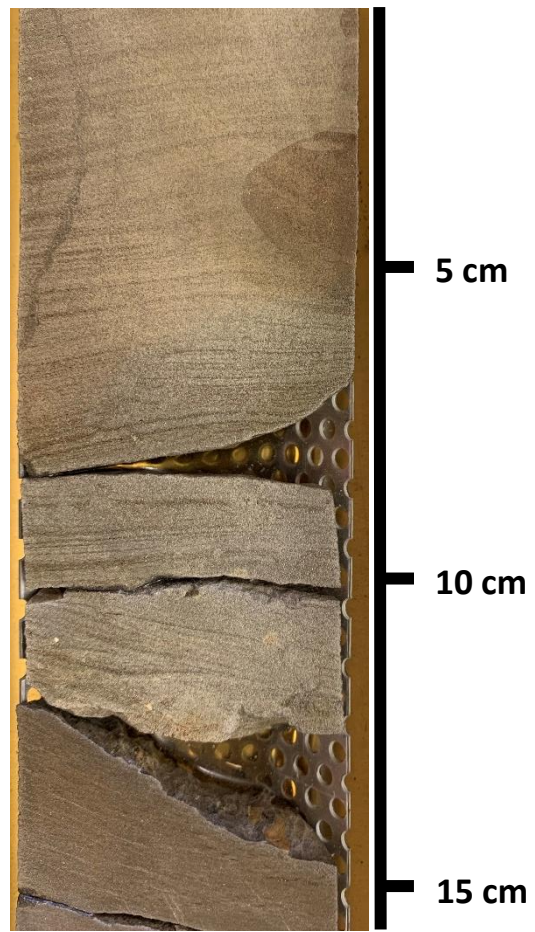
### *Interpretation*

This facies is commonly associated with turbidity currents that deposit part B of the Bouma sequence.

(a) 7230/05-U-04  
72-73 m



(b) 7230/05-U-04  
73-74 m



**Figure 12:** Core photos showing planar laminated sandstone. (a) Planar laminated sandstone overlain by rippled sandstone. (b) Laminated sandstone overlying mudstone.

## **Rippled sandstone facies**

### *Description*

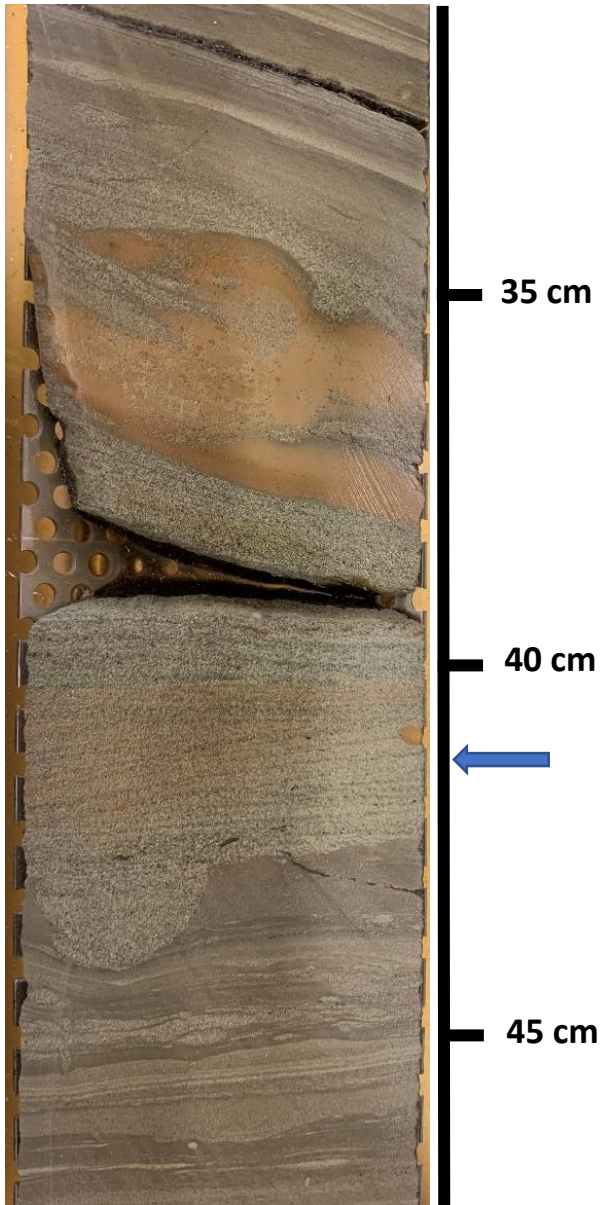
This facies has a light grey colour and consists of very fine to medium sand. The beds are a few centimetres thick and show cross lamination (Figure 13). The upper boundary is mostly sharp, and the lower boundary is sharp or gradual. This facies is often underlain by laminated sandstone and often overlain by mud.

### *Interpretation*

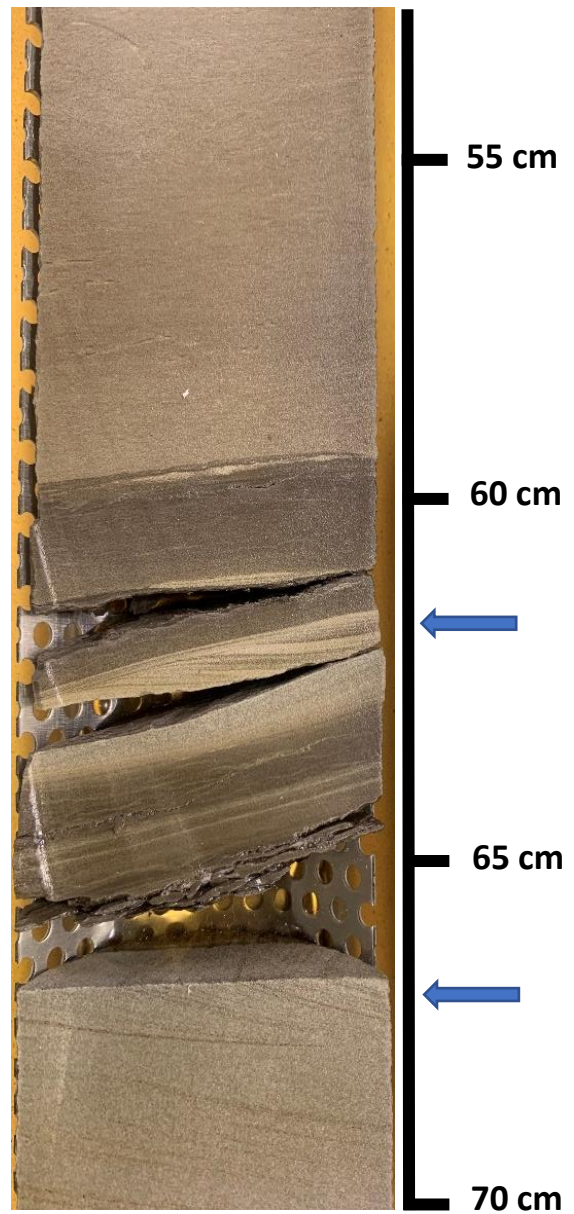
This facies is commonly associated with turbidity currents that deposit Bouma C.



(a) 7230/05-U-06  
93-94 m



(b) 7230/05-U-04  
72-73 m



**Figure 13:** Core photos showing rippled sandstone indicated by the arrows. (a) Rippled sandstone overlying a thin layer of parallel laminated sandstone and underlying laminated sandstone. (b) Rippled sandstone overlying a thicker layer of parallel laminated sandstone and underlying mudstone.

## **Heterolithic facies**

### *Description*

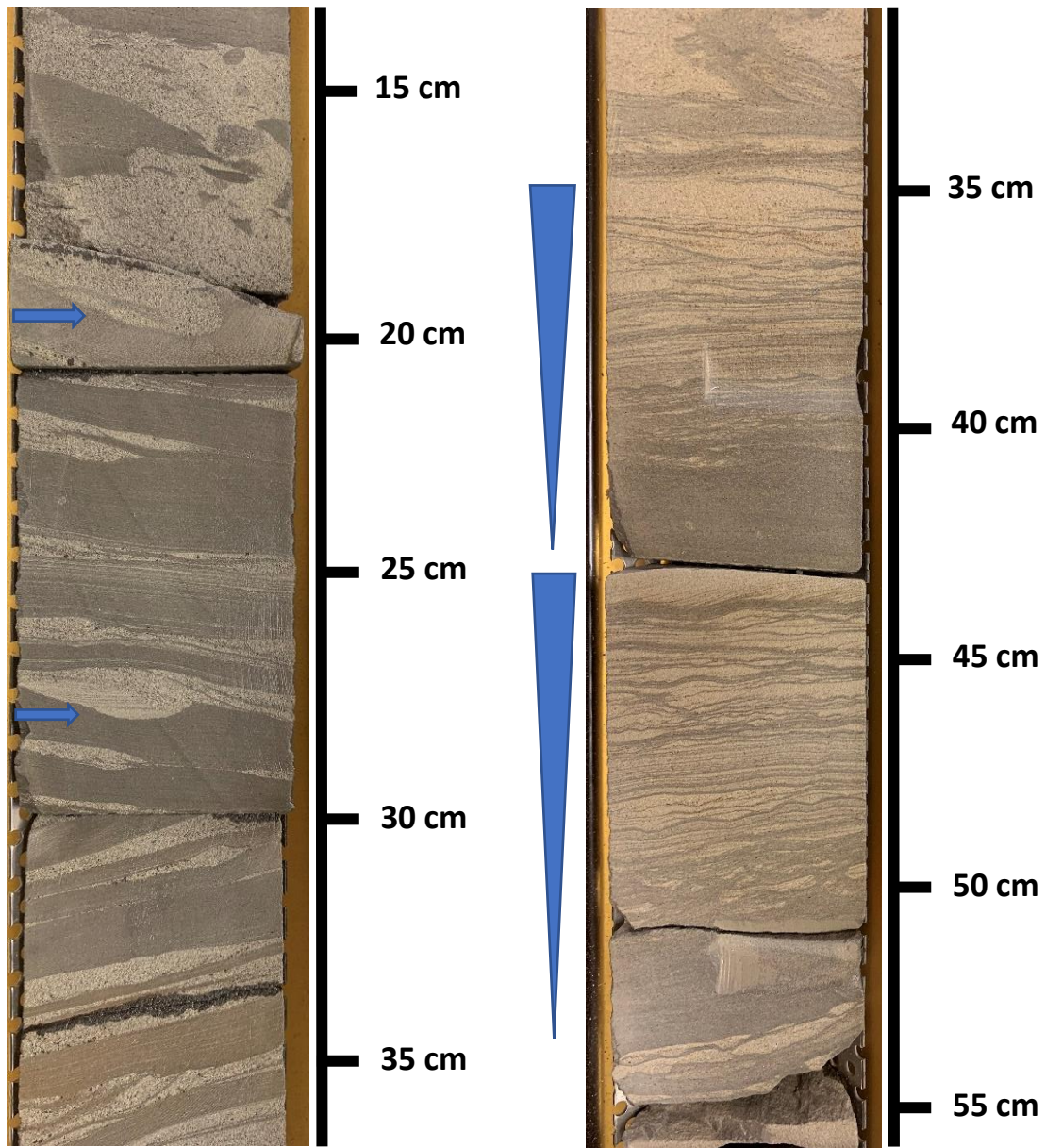
This facies is made up of both mudstone and sandstone (Figure 14). It is often bioturbated and the intensity of the bioturbation varies. Some primary depositional structures are still present. The amount of sandstone and mudstone varies. In some places there is more mudstone than sandstone, this is called lenticular bedding, in some places the amounts of sandstone and mudstone are equal, this is called wavy bedding, and in some places there is more sandstone than mudstone which is called flaser bedding. The beds are sometimes graded upwards from lenticular to flaser bedding.

### *Interpretation*

This facies is common in a tidal influenced environment. There are regular changes in energy during tidal cycles. This allows sand to be transported and deposited at high energy stages of the cycle while mud is deposited from suspension at low energy stages.

(a) 7230/05-U-06  
74-75 m

(b) 7230/05-U-03  
93-94 m



**Figure 14:** Core photos showing heterolithics. (a) Alternating layers of sand and mud, possible flute cast (blue arrows). (b) Two cycles of upward grading from mudstone to flaser bedding.

## **Distorted heterolithic facies**

### *Description*

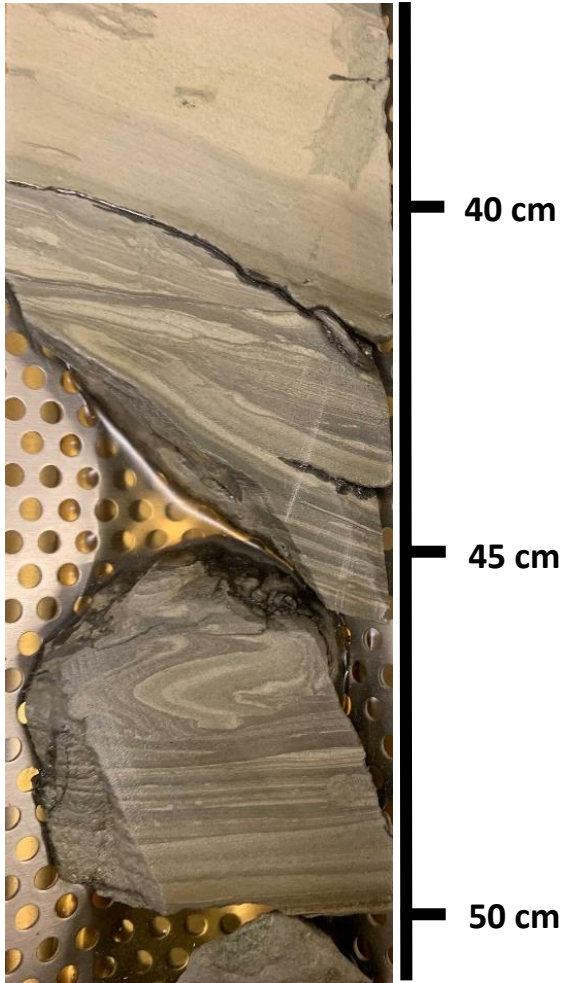
This facies consists of thin dark grey and lighter grey laminae. The grain size composition varies but the most common grain sizes are clay, and silt or very fine sand. This thinly interbedded sandstone and mudstone has been sheared and deformed. The original lamination is still visible but is folded and not broken up (Figure 15). This facies is a few centimetres to about half a metre thick. It is discordant with overlying and underlying beds, and both the upper and lower boundary are sharp.

### *Interpretation*

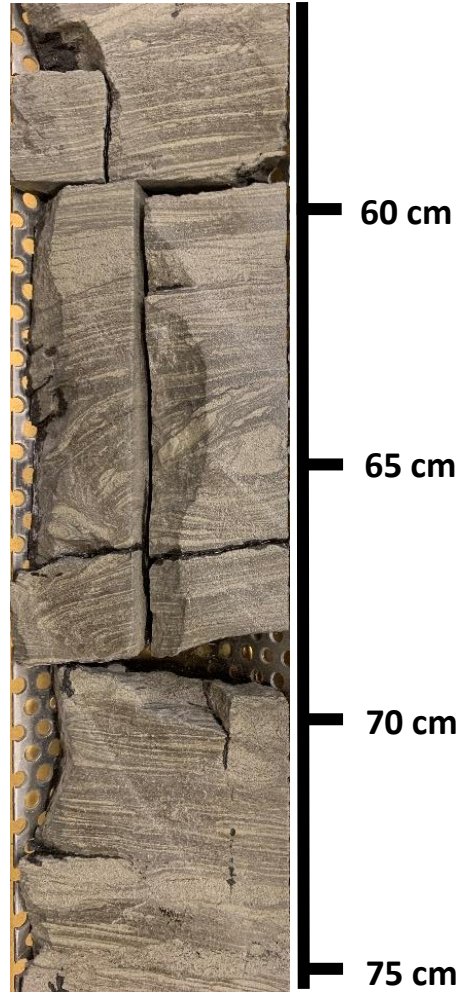
This facies is characteristic of a slump deposit. A slump results from disturbance of the original structures and is identified by the sheared and deformed original layers. The mechanism of deposition is en masse freezing.



(a) 7230/05-U-06  
95-96 m



(b) 7230/05-U-06  
35-36 m



**Figure 15:** Core photos showing distorted heterolithics. (a) Muddy distorted heterolithic bed. (b) Sandy distorted heterolithic bed.

## **Chaotic facies**

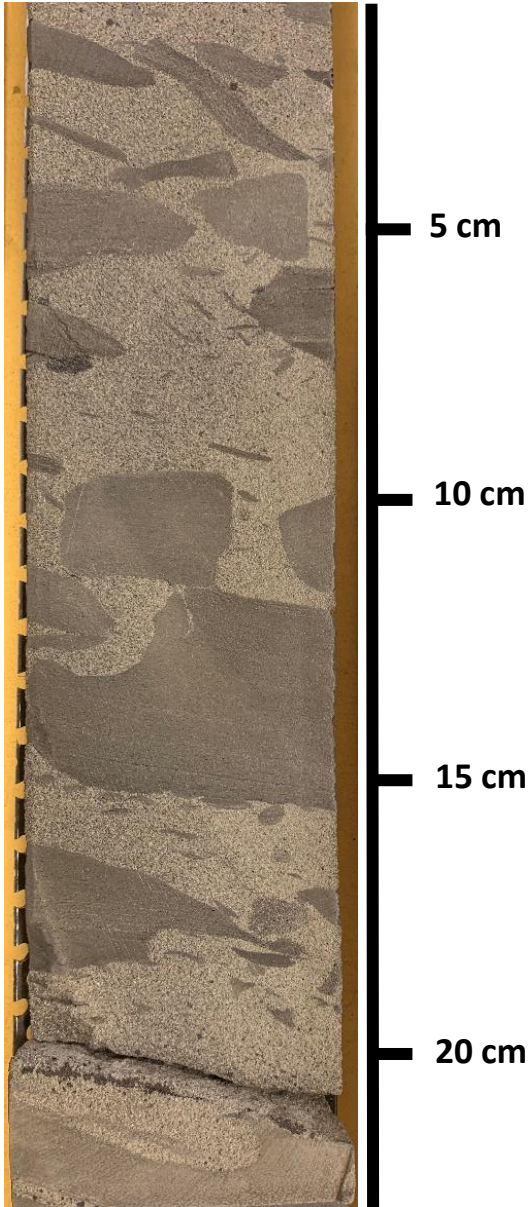
### *Description*

This facies consists of a light grey sandstone matrix with dark mudstone clasts floating in it (Figure 16). The clasts vary in size and are angular/sub angular. The clasts have no preferred orientation or grading. The upper boundary is often sharp when overlain by mudstone and often gradual when overlain by sandstone. The lower boundary is often gradual when underlain by sandstone and often sharp when underlain by mudstone or heterolithics.

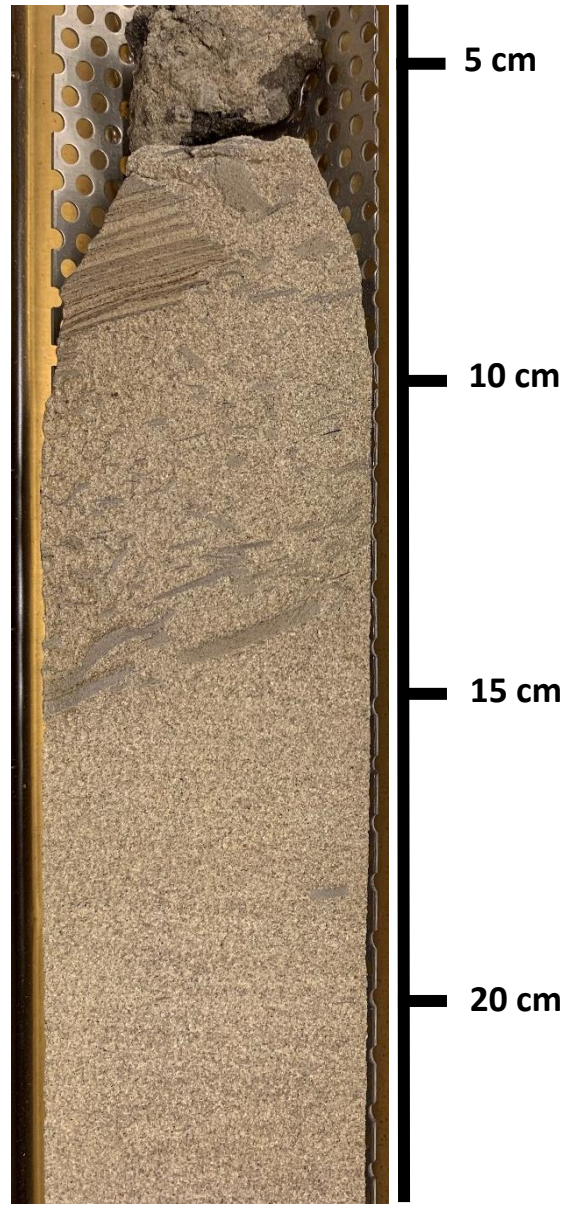
### *Interpretation*

This facies is characteristic of debrites. The floating mud clasts are suspended within the sandstone matrix. It is the strength of the matrix that supports the suspended sediments. The sediments are deposited by cohesive freezing.

(a) 7230/05-U-06  
74-75 m



(b) 7230/05-U-03  
67-68 m



**Figure 16:** Core photos showing chaotic facies. (a) Sub angular mud clasts floating in a sandstone matrix. (b) Chaotic facies overlying a massive sandstone.



## Muddy sandstone facies

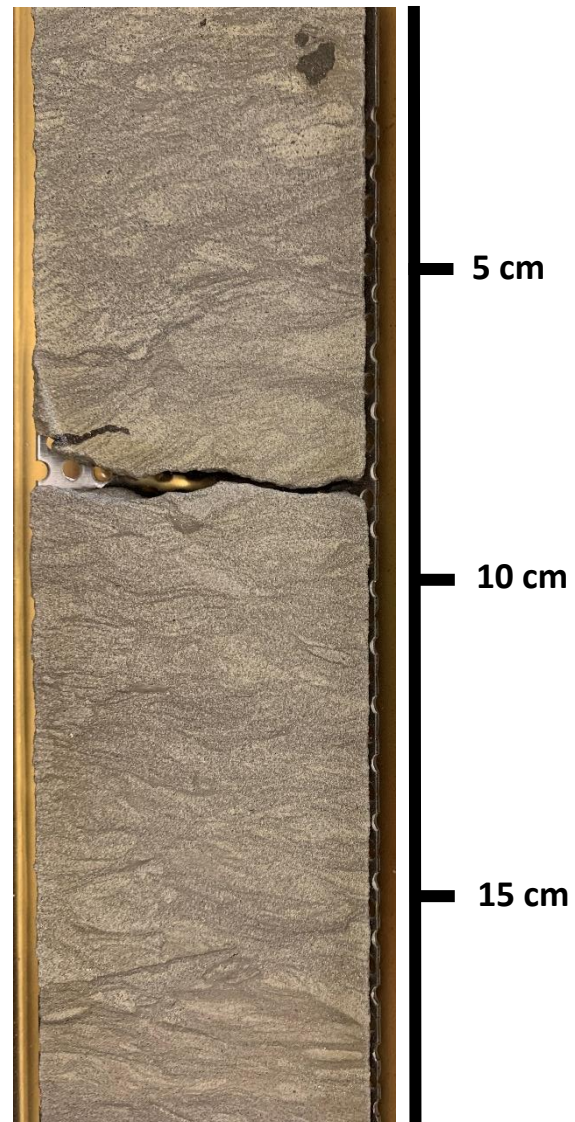
### *Description*

This is a sandstone with mud mixed into it (Figure 17). The colour is grey or sometimes greenish grey due to the presence of glauconite. This facies can be many metres thick and it is often heavily bioturbated. It is sometimes graded.

### *Interpretation*

This facies was deposited by processes similar to those that deposited the heterolithics, where conditions varied between energetic and calm due to tides allowing for the deposition of mud at times and for the deposition of sand at other times. This was then followed by intense bioturbation.

7230/05-U-05  
43-44 m



*Figure 17: Core photo showing heavily bioturbated muddy sandstone.*



## **Laminated mudstone facies**

### *Description*

#### *Laminated mudstone with silt laminae*

This facies has a dark grey colour and consists mainly of silt and clay. Silt rich laminae which have a lighter grey colour are common (Figure 18a). The beds are often several metres thick. The boundaries are sharp or gradual.

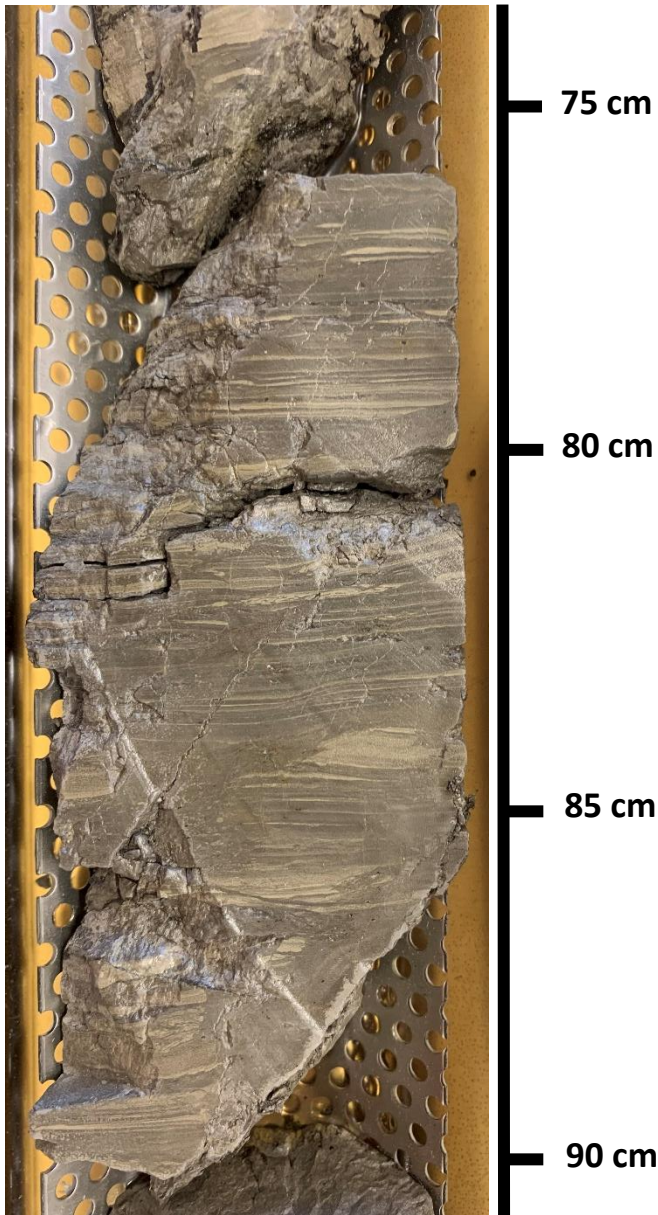
#### *Laminated mudstone with siderite laminae*

This facies has a dark grey colour and consists mainly of silt and clay. Reddish siderite or pyrite laminae are present in this facies (Figure 18b). The beds are often several metres thick. The boundaries are sharp or gradual. This mudstone overlies a carbonate mudstone.

### *Interpretation*

See section 3.2 Microstructures in mudstone.

(a) 7230/05-U-04  
56-57 m



(b) 7231/01-U-01  
42-43 m



**Figure 18:** Core photos showing laminated mudstone. (a) Laminated mudstone with silt laminae. (b) Laminated mudstone with red pyrite or siderite laminae.

### **Slightly bioturbated clayey mudstone facies**

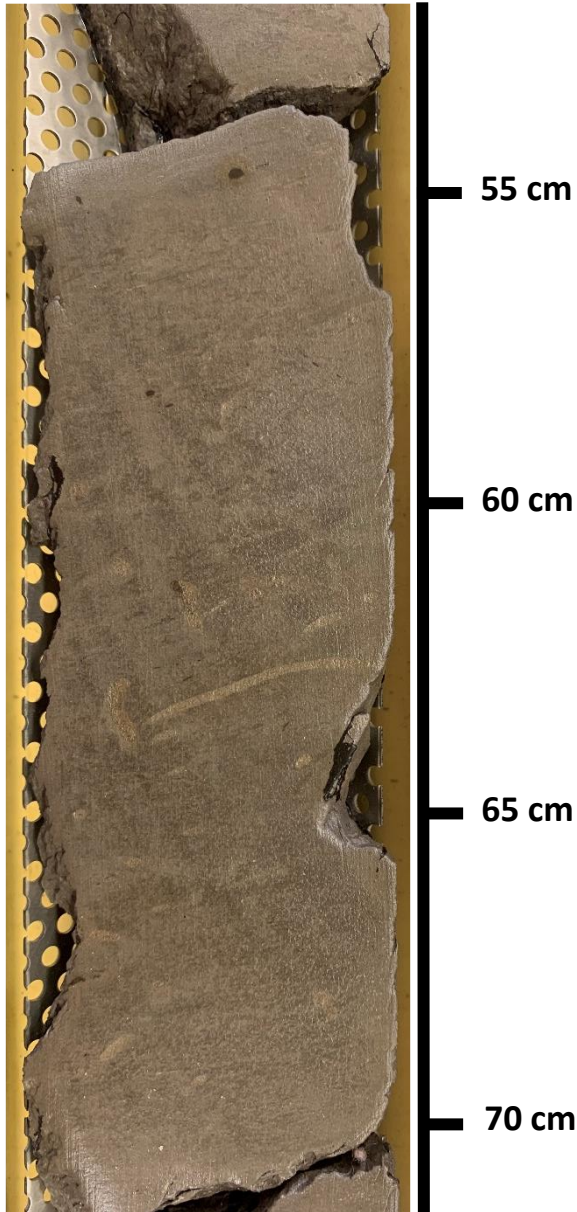
#### *Description*

This facies consists of a clay rich mudstone. It has a dark grey colour, and it is slightly bioturbated (Figure 19). The thickness of this facies is half a metre to two metres. It has gradual boundaries, and it is often overlain and underlain by bioturbated silty mudstone.

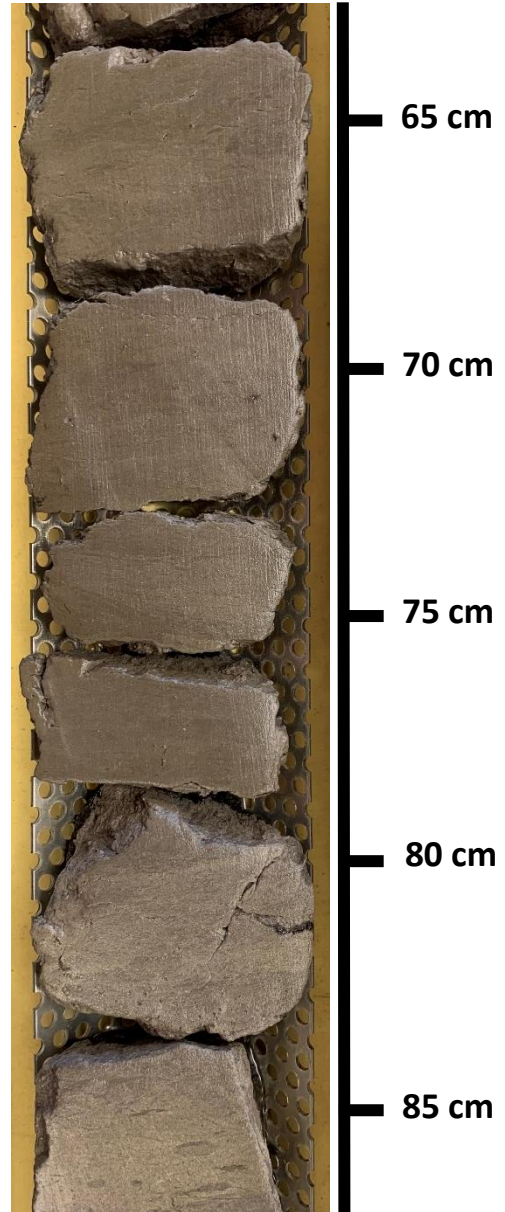
#### *Interpretation*

See section 3.2 Microstructures in mudstone.

(a) 7231/04-U-01  
71-72 m



(b) 7231/04-U-01  
70-71 m



**Figure 19:** core photos showing slightly bioturbated clayey mudstone. (a) Slightly bioturbated clayey mudstone. (b) Gradual upwards transition from bioturbated silty mudstone to slightly bioturbated clayey mudstone.

## **Bioturbated silty mudstone facies**

### *Description*

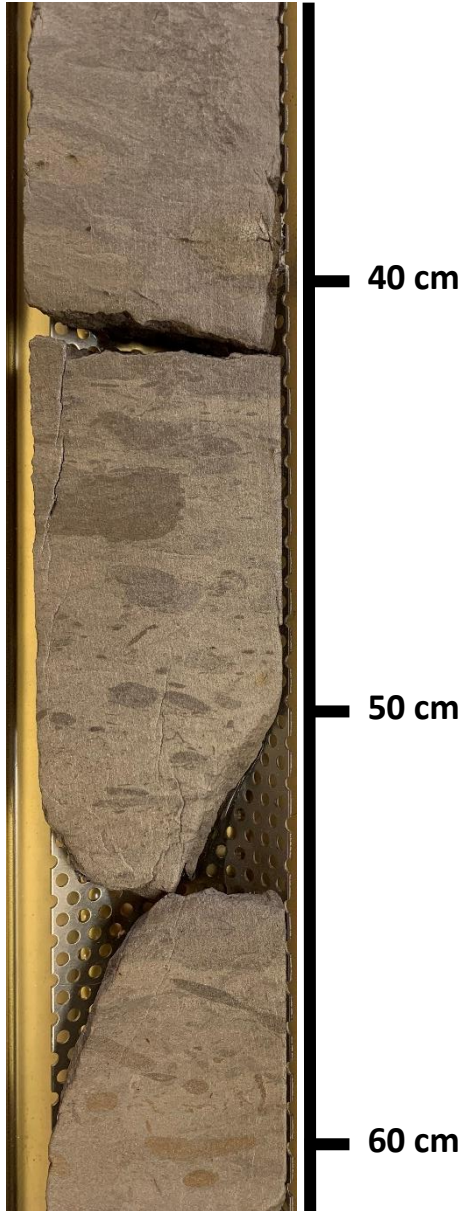
This facies has a grey colour and consists of silty mudstone (Figure 20). It is bioturbated and the burrows are filled with claystone and are therefore darker than the surrounding mudstone. The thickness varies from half a metre to several metres. The boundaries are gradual, and this facies is underlain and overlain by dark grey clay rich mud with sparse bioturbation.

### *Interpretation*

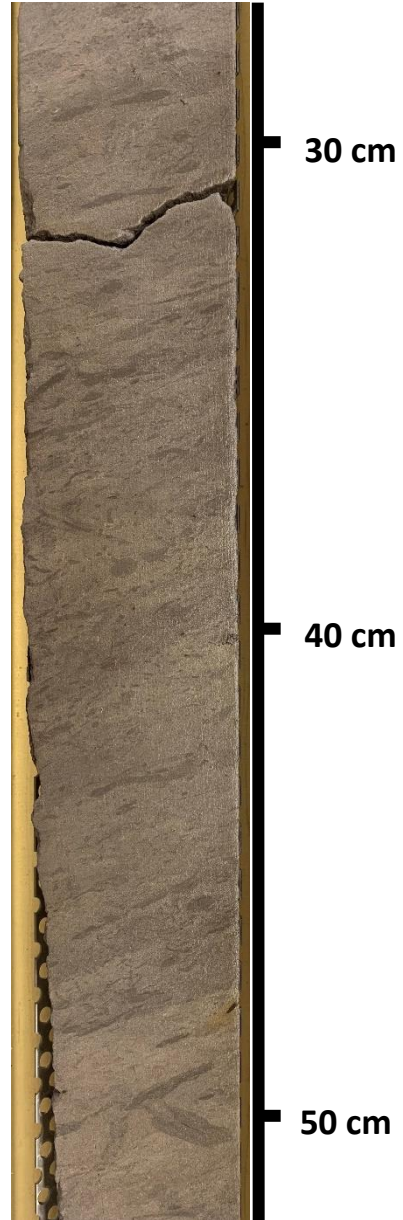
See section 3.2 Microstructures in mudstone.



(a) 7231/04-U-01  
72-73 m



(b) 7231/04-U-01  
73-74 m



**Figure 20:** Core photos showing bioturbated silty mudstone. (a) Bioturbated silty mudstone with a gradual upper boundary transitioning to slightly bioturbated clayey mudstone. (b) Bioturbated silty mudstone.

## **Shale facies**

### *Description*

#### Shale:

The dominant grainsize in this facie is clay. It is fissile and it has a dark grey colour (Figure 21a). This facies is often several metres thick and has sharp or gradual boundaries.

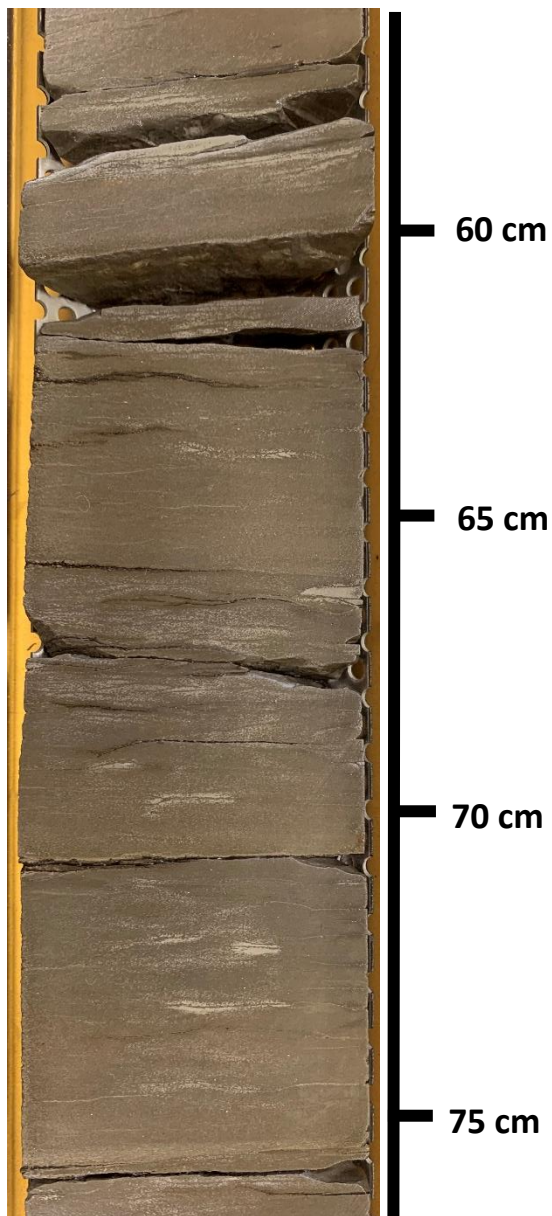
#### Black Shale

In this facies the dominant grainsize is clay. It is fissile and is often black which suggests that it is rich in organic matter. Fossils, like ammonites, shells and gastropods, as well as cone in cone structures, calcite and pyrite concretions and silt rich laminae appear occasionally throughout the shale (Figure 21b). This facies is often several metres thick and has sharp or gradual boundaries.

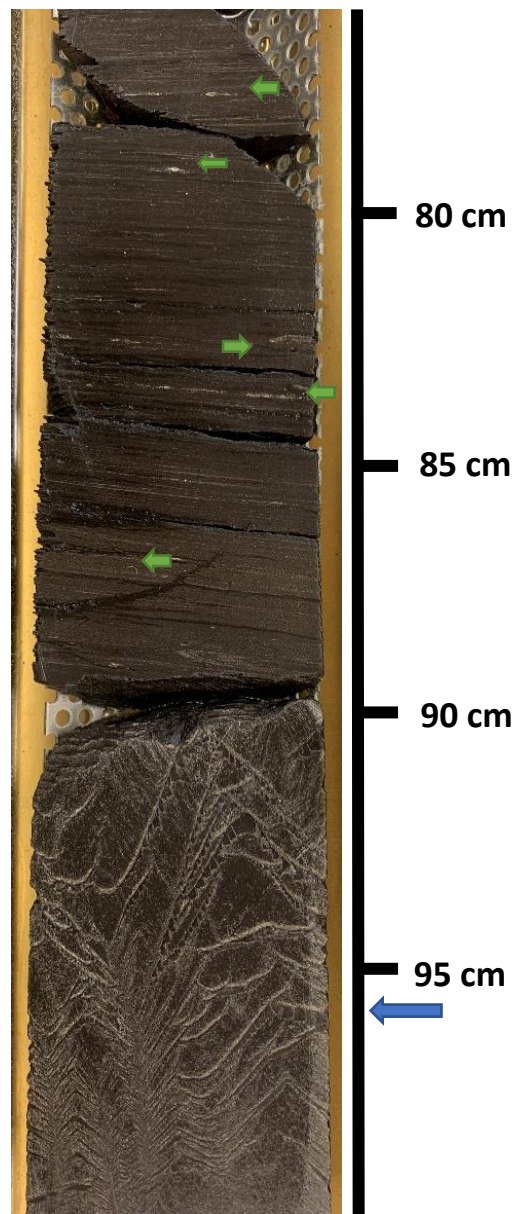
### *Interpretation*

See section 3.2 Microstructures in mudstone.

(a) 7230/05-U-04  
65-66 m



(b) 7230/05-U-02  
35-36 m



**Figure 21:** Core photos showing shales. (a) Shale. (b) Black shale with cone in cone structures (blue arrow) and fossil fragments (green arrows).



## **Mottled claystone facies**

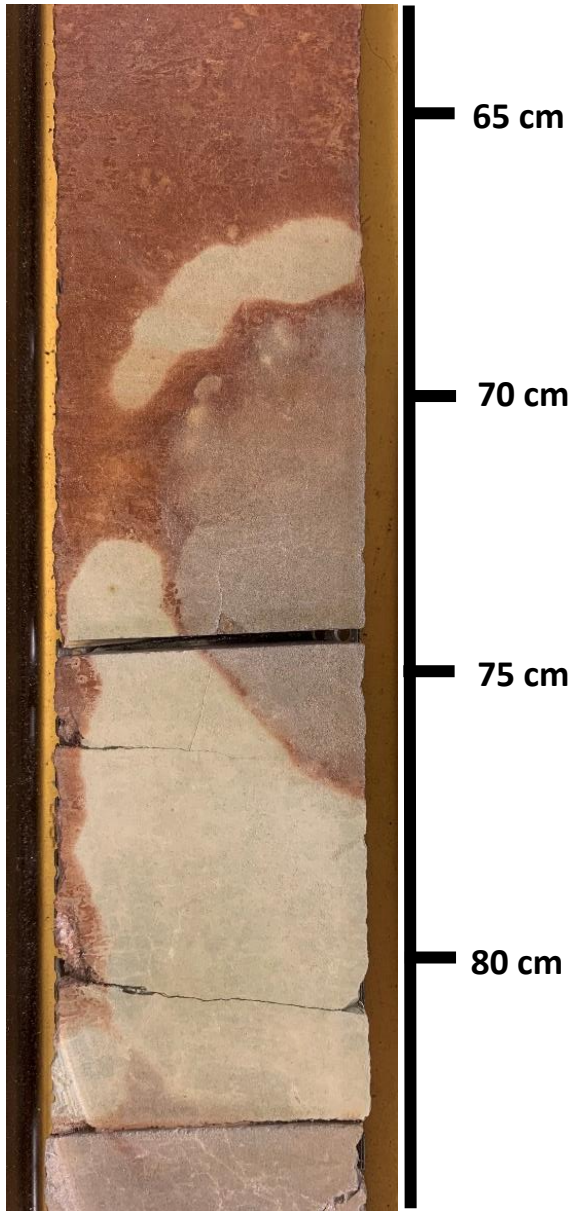
### *Description*

This facies consists mostly of claystone or clayey mudstone. The colour varies from a reddish grey to greenish grey in a mottled pattern (Figure 22). It is not fissile. Rootlets and concretions appear in this facies. It can be over a metre thick, and the lower boundary is often gradual, while the upper boundary is often sharp. It is often underlain by very fine sandstone, and it is often overlain by mudstone.

### *Interpretation*

The mottling is post depositional and it is caused by changes in the water table causing the conditions to vary between oxidizing and reducing (Nichols, 2009b). When the water table is low the sediments are exposed to the air making the conditions oxidising, resulting in the red colour. When the water table is high the sediments are less exposed to the air making the conditions reducing which results in a green colour. The mottling and the rootlets are characteristic of soils and indicate a depositional environment very close to or on the shore like coastal plain or delta plain. The sediments are deposited through suspension settling.

(a) 7230/05-U-03  
108-109 m



(b) 7230/05-U-06  
43-44 m



**Figure 22:** Core photos showing mottled claystone. (a) Red and white coloured mottled claystone. (b) Multi coloured mottled claystone, possible rootlet indicated by arrow.

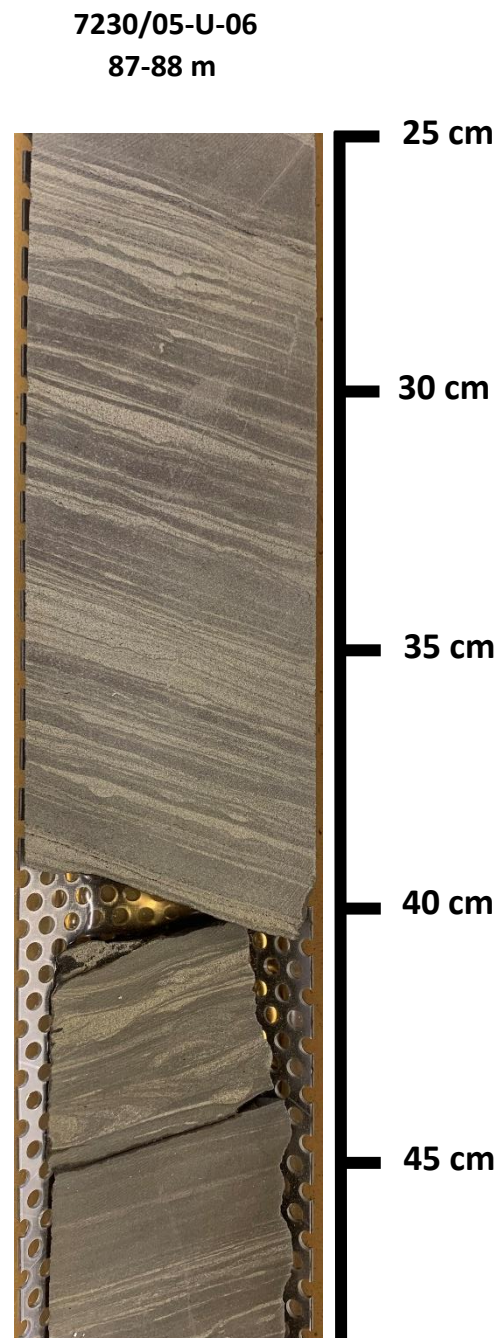
## Interlaminated sandstone and mudstone facies

### *Description*

This facies consists of alternating thin layers of sandstone and mudstone as seen in Figure 23. The sandstone layers are light grey and consist of very fine sand. The mudstone layers are dark grey and consist of clay and silt. Sometimes the boundaries are sharp, but they can also be gradual where the laminae are fining upwards. Sometimes the layers are disturbed by bioturbation. The sequences are often very thick, up to several metres.

### *Interpretation*

Alternation between multiple events of varying flow strength. The mud was deposited through suspension settling under calm conditions. During high energy events like storms the flow strength is higher, which enables the transportation and deposition of sand. This results in an alternation between mud and sand layers.



*Figure 23: Core photo showing interlaminated sandstone and mudstone.*

## **Shell bed facies**

### *Description*

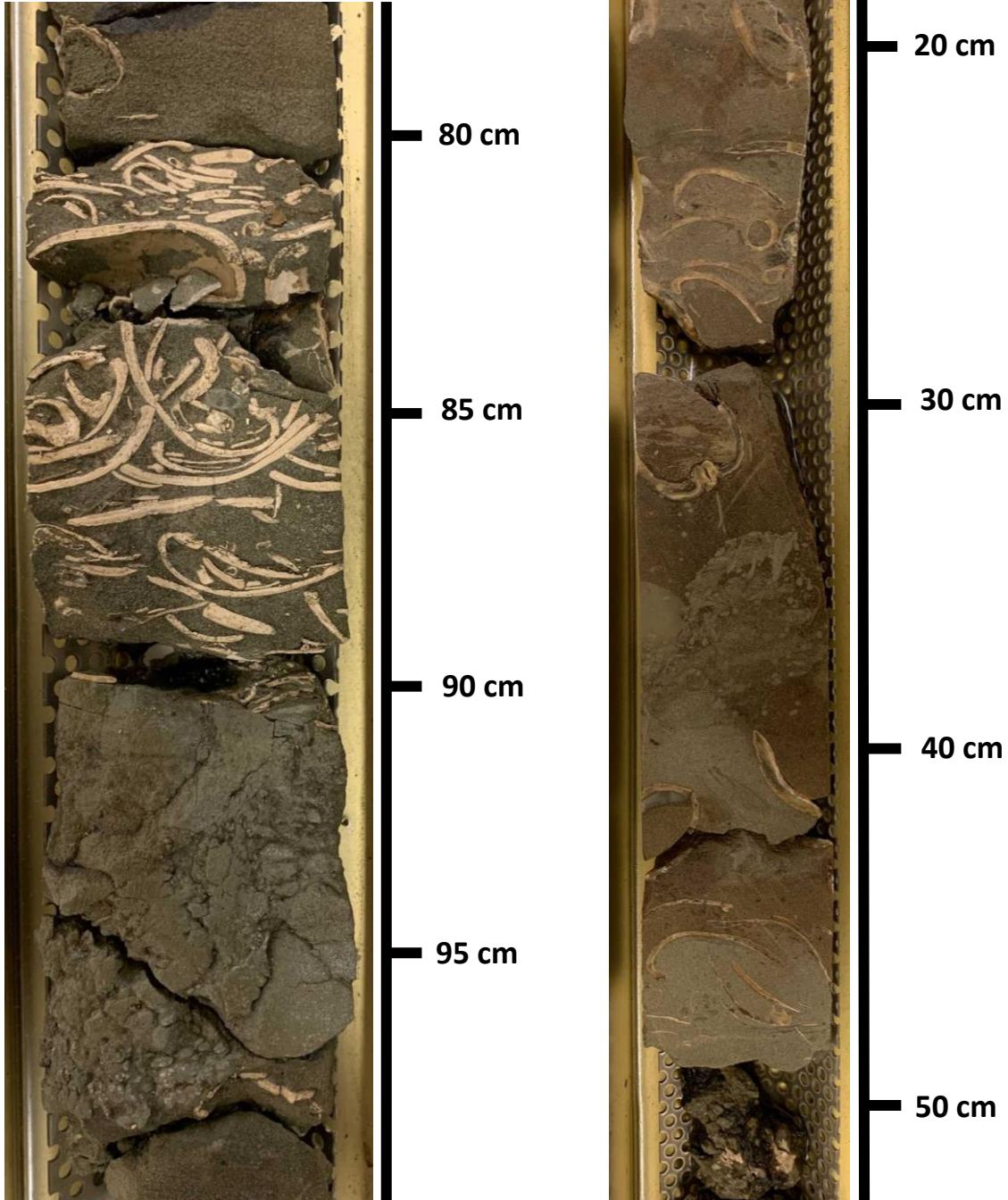
This facies consists of large shells in a sandstone or mudstone matrix (Figure 24). The colour of the matrix is mostly a greenish grey but in some places it is mottled. The shells are mostly whole or broken into large pieces, and their orientation varies from horizontal to vertical. The beds are a few centimetres to several decimetres thick. This facies has sharp or gradual boundaries and is often underlain and overlain by massive or slightly laminated sandstone.

### *Interpretation*

This facies is characteristic of lagoonal deposits. The shells and pieces of shells are large which indicates that they have not been transported very far which in turn indicates calm conditions. Mottling is typical of soil formation which indicates that the deposit was exposed to air at some point and therefore must have been deposited very close to land.

(a) 7230/05-U-09  
43-44 m

(b) 7230/05-U-09  
30-31 m



**Figure 24:** Core photos showing shell beds. (a) Large shells in a greenish grey sand matrix. (b) large shells in a mottled and bioturbated muddy sandstone matrix.

## **Carbonate facies**

### *Description*

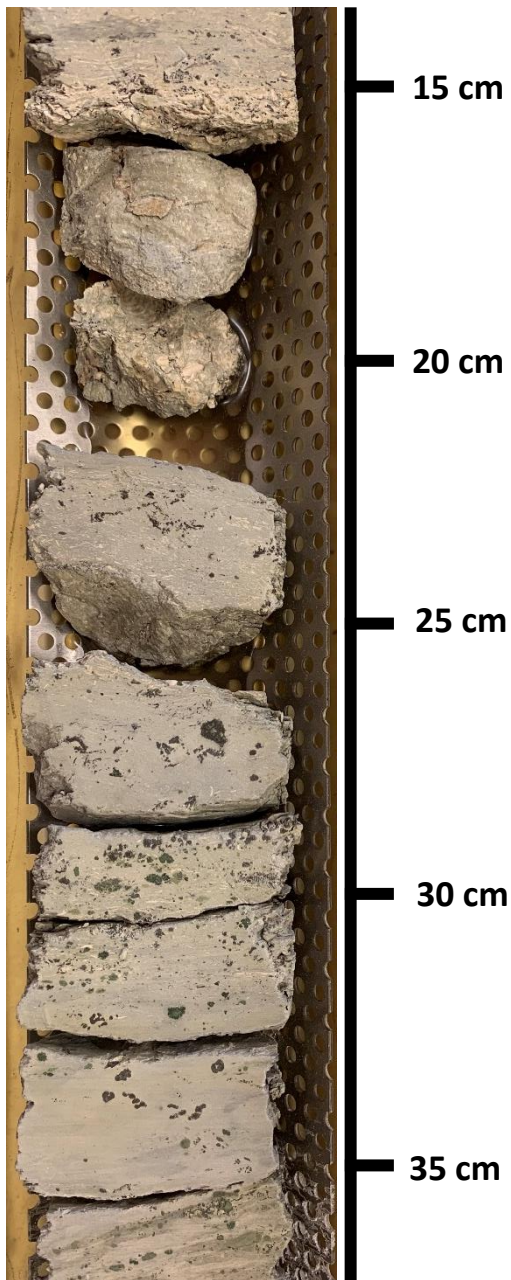
This facies is white to light grey coloured and it has a sharp lower boundary and a gradual upper boundary. It is about four and a half metres thick in core 7231/01-U-01 (Figure 39 a, d). The lower part of the carbonate is a mudstone with shell fragments (Figure 25a) that transitions to wackestone and then to packstone (Figure 25b). Further up it transitions back to wackestone and then mudstone. The carbonate overlies a black shale and is overlain by clastic laminated mudstone. This facies contains fossil fragments but no whole fossils.

### *Interpretation*

The fragmented fossils indicate that they are not in situ and that they have been transported some distance. The coarsening upwards from mudstone to packstone is characteristic of outer to mid carbonate ramp deposits (Nichols, 2009c). Gravity currents transport bioclastic debris on to the shelf and form mudstone deposits on the outer ramp and wackestone and packstone deposits on the mid shelf.



(a) 7231/01-U-01  
64-65 m



(b) 7231/01-U-01  
62-63 m

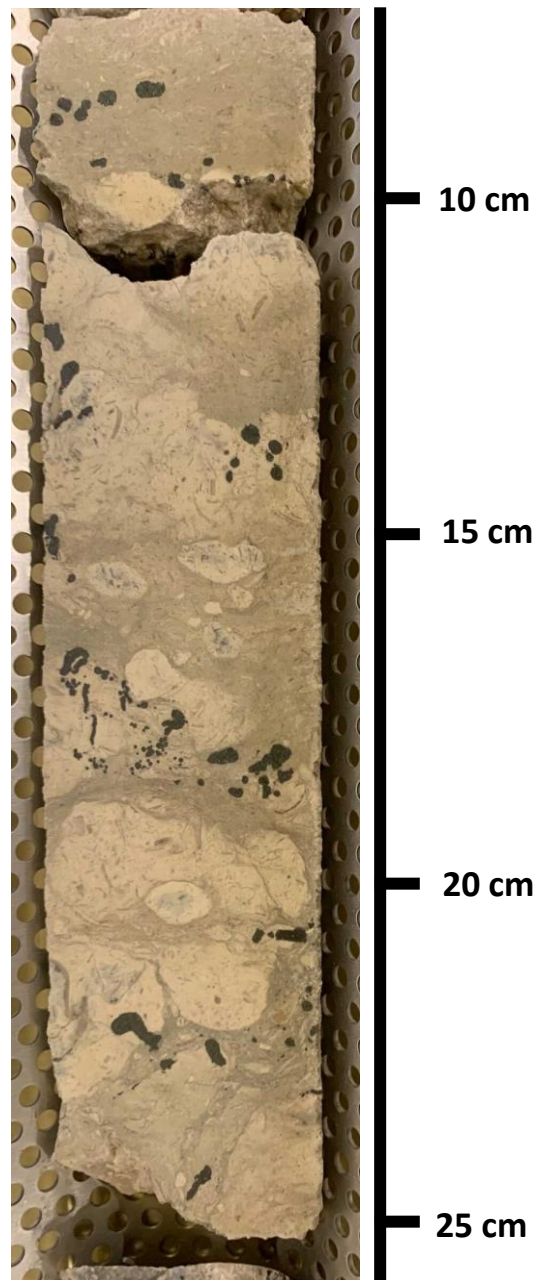


Figure 25: Core photos showing carbonates. (a) Mudstone gradually transitioning to wackestone. (b) Packstone.

## 4.2 Microstructures in mudstone

Five thin sections, one from laminated mudstone facies, one from slightly bioturbated clayey mudstone facies, one from bioturbated silty mudstone facies and two from the shale facies were looked at under the microscope to look at possible microstructures.

### **Laminated mudstone**

#### *Description*

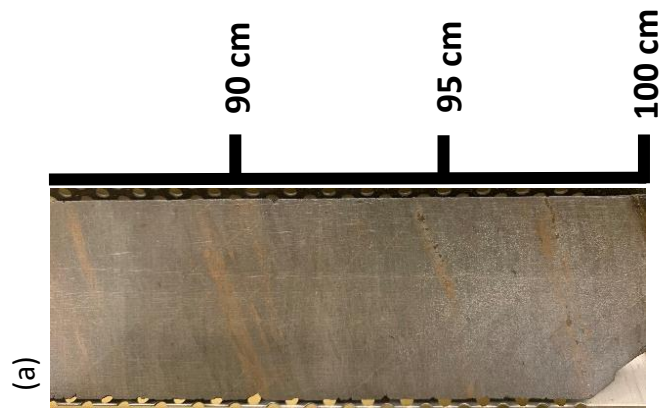
This facies has a dark brown colour and consists mainly of clay and silt. It is laminated with some dark discontinuous clay laminae (Figure 26).

#### *Interpretation*

Silt separates from mud under transport which results in differential settling. Silt deposits first while clay accumulates and eventually deposits rapidly and form a clay layer (Bowen and Stow, 1978; Yawar and Schieber, 2017). Another way of getting lamination in mud is by the deposition of ripples in mud, from wave-enhanced sediment-gravity flows (WESGFs), that are compacted post deposition and therefor appear horizontal (Macquaker et al., 2010). This facies however dos not have the characteristic three part stratification shown in Macquaker et al. (2010) which make it unlikely that this facies is the result of WESGFs.



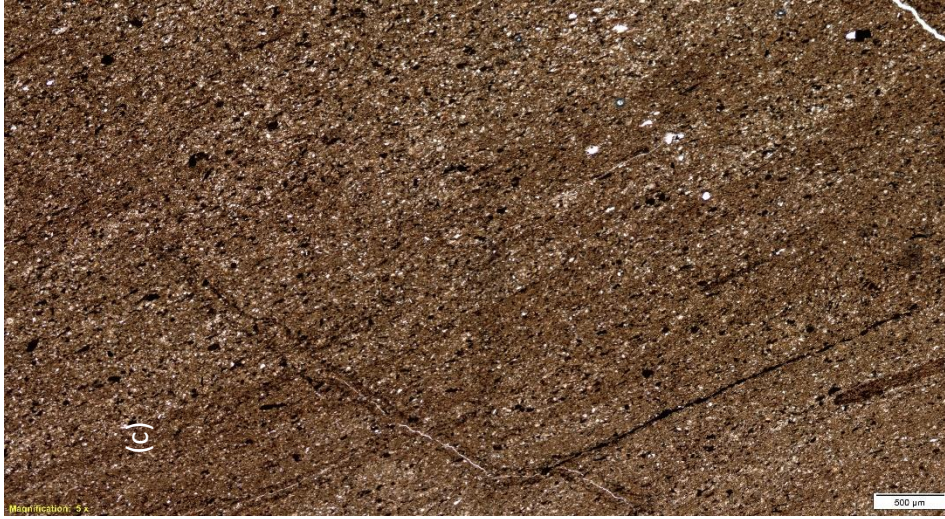
7231/01-U-01, 42,96m



(a)



(b)



**Figure 26:** Laminated mudstone with siderite or pyrite laminae (a) core photo of the interval from which the thin section was taken, (b) full scan of the thin section (5x magnification),

### **Slightly bioturbated clayey mudstone**

#### *Description*

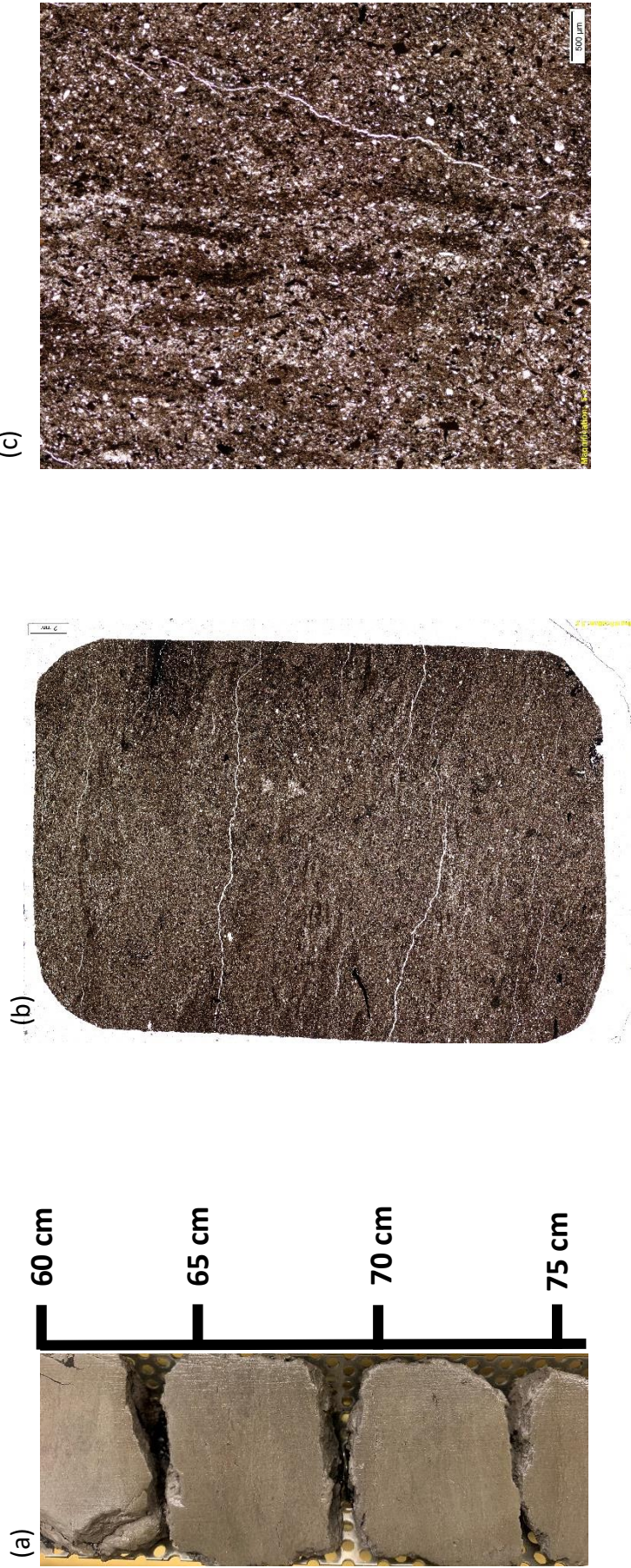
This facies appears massive in the core probably due to the dark colour (Figure 27a). It contains both silt and clay. When this facies is looked at under the microscope some discontinuous patches and laminae of mudstone are revealed (Figure 27b, c).

#### *Interpretation*

This facies was deposited through suspension settling and bioturbated slightly post deposition.



7231/01-U-04, 70,59m



**Figure 27:** Slightly bioturbated clayey mudstone (a) core photo of the interval from which the thin section was taken, (b) full scan of the thin section (5x magnification), (c) photomicrograph showing dark discontinuous patches of mud in a slightly lighter coloured mudstone (5x magnification).

## **Bioturbated silty mudstone**

### *Description*

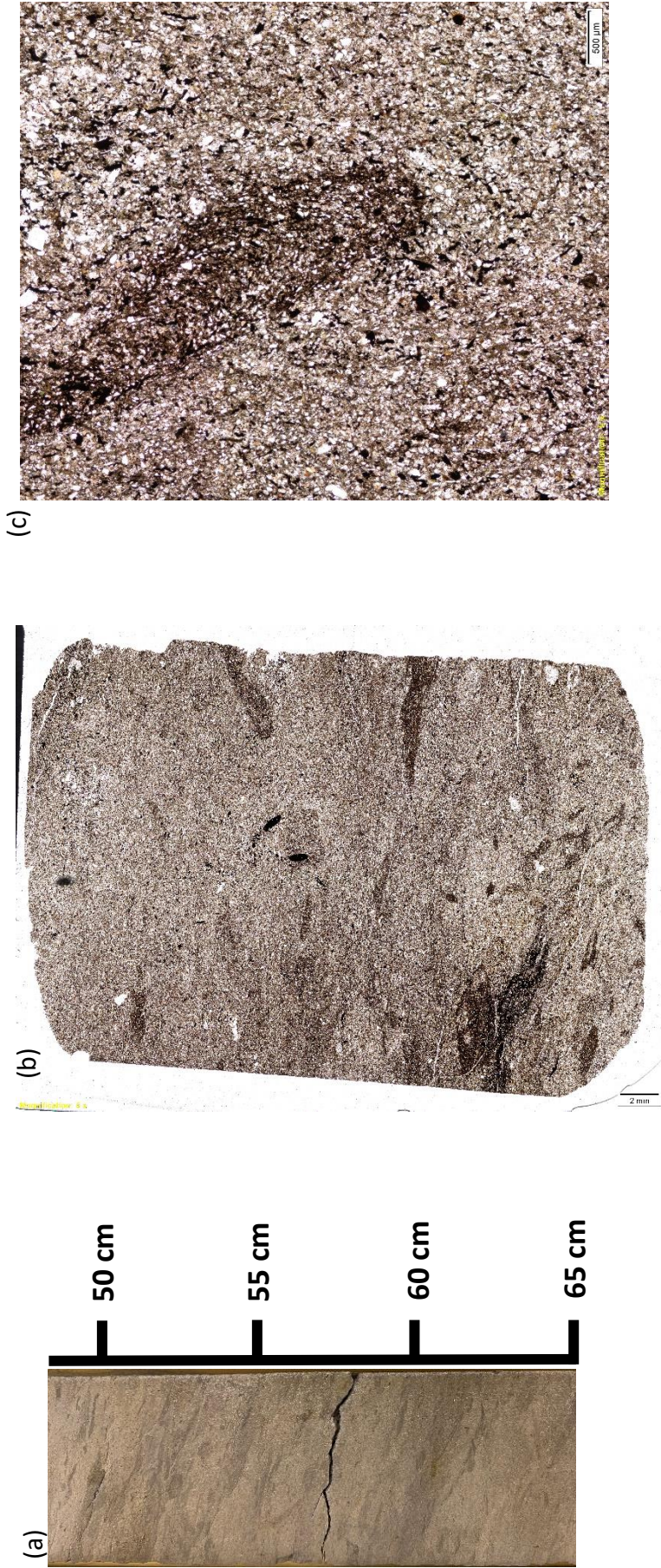
This facies has a light grey colour and consists of silt and some sand. It contains many dark discontinuous patches of clayey mud (Figure 28). These patches have no preferred orientation.

### *Interpretation*

The patches are likely burrows. This facies was deposited through suspension settling and bioturbated post deposition.



7231/01-U-04, 74,59m



**Figure 28:** Bioturbated silty mudstone (a) core photo of the interval from which the thin section was taken, (b) full scan of the thin section (5x magnification), (c) photomicrograph showing a dark clay rich burrow in a light grey coloured siltstone (5x magnification).

## **Shale**

### *Description*

This facies is black and it is made up of very thin layers of clay (Figure 29 and Figure 30). It contains a few fossil fragments and a few pieces of a red/orange mineral (Figure 29c). There are also some silt enriched laminae in this facies (Figure 30c).

### *Interpretation*

The dark colour of this facies could mean that it is rich in organic matter which indicates anoxic or dysoxic depositional conditions which suggests that this facies was deposited in a restricted basin. The mechanism of deposition was suspension settling. There are some silt enriched laminae in this facies that could be distal turbidites.

7231/01-U-01, 72,85m

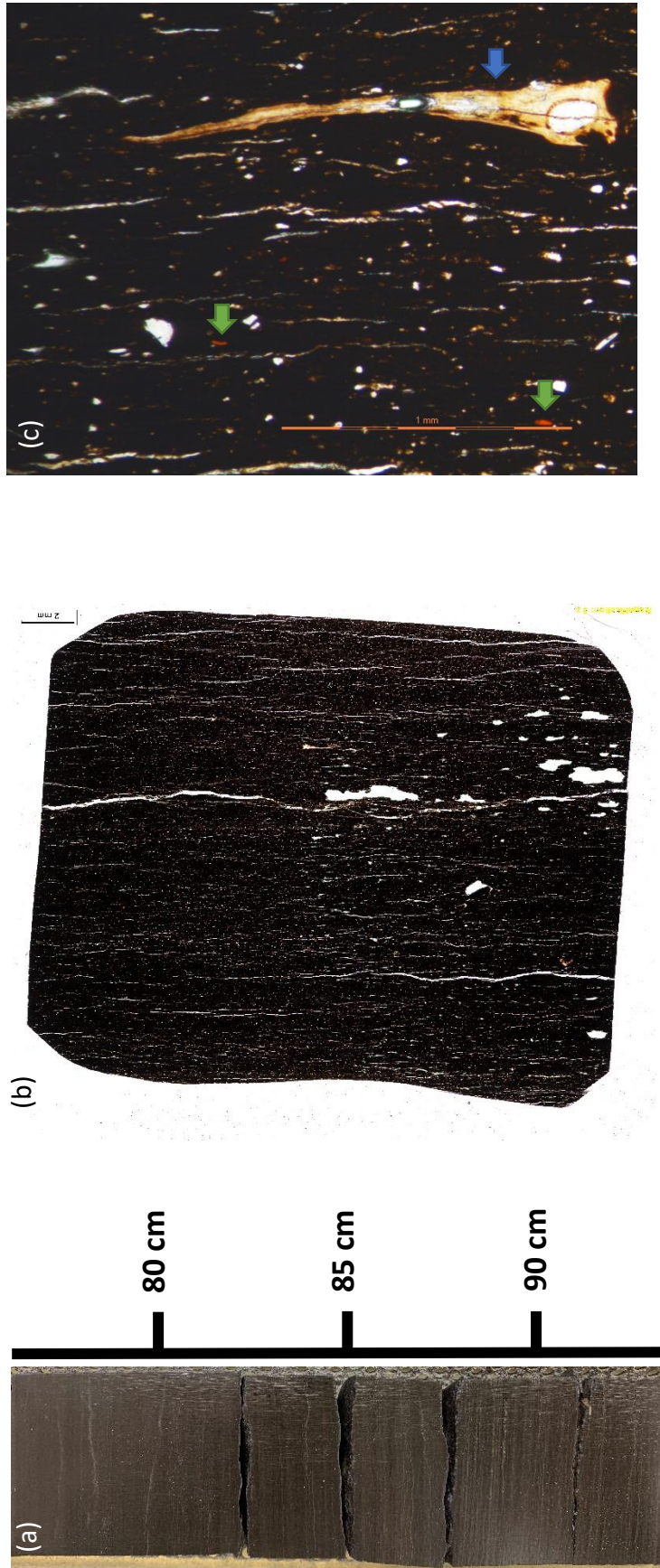
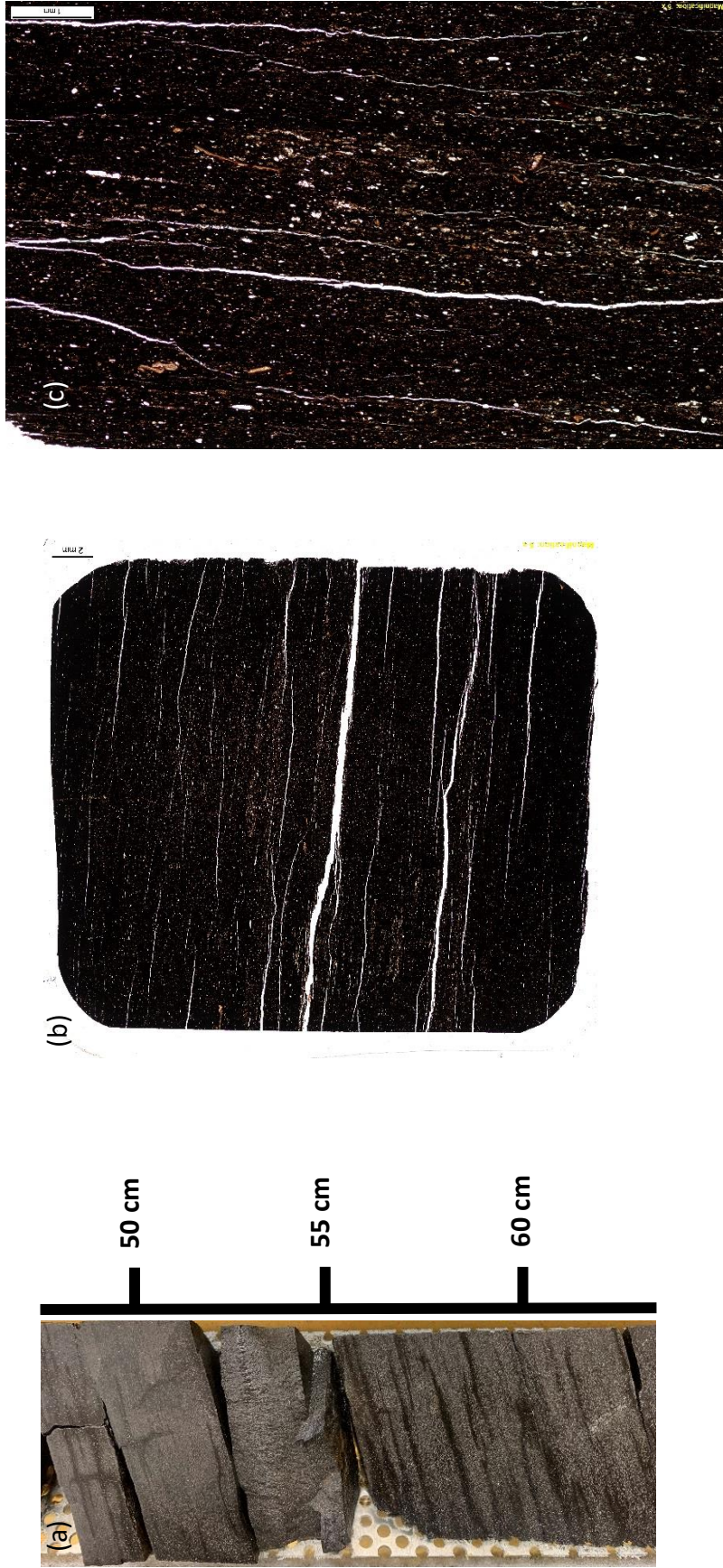


Figure 29: Black shale (a) core photo of the interval from which the thin section was taken, (b) full scan of the thin section (5x magnification), (c) scan showing a fossil fragment (blue arrow) and some red pieces of mineral (green arrows) in the black shale (5x magnification).



7230/05-U-02, 46,57m



**Figure 30:** Black shale (a) core photo of the interval from which the thin section was taken, (b) full scan of the thin section (5x magnification), (c) scan showing silt enriched lamina (5x magnification).



### 4.3 Graphical sedimentary logs, descriptions, and interpretations of all cores

The cores were described and interpreted, and graphical sedimentary logs were made for each core. The bioturbation intensity, heterolithics, mottling, facies and depositional environments were plotted against core depth. The interpretations of depositional environments in this section are based on observations and facies interpretations that are presented in section 3.1 Facies and section 3.2 Microstructures in mudstone.

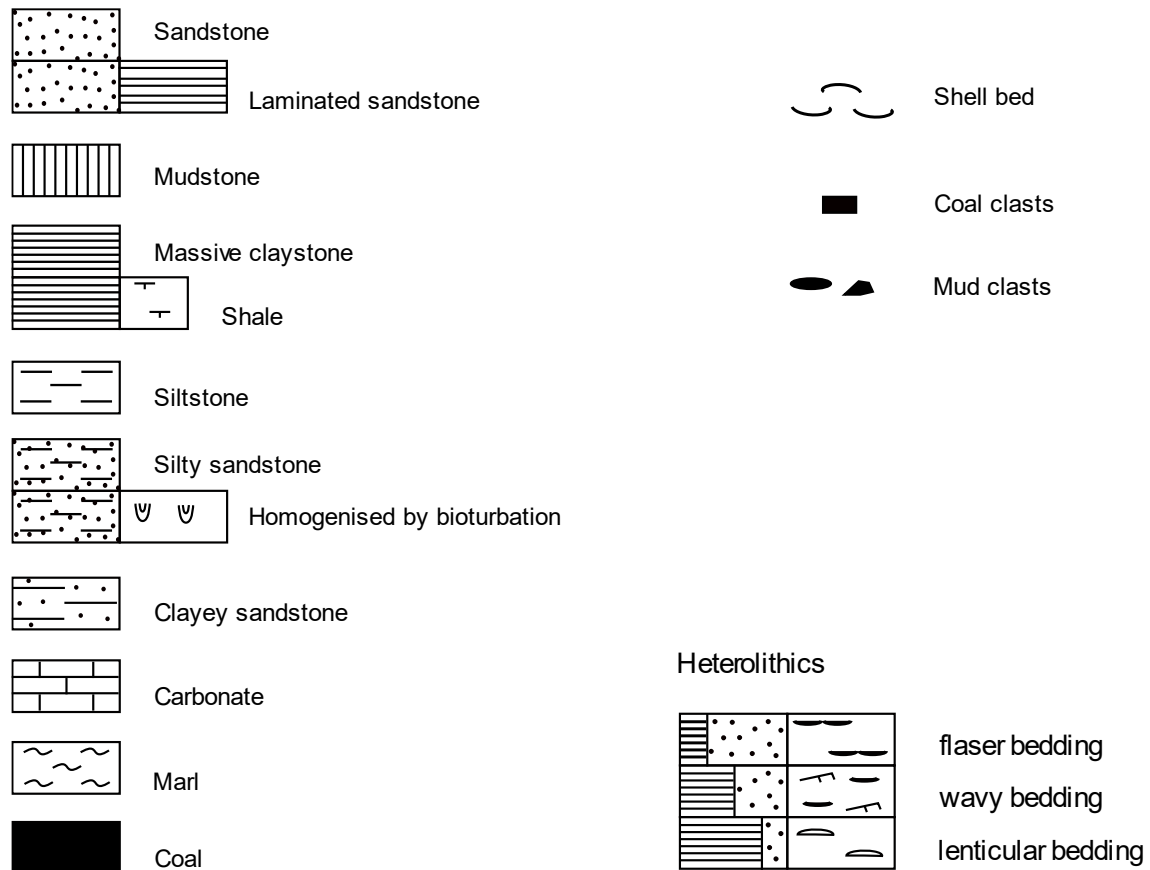


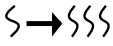

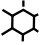













Figure 31: Legend (Lithology)

## Sedimentary structures and fossil content

	Rootlets		Glaucinite
	Bioturbation		Fossil
	Mottling		Fossilfragment
	Slump		Gastropod
	Current ripple		Bivalve
	Wave ripple		Ammonite
	Water escape structure		Cone in cone
			Concretions

**Figure 32:** Legend (structures)

	Mudstone		Mottled clay
	Sandstone		Clay
	Heterolithic		Coarsening upwards sandstone
	Muddy sandstone		Fining upwards sandstone
	Laminated mudstone		Distorted heterolithic
	Silty mudstone		Chaotic facies
	Rippled sandstone		Conglomerate
	Silt		Black shale
	Coal		Marl
	Carbonate		Shell bed
	Slightly bioturbated mudstone		

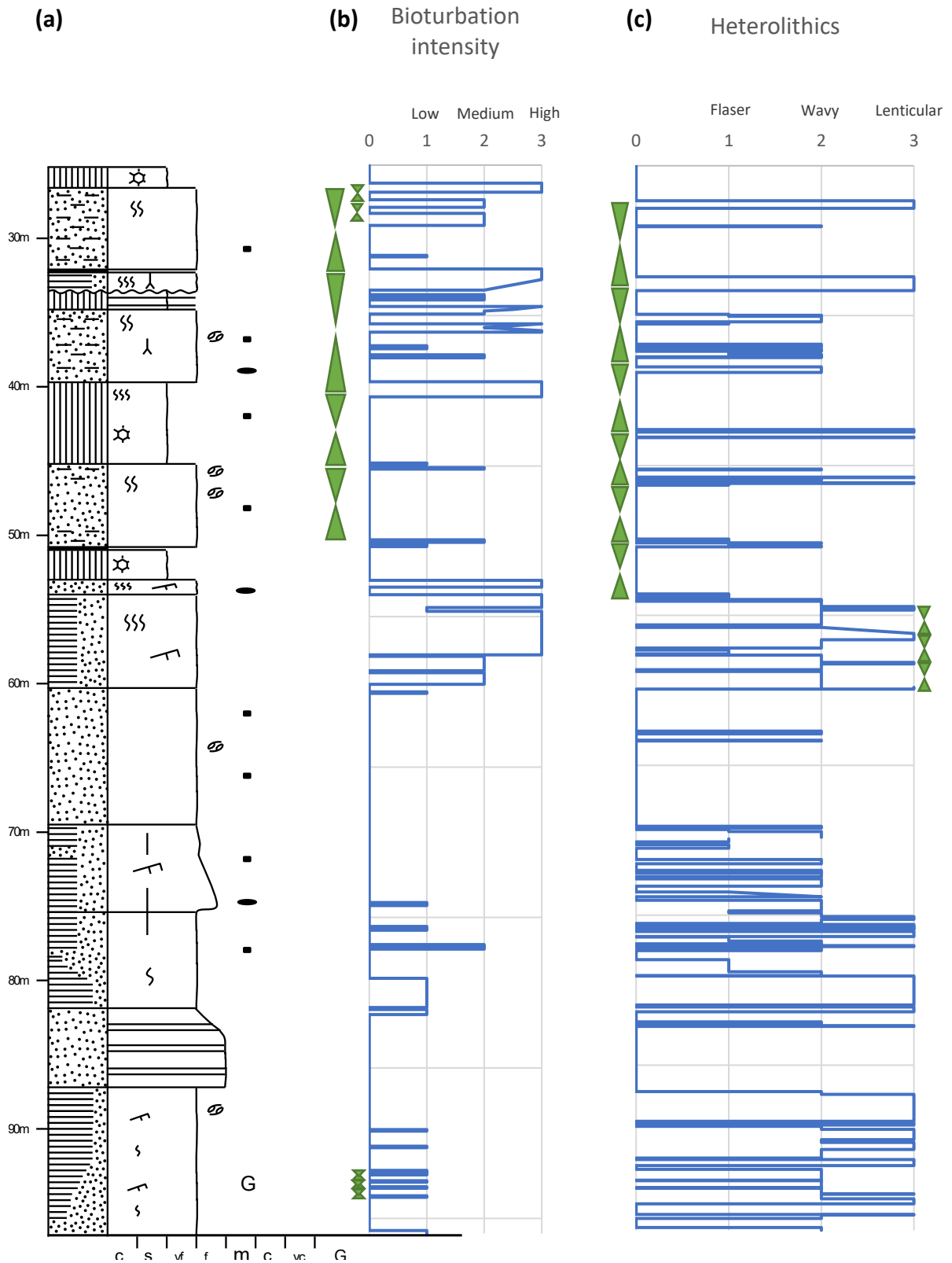
**Figure 33:** Legend (facies)

### **Core 7230/05-U-06**

The results for core 7230/05-U-06 are shown in Figure 34. The legends for this and the following cores are shown in Figure 31, Figure 32 and Figure 33.

This core was deposited as part of the Kobbe Formation in the Middle to Late Anisian (Bugge et al., 2002). It shows an overall regression where the depositional environment changes from inner shelf to coastal. This core consists of muddy heterolithics, interpreted as inner shelf deposits, overlain by sandstones, interpreted as shoreface deposits, followed by three cycles of gradual transition from heterolithics, interpreted as tidal deposits, to fining upwards sandstones with rootlets and coal and then mottled clay, interpreted as coastal deposits, stacked on top of each other, as shown in Figure 34 e and f. There is an overall increase in bioturbation intensity towards the top of the core as the environment becomes shallower. These interpretations of depositional environments are the same as in Bugge et al. (2002).

There seem to be cyclic variations in both bioturbation intensity and in the clay content in the heterolithics throughout this core and it looks like the bioturbation intensity is high when the clay content in the heterolithics is high. There are also some cyclic variations in the mottling in this core but only in a limited part.





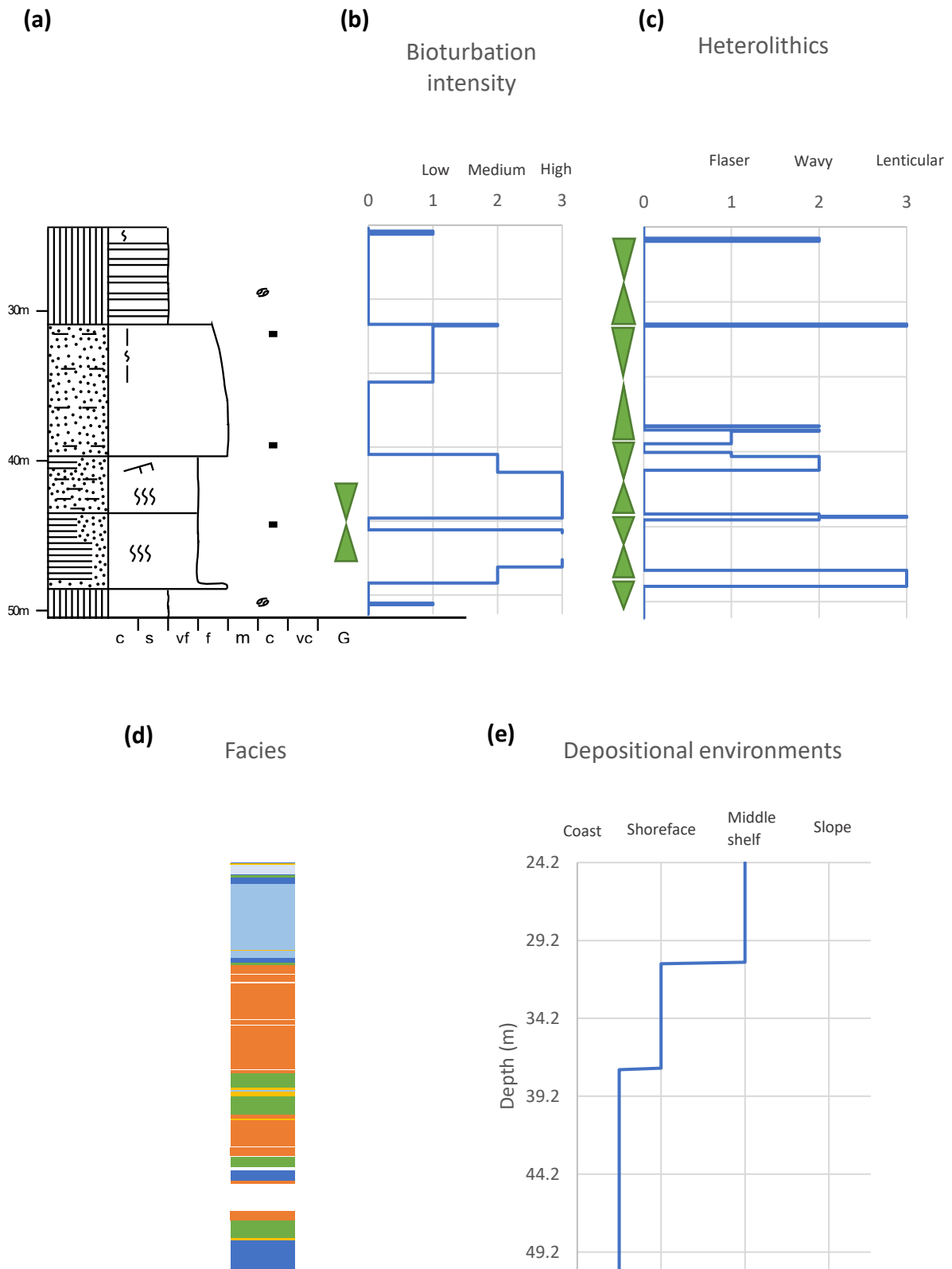
### **Core 7230/05-U-05**

The observations from core 7230/05-U-05 are shown in Figure 35.

The rocks in this core were deposited as part of the Kobbe Formation in the Late Anisian (Bugge et al., 2002). This core shows an overall transgression where the depositional environment changes from tidal to middle shelf. The core consists of heterolithics interpreted as tidal deposits overlain by muddy sandstones interpreted as shoreface deposits that are overlain by mudstones interpreted as middle shelf deposits (shown in Figure 35d and e). These interpretations of depositional environments are the same as in Bugge et al. (2002).

There is an overall decrease in bioturbation intensity towards the top of the core as the depositional environment becomes deeper (Figure 35b). There are some cyclic changes in both the bioturbation intensity and heterolithics.





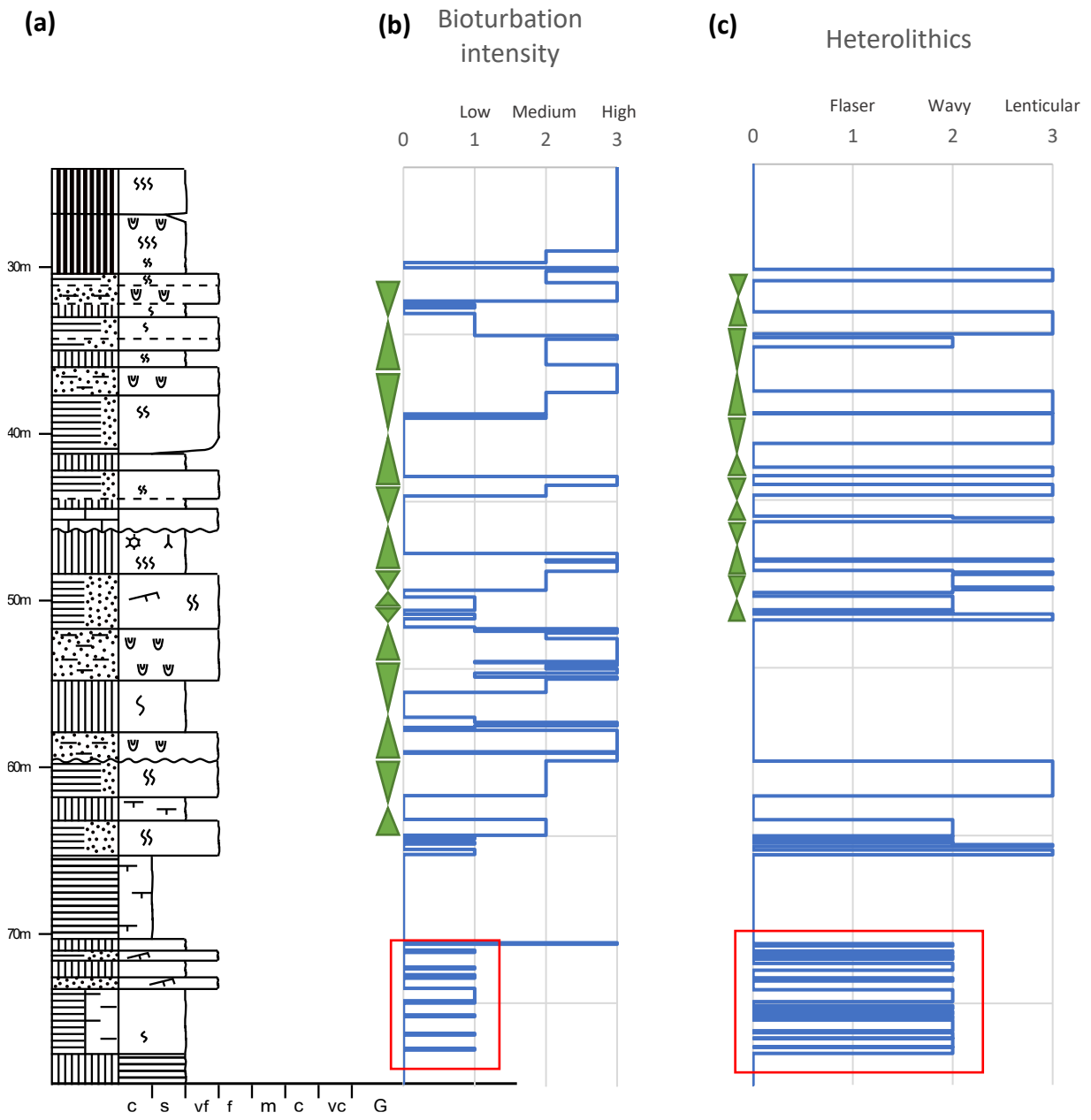
**Figure 35:** Core 7230/05-U-05. (a) overview log, (b) variations in bioturbation intensity, (c) heterolithics, (d) facies and (e) depositional environments. Cycles are indicated by the green arrows; increase or decrease in bioturbation intensity in (b) and increase or decrease in amount of mud in (c).

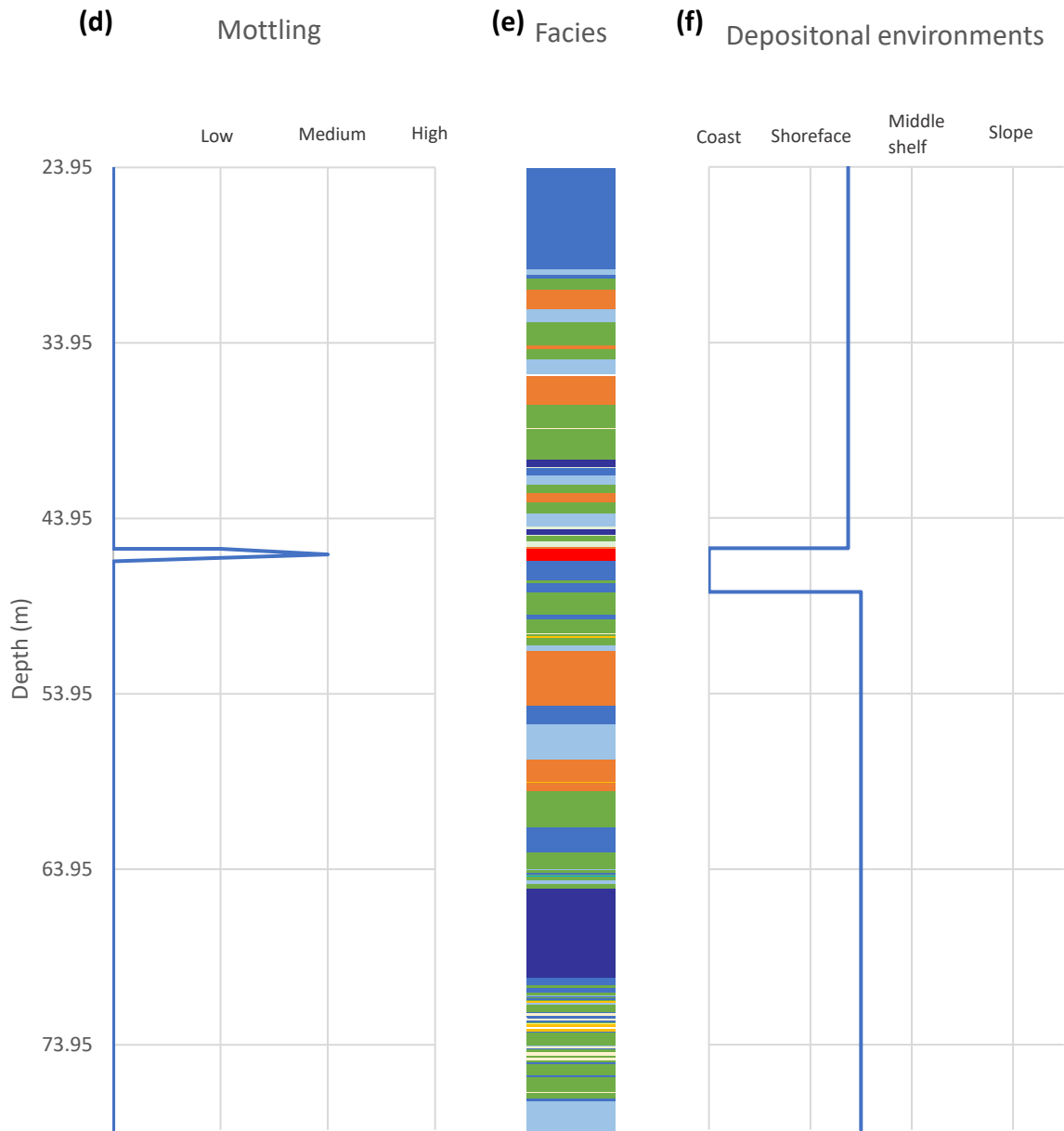
## **Core 7230/05-U-04**

The results for core 7230/05-U-04 are shown in Figure 36.

The rocks in this core are part of the Snadd Formation and were deposited in the Ladinian (Bugge et al., 2002). The core shows a regression followed by a transgression. It consists of mudstones and muddy heterolithics, interpreted as inner shelf deposits, overlain by mottled clay, interpreted as coastal deposits, overlain by mudstones and muddy heterolithics, interpreted as inner shelf deposits, shown in Figure 36e and f. These interpretations of depositional environments are the same as in Bugge et al. (2002).

This core contains mostly mudstones and heterolithics and has a low sandstone content. There are cyclic variations in the bioturbation intensity and the heterolithics throughout the core. There are very clearly cyclic changes in bioturbation intensity, heterolithics and facies below 70 metres in this core. The facies also vary considerably in the same parts of the core where the bioturbation intensity and heterolithics vary.





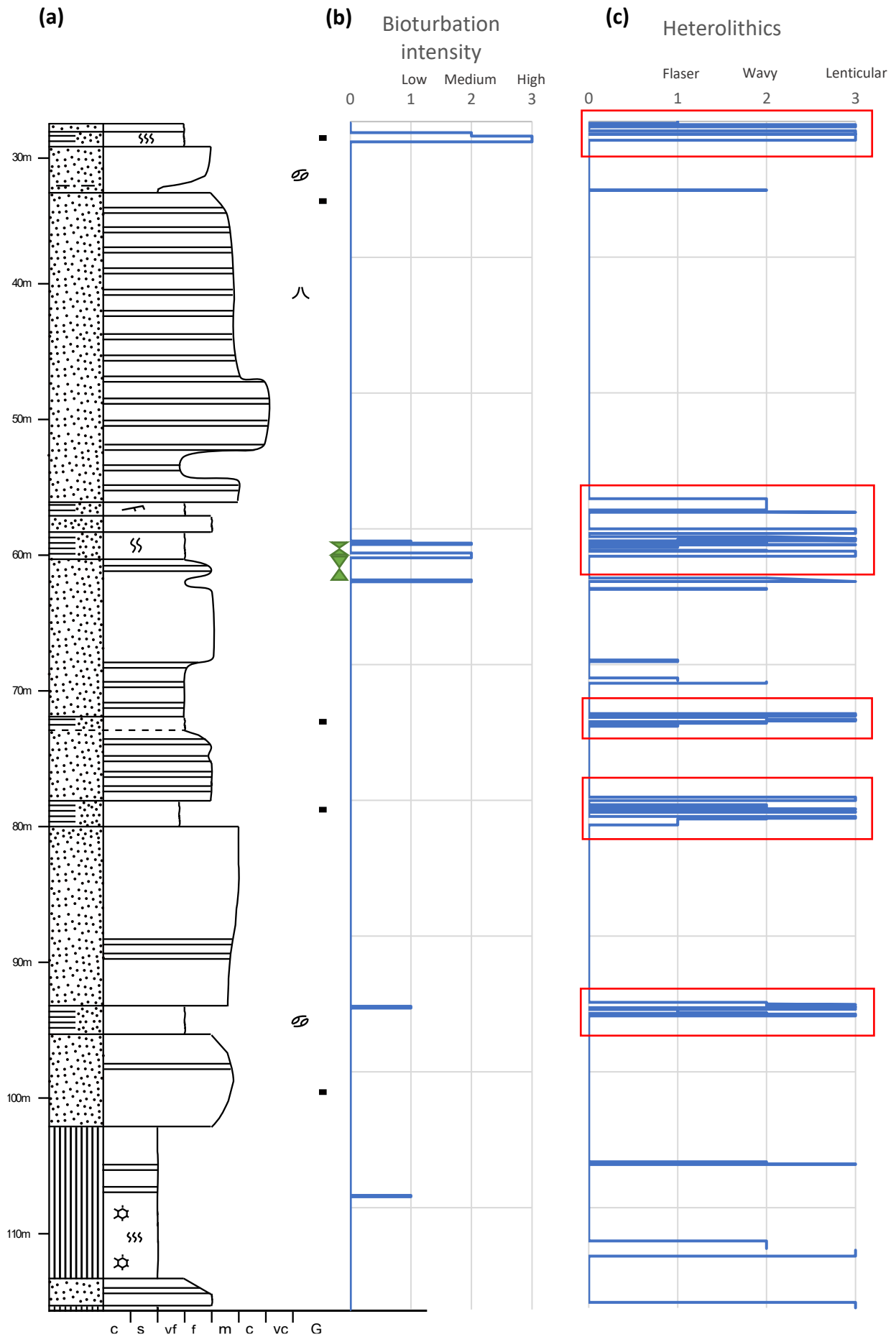
**Figure 36:** Core 7230/05-U-04. (a) overview log, (b) variations in bioturbation intensity, (c) heterolithics, (d) mottling, (e) facies and (f) depositional environments. Cycles are indicated by the green arrows; increase or decrease in bioturbation intensity in (b) and increase or decrease in amount of mud in (c). The red boxes indicate cycles that are too small to indicate with green arrows.

### **Core 7230/05-U-03**

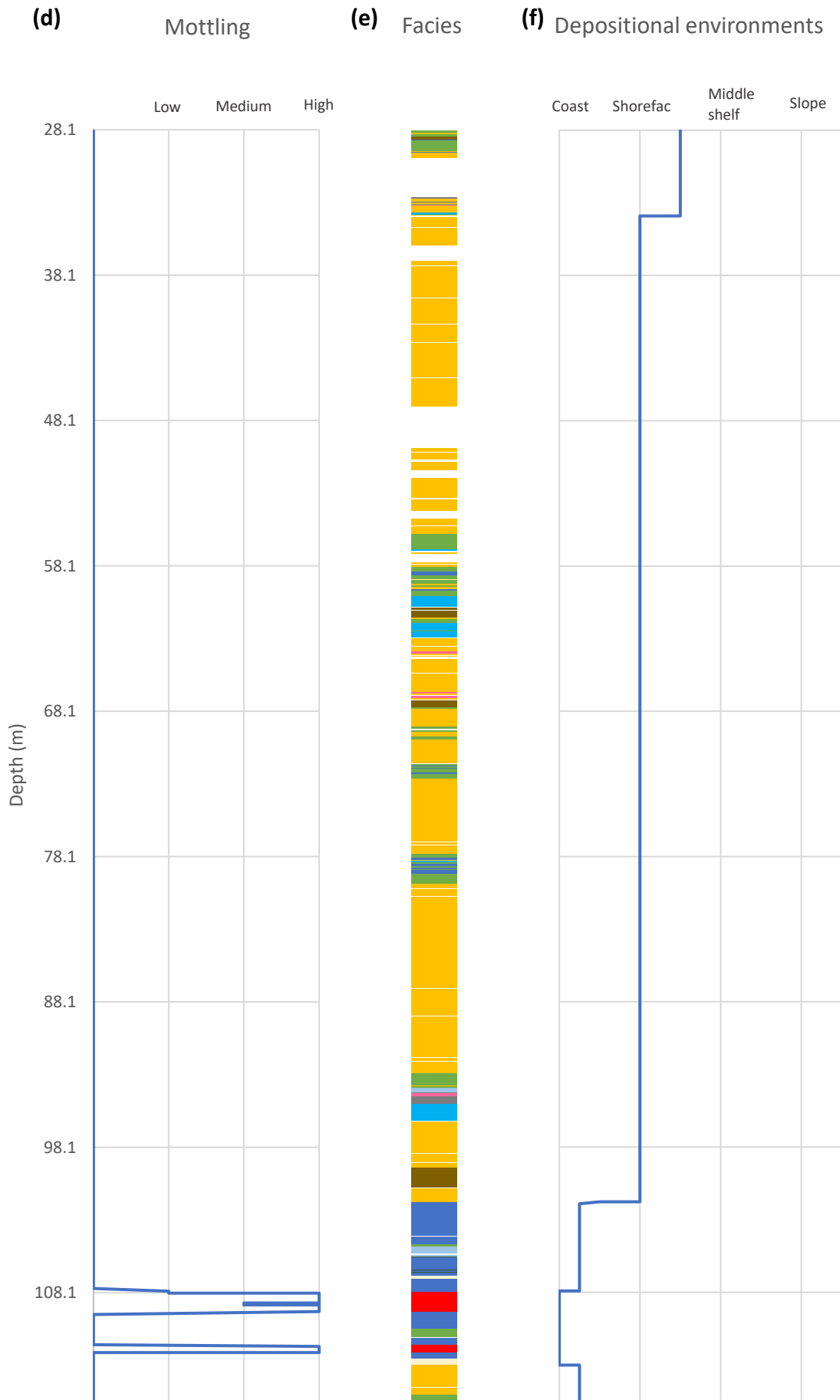
The results for core 7230/05-U-03 are shown in Figure 37.

This core is part of the upper part the Snadd formation (deposited possibly in the Late Carnian to Early Norian), the Fruholmen Formation (deposited in the late Norian to Rhaetian) and the lower part of the Stø Formation (deposited in the Late Toarcian) (Bugge et al., 2002). It shows an overall transgression where the environment changes from coastal to inner shelf. This core consists of fining upwards sandstones and mottled clay, interpreted as coastal deposits, overlain by alternating thick layers of sandstone and thinner layers of heterolithics, interpreted as shoreface deposits, overlain by muddy heterolithics, interpreted as inner shelf deposits (Figure 37e, f). These interpretations of depositional environments are the same as in Bugge et al. (2002).

There are cyclic variations in the heterolithics throughout the core and some cyclic variations in the bioturbation intensity.







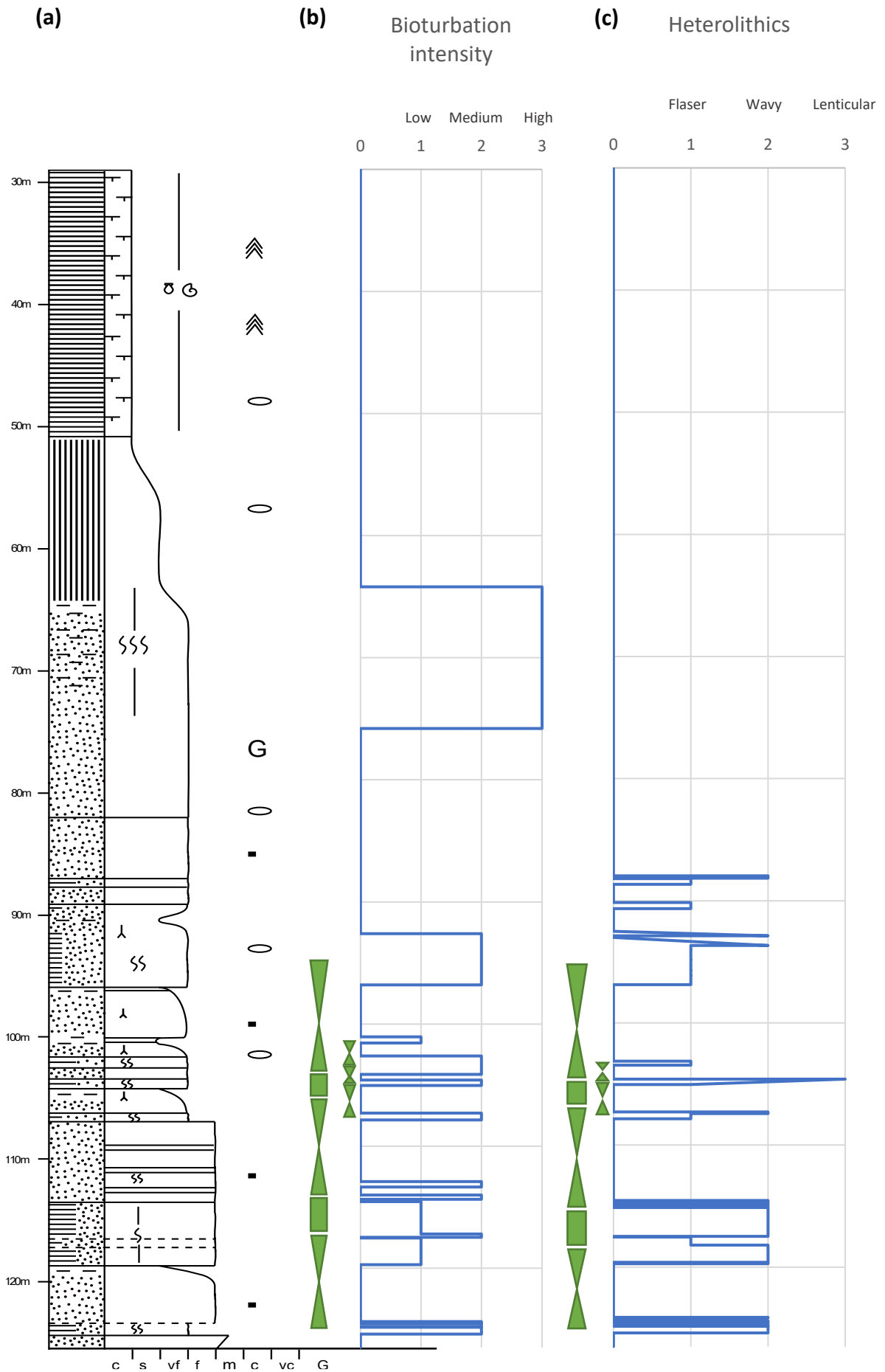
**Figure 37:** Core 7230/05-U-03. (a) overview log, (b) variations in bioturbation intensity, (c) heterolithics, (d) mottling, (e) facies and (f) depositional environments. Cycles in the bioturbation intensity are indicated by green arrows. The red boxes indicate cycles in the heterolithics which are too small to indicate with arrows.

## Core 7230/05-U-02

Figure 38 shows the results for core 7230/05-U-02.

This core is part the Stø Formation (deposited in the Late Toarcian possibly to Aalenian and possibly in the Bajocian), the Fugle Formation (deposited in the Early to Middle Bathonian, Late Bathonian and Early Callovian) and the Hekkingen Formation (deposited in the Late Oxfordian, Early Kimmeridgian and Late Kimmeridgian) (Bugge et al., 2002). It shows an overall transgression where the environment changes from coastal to anoxic basin. The core consists of two cycles of fining upwards sandstone with rootlets and pieces of coal, interpreted as coastal deposits, overlain by heterolithics, interpreted as tidal deposits, which are overlain by sandstones, interpreted as shoreface deposits, followed by mudstones, interpreted as shelf deposits, overlain by black shale, interpreted as anoxic basin deposits (Figure 38d, e). These interpretations of depositional environments are the same as in Bugge et al. (2002).

There are cyclic variations in the bioturbation intensity and heterolithics in the lower half of the core shown in Figure 38b, c. The bioturbation intensity appears to be high when the clay content in the heterolithics is high.



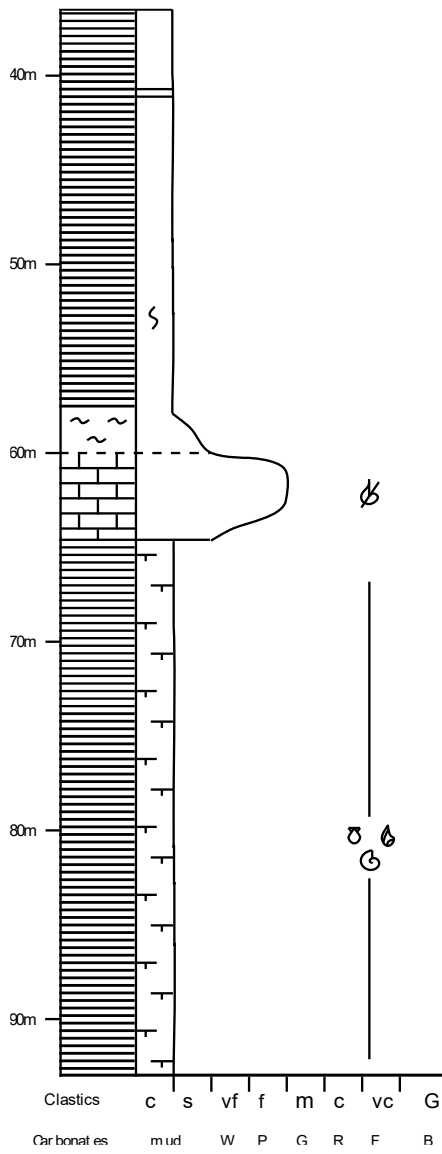


## **Core 7231/01-U-01**

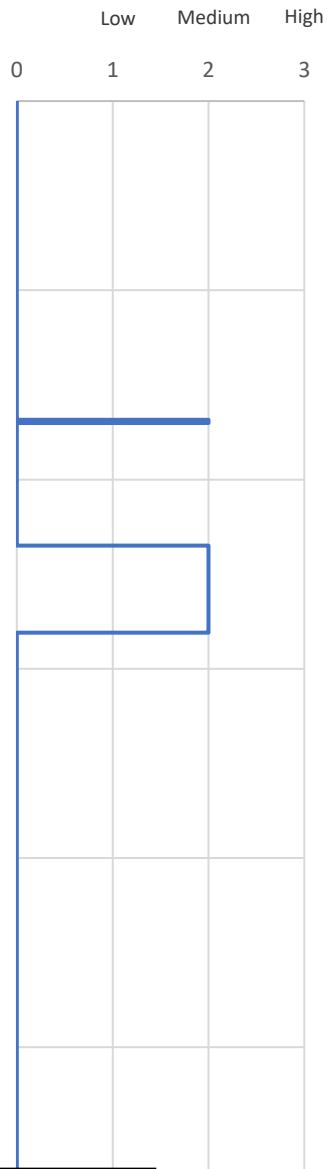
The results for core 7231/01-U-01 are shown in Figure 39.

This core is part of the Hekkingen Formation (deposited in the Oxfordian, Kimmeridgian and Early Volgian), the Klippfisk Formation (deposited in the Early Hauterivian) and the Kolje Formation (deposited in the Early Barremian) (Bugge et al., 2002). The black shales of the Hekkingen Formation, interpreted as anoxic basin deposits, are abruptly overlain by about 5 metres of carbonates of the Klippfisk Formation interpreted as inner shelf carbonate ramp deposits which are overlain by mudstones of the Kolje Formation interpreted as outer shelf deposits (shown in Figure 39c). So the core shows a regression followed by a transgression (Figure 39d). These interpretations of depositional environments are the same as in Bugge et al. (2002). There are no visible cyclic changes in any of the indicators in this core.

(a)



(b) Bioturbation intensity

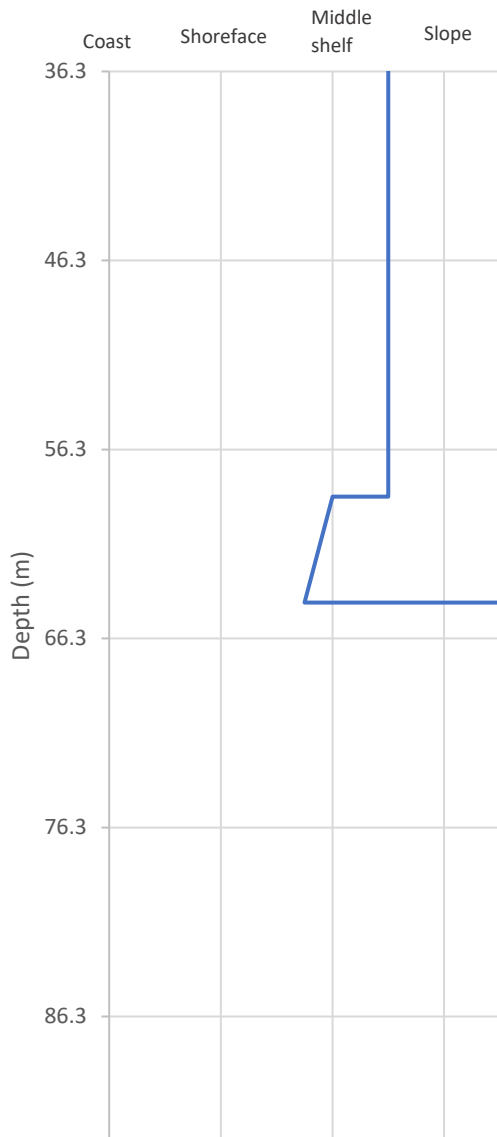


(c) Facies





**(d)** Depositional environments



**Figure 39:** Core 7231/01-U-01. (a) overview log, (b) variations in bioturbation intensity, (c) facies and (d) depositional environments.

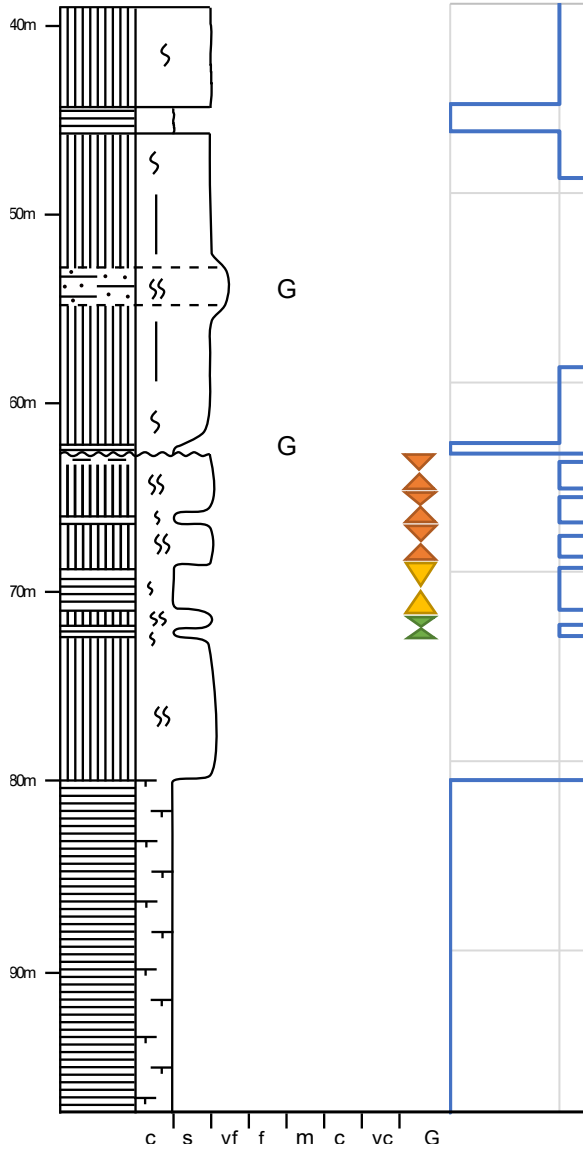
## **Core 7231/04-U-01**

The observations from core 7231/04-U-01 are shown in Figure 40.

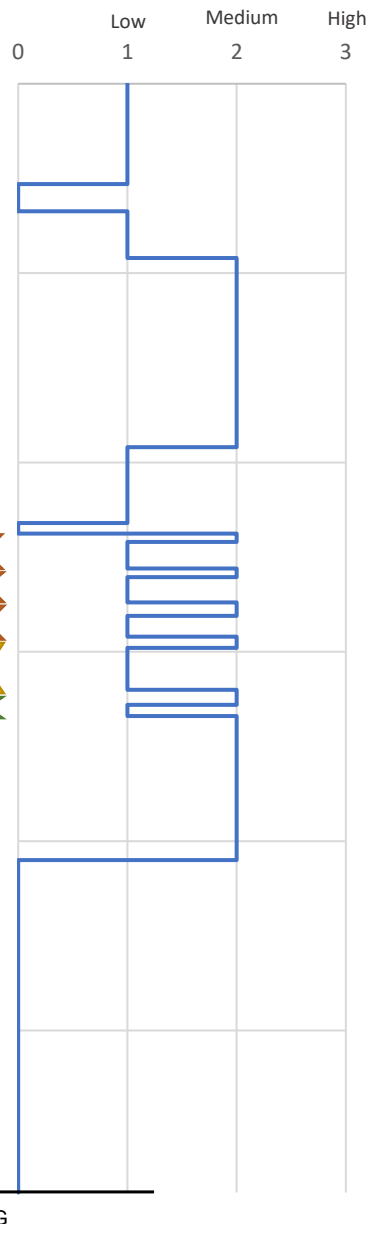
This core is part of the Kolje Formation (deposited from the Aptian to Early Albian) and the Kolmule Formation (deposited in the Middle Albian). It shows a small sea level fall followed by a small sea level rise. It consists of clayey mudstones interpreted as outer shelf deposits overlain by mudstones interpreted as middle shelf deposits overlain by siltier mudstones interpreted as inner shelf deposits with an erosive upper boundary overlain by mudstones interpreted as middle shelf deposits (Figure 40). These interpretations of depositional environments are the same as in Bugge et al. (2002).

There is very little variation in facies in this core but the bioturbation intensity varies considerably. Between 60 and 75m there are five cycles of increasing and decreasing bioturbation intensity.

(a)



(b) Bioturbation intensity

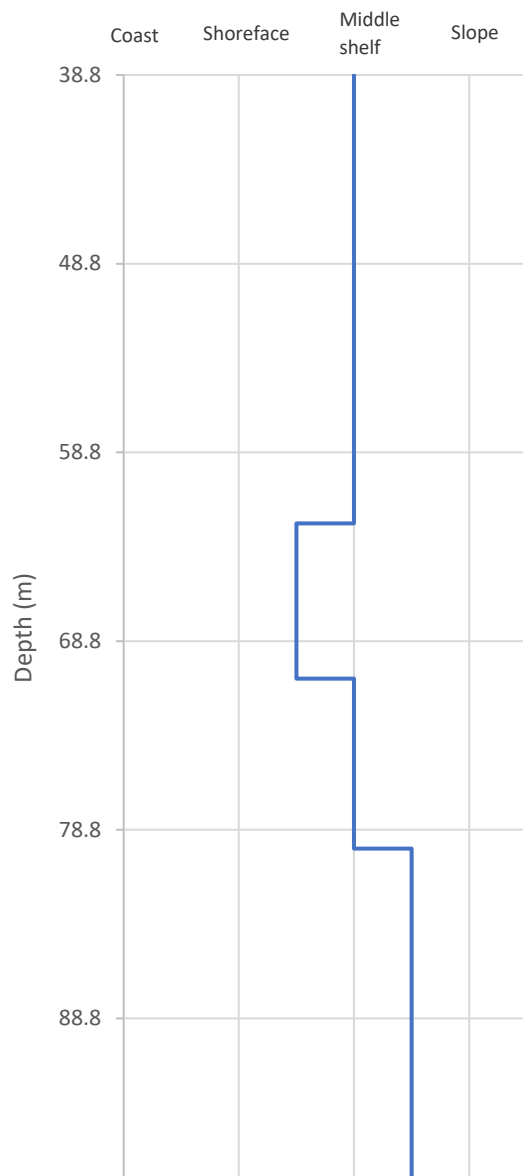


(c) Facies



(d)

### Depositional environments



**Figure 40:** Core 7231/04-U-01. (a) overview log, (b) variations in bioturbation intensity, (c) facies and (d) depositional environments. The green arrows indicate a 200ka cycle, the yellow arrows indicate a 400ka cycle and the orange arrows indicate tree 260ka cycles.

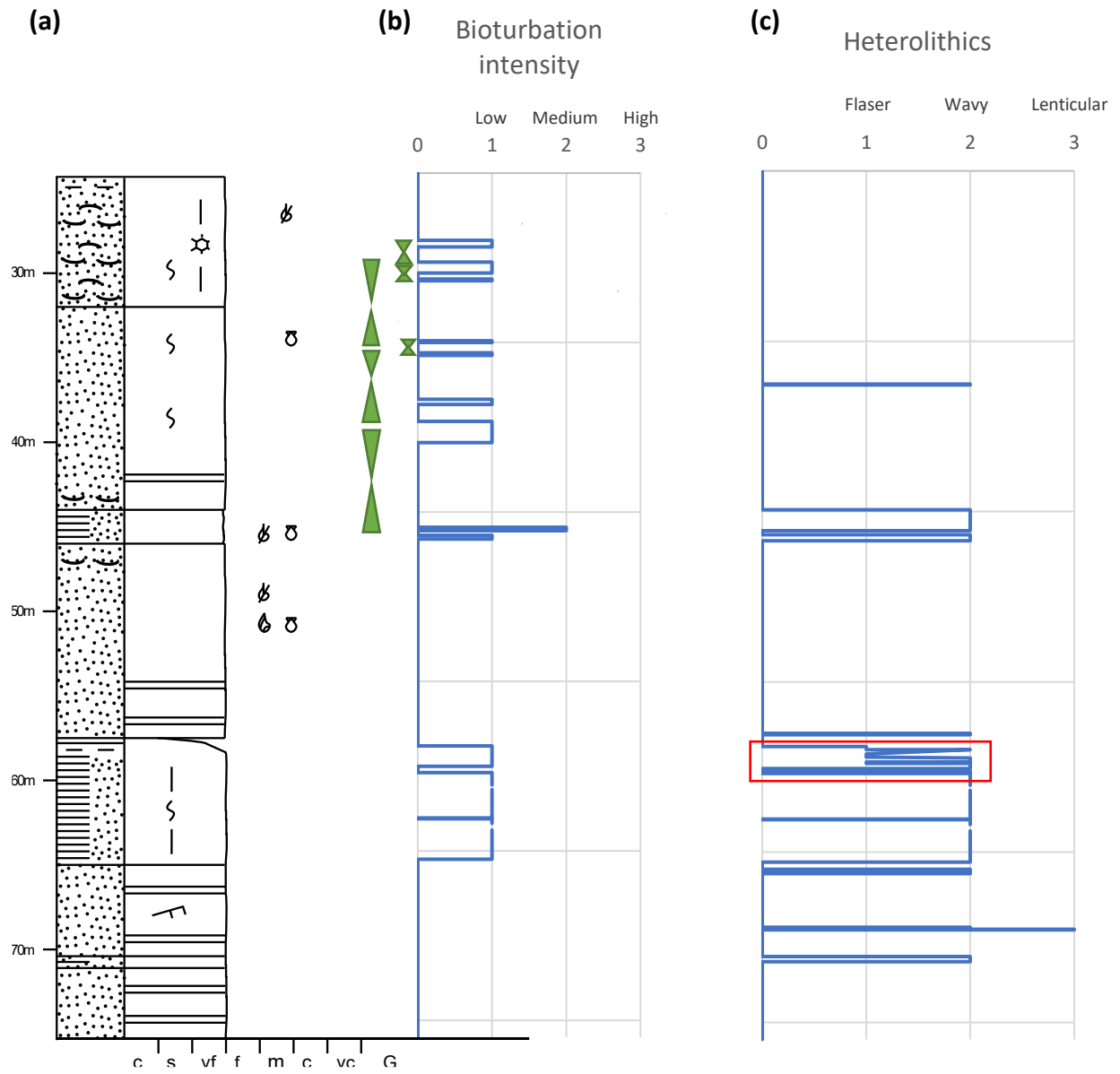
### **Core 7230/05-U-09**

The results for core 7230/05-U-09 are shown in Figure 41.

This core is part of the Kolmule Formation and was deposited from Late Albian to Early Cenomanian (Bugge et al., 2002). Figure 41f shows that this core shows an overall regression and consists of sandstones interpreted as shoreface deposits overlain by muddy heterolithics interpreted as inner shelf deposits followed by two cycles of sandstones, interpreted as shoreface deposits, overlain by shell beds, interpreted as lagoonal deposits, stacked on top of each other. These interpretations of depositional environments are the same as in Bugge et al. (2002).

This core consists mainly of sandstones, heterolithics and shell beds as shown in Figure 41e. There are cyclic changes in the bioturbation intensity and heterolithics in parts of this core (Figure 41b, c).







## 5. Discussion

Small scale changes have been seen in coastal to inner shelf environments and in several different sedimentary structures and lithologies. Examples of such changes can be seen in Figure 42. The depositional environments were interpreted based on observations and facies interpretations. The interpretations here matches those in Bugge et al. (2002). The durations and possible causes of these changes will be discussed here.

### 5.1 Duration of the small scale variations

There are several different ways to determine cyclicity and a very common method for especially Milankovitch cyclicity is to use Fourier analysis (Kochhann et al., 2020; Marshall et al., 2017; Milana and Lopez, 1998; Williams, 1991). Fourier analysis was not used here because the cores are short and there are not enough variations in each core to obtain meaningful results with this method. The cycles found in these cores are also not continuous and often consist of many single cycles or intervals with only a few cycles. This is another reason that some of the standard methods could not be used, but by using the detailed biostratigraphy from Bugge et al. (2002) the durations could still be determined and therefore interpreted. Another way of finding indications of Milankovitch cyclicity is by looking at the ratios of thickness of the core (Olsen, 1990). This method is not used here because Bugge et al. (2002) presented a detailed biostratigraphy.

The durations of the small scale variations were found by using the sedimentation rates to translate thickness of change to duration of change. The sedimentation rates were calculated by dividing the thickness of the cores or parts of cores with approximate durations of sedimentation. The durations of deposition in the cores or part of the core were found using figure 6 in Bugge et al. (2002) (reproduced here in Figure 43). This figure was used instead of the most recent dates because the biostratigraphy was used by Bugge et al. (2002) to make a linear timeline which made it very easy to read the durations directly from the figure. When the ages were not clear the duration of deposition was found by multiplying the duration of the stage with the duration of deposition/duration of the stage ratio. For example, in the case of core 7230/05-U-06 which was deposited in the Anisian the height of the core and the height of Anisian was measured on the figure. The measured height of the core was divided by the measured height of the stage in the image to find the relationship between duration of the Anisian and the duration of deposition. This was then multiplied with the actual duration of the Anisian which was read directly from the figure. The duration of the cyclic changes was calculated for different observed structures and lithologies in different cores as indicated in Table 1.

There are cycles with a duration around 40ka in the lower part of core 7230/05-U-04 and the middle part of core 7230/05-U-03. This duration indicates that these cycles could be the result of obliquity. Cycles with a duration around 20ka were found in the lower parts of the cores 7230/05-U-06 and 7230/05-U-04, these cycles could be the result of precession (Table 1). Possible Milankovitch cycles have been found in the bioturbation intensity, heterolithics

and in the mottling. There are cyclic changes in the coastal to middle shelf environments and possible Milankovitch cycles in the inner shelf, shoreface and coastal environments. In the outer shelf to anoxic basin environments no cyclicity is visible in any of the sedimentary structures or lithologies.

In all the coastal to middle shelf environments including the tidal and middle shelf environments there are cycles that have very long durations. This can be seen in several of the cores. For example in core 7230/05-U-02 the heterolithics and bioturbation intensity show 890 ka cycles in coastal to shoreface environment (Figure 38), and in core 7231/04-U-01 the bioturbation intensity shows 200, 260 and 400ka cycles in the inner and middle shelf environment (Figure 40). There are also cycles that have durations that fall in between eccentricity and obliquity, as in core 7230/05-U-03, 7230/05-U-06 and 7230/05-U-09 where the heterolithics show 60-65 ka cycles in shoreface (Figure 37), coastal (Figure 34) and inner shelf (Figure 41) environments. These cycles may therefore have other origins than Milankovitch cycles; however it is possible that some of the long cycles may be long eccentricity cycles. Because dates from 2002 were used for the calculations of the durations of changes, the changes may have somewhat shorter or longer durations if calculated with more recent dates and could therefore be the result of Milankovitch cycles.

There are also cyclic changes in the depositional environments in core 7230/05-U-06 (Figure 34f) and 7230/05-U-02 (Figure 38 e). These changes have very long durations of about 750ka and 2Ma and could possibly be the result of long eccentricity cycles.

Cyclicity has been seen in some environments but not all of them. This might be because the sediments in the outer shelf to anoxic basin environments where no cyclicity has been observed consist mostly of mud. In such fine grained sediments, it is very hard to see any structures at all and they therefore often appear massive which makes any changes that might be in the sediments very hard to see. Lab analysis is needed to study small scale changes in these environments.

Many single cycles have been found in these cores and ascribing each of these cycles to Milankovitch on their own is probably not very reliable, but as this is something that is seen many times it might be more reliable collectively. There are often just a few cycles at a time and a reason for this could be rapid changes in environments. For example, just a few cycles occur when the environment changes from shoreface to tidal and back to shoreface at around 45 metres depth in core 7230/05-U-09 (Figure 41)

There are some uncertainties with the calculated duration of changes. The sedimentation rates used to determine the durations are based on the approximate duration of deposition, which is not based on the most recent dates. It was also assumed that the sedimentation rates did not change much during the deposition of each core which might not be the case. This could have affected the accuracy of the sedimentation rates and therefore the durations of the changes that were calculated. Nonetheless, all of these effects are probably

relatively small so even if the calculated durations of changes are slightly inaccurate the changes could still be the result of Milankovitch cycles.

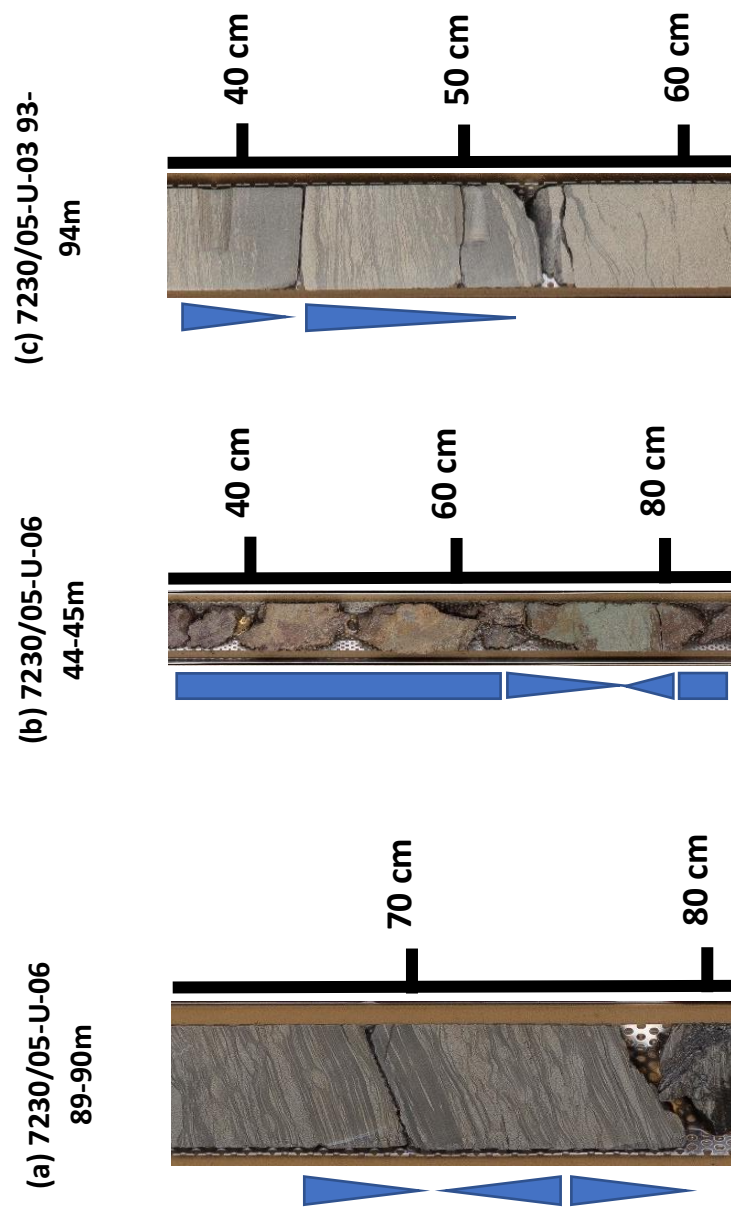


Figure 42: Examples of small scale changes in (a) bioturbation intensity, (b) mottling and (c) heterolithics.

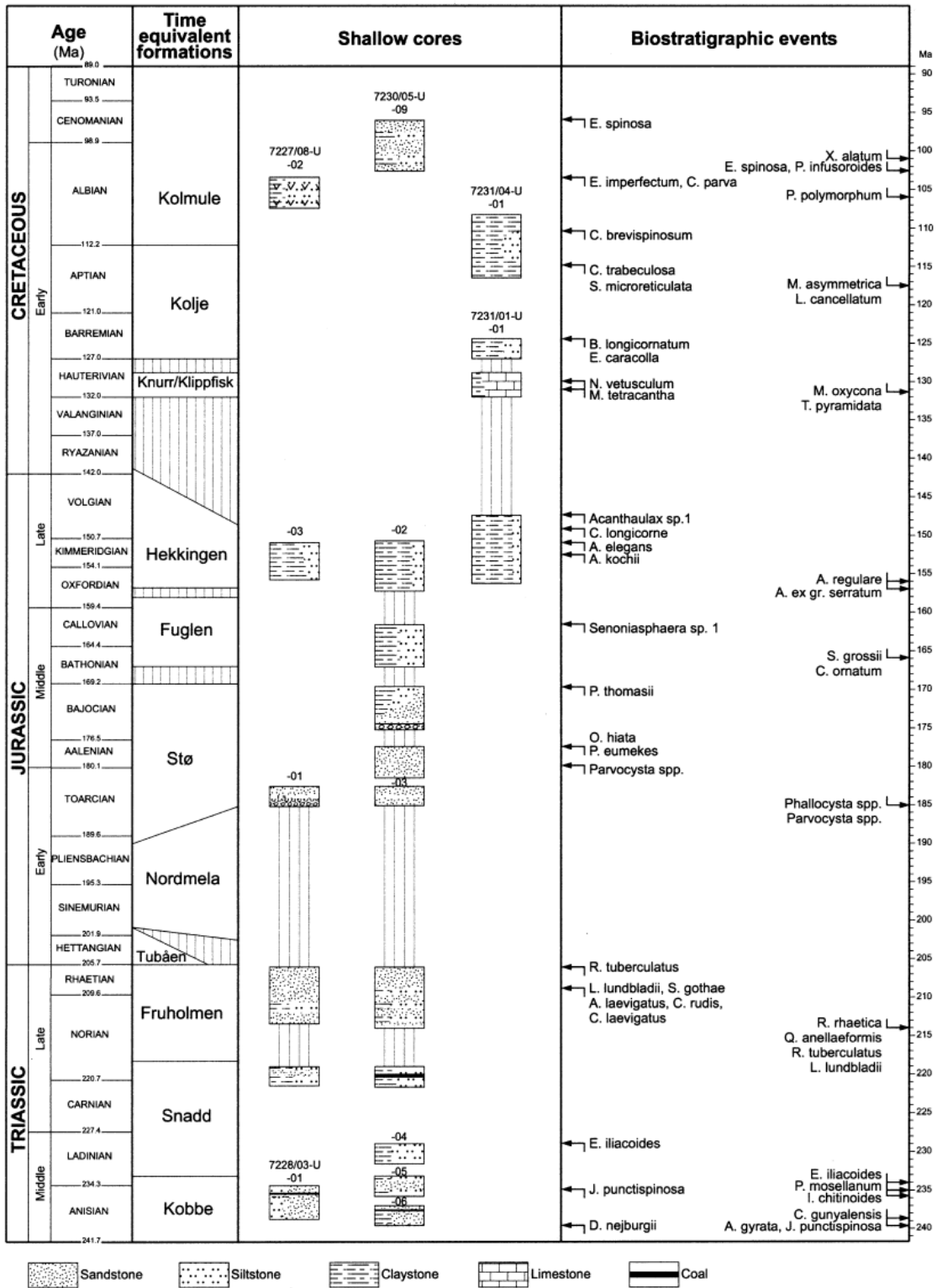


Figure 43: Chronogram of the cores. From Bugge et al. (2002).



*Table 1: The durations of sedimentation, sedimentation rates and duration of changes for each core or part of core.*

Core	Duration of sedimentation (Ma)	Thickness of core (m)	Sedimentation rate (cm/ka)	Changes in:	Depth interval (m)	Cycles	Duration of cycle (ka)
7230/05-U-07	2.59	71	2.74	Bioturbation	93.8 - 92.3	3	18
					52.8 - 26.4	5	190
					28.4 - 26.4	2	36
					52.8 - 27.54	6	150
					60.11 - 54.84	3	64
7230/05-U-05	2.86	26.1	0.92	Environments	45.98 - 43.73	2	41
					82.62 - 25.2	3	750
					50.3 - 24.2	5	570
7230/05-U-04	2.76	54.9	1.99	Bioturbation	76.8 - 70.48	8	40
					65.1 - 29.7	8	220
7230/05-U-03 (Snadd Fm.)	2.96	13.6	0.46	Heterolithic	76.93 - 70.52	14	23
					51.11 - 30.89	6	170
					93.5 - 93.16	3	25
7230/05-U-03 (Fruholmen Fm.)	7.98	67.9	0.85	Bioturbation	61.9 - 59.15	2	160
					60.14 - 58.47	3	65
7230/05-U-02 (Stø Fm. 1)	4.07	43.5	1.07	Heterolithic	72.44 - 71.73	2	40
					79.31 - 77.88	4	40
					29.51 - 28.25	3	225
7230/05-U-02 (Stø Fm. 2)	5.84	17.8	0.31	Bioturbation	124.2 - 95.6	3	890
					106.65 - 100.36	3	195
					124.18 - 95.67	3	890
					106.65 - 102.26	2	200
					125.3 - 81.8	2	2030
7230/05-U-02 (Fuglen Fm.)	5.44	13	0.24	—	—	—	No visible cyclicity
					—	—	No visible cyclicity
					—	—	No visible cyclicity
					—	—	No visible cyclicity
					—	—	No visible cyclicity
7231/01-U-01 (Hekkingen Fm.)	8.32	28.4	0.34	—	—	—	No visible cyclicity
					—	—	No visible cyclicity
					—	—	No visible cyclicity
7231/01-U-01 (Klippfisk Fm.)	3.21	4.62	0.14	—	—	—	No visible cyclicity
					—	—	No visible cyclicity
7231/01-U-01 (Kølje Fm.)	2.63	23.5	0.90	—	—	—	No visible cyclicity
					—	—	No visible cyclicity
					—	—	No visible cyclicity
7231/04-U-01	8.35	58.6	0.70	Bioturbation	72.2 - 70.8	1	200
					70.8 - 68	1	400
					68 - 62.56	3	260
7230/05-U-09	6.83	51	0.75	Bioturbation	45.7 - 24.1	4	720
					34.85 - 34.1	1	100
					30.45 - 28.45	2	130
					59.2 - 57.9	3	58

## 5.2 Causes of the small scale variations

As sand dominated heterolithics often are deposited in intertidal areas and mud dominated heterolithics often are deposited further out in calmer sub tidal areas (Donselaar and Geel, 2007) changes in heterolithics can be caused by changes in sea level. A change in sea level would lead to a change in energy and a change in the fluvial, wave or tidal influence. A rise in sea level would lead to calmer conditions and an increased amount of clay in the heterolithics. A sea level fall would lead to more energetic conditions with more influence from the tides which would lead to an increase in the amount of sand in the heterolithics.

Variations in bioturbation intensity can be caused by changes in the amount of oxygen and nutrients available for the living organisms. An increase in oxygen or nutrient availability may lead to an increase in bioturbation intensity and a decrease in oxygen or nutrient availability may lead to a decrease in bioturbation intensity. These changes in oxygen and nutrient availability can be caused by changes in climate and or sea level. Changes in climate can lead to changes in the amount of runoff which in turn can lead to changes nutrient availability which can lead to changes in bioturbation intensity.

As some living organisms are very sensitive to the temperature, changes in temperature could also lead to variations in the bioturbation intensity. Changes in salinity may also lead to changes in bioturbation intensity.

### 5.3 Further work

In core 7230/05-U-04 both possible obliquity and precession cycles are seen but not in the same sedimentary structure. The bioturbation intensity shows possible obliquity cycles and in that same section of the core the heterolithics show possible precession cycles. The reason for this is unclear, and further work will be necessary to look at this in more detail.

No cyclicity was found in the outer shelf to anoxic basin environment. Because the sediments in these environments are very fine grained there might still be cyclicity there that just are not visible. Further work with lab analysis will be necessary to determine if there are Milankovitch cyclicity in these environments.

## 6. Conclusion

This work looked at small scale changes within different depositional environments in cores from the Nordkapp Basin. This was done by describing the cores thoroughly, interpreting the facies and plotting the facies along with bioturbation intensity, heterolithics, mottling and depositional environments against core depth.

There are changes at a smaller scale, 0.4 to 10 metres, than what has been reported previously, which was at thicknesses of more than 10 to several tens of metres. Small scale changes have been found in the bioturbation intensity, heterolithics and mottling in coastal to inner shelf environments, but they are most visible in the bioturbation intensity and heterolithics.

Some of the changes found in these cores have durations that indicate that they could be the result of Milankovitch cycles. Possible precession, obliquity and long and short eccentricity cycles have been found in these cores in the coastal shoreface and inner shelf environments along with cycles with durations that are too long to be Milankovitch cycles.

The outer shelf to anoxic basin environments show no visible cyclicity because these deposits are very fine grained which makes it hard to see any changes that might be there.

## References

- Bowen, A.J. and Stow, D.A.V.** (1978) Origin of lamination in deep sea, fine-grained sediments. *Nature (London)*, **274**, 324-328.
- Brekke, H., Sjulstad, H.I., Magnus, C. and Williams, R.W.** (2001) Sedimentary environments offshore Norway—an overview. In: *Norwegian Petroleum Society Special Publications*, **10**, pp. 7-37. Elsevier.
- Bugge, T., Elvebakk, G., Fanavoll, S., Mangerud, G., Smelror, M., Weiss, H.M., Gjelberg, J., Kristensen, S.E. and Nilsen, K.** (2002) Shallow stratigraphic drilling applied in hydrocarbon exploration of the Nordkapp Basin, Barents Sea. *Marine and Petroleum Geology*, **19**, 13-37.
- de Boer, P.L. and Smith, D.G.** (1994) Orbital forcing and cyclic sequences. *Spec. Publs Int. Ass. Sediment.*, **19**, 1-14.
- Donselaar, M.E. and Geel, C.R.** (2007) Facies architecture of heterolithic tidal deposits: the Holocene Holland Tidal Basin. *Netherlands Journal of Geosciences*, **86**, 389-402.
- Faleide, J.I., Tsikalas, F., Breivik, A.J., Mjelde, R., Ritzmann, O., Engen, O., Wilson, J. and Eldholm, O.** (2008) Structure and evolution of the continental margin off Norway and the Barents Sea. *Episodes*, **31**, 82-91.
- Gabrielsen, R.H. and Norge, O.** (1990) *Structural elements of the Norwegian continental shelf : 6 : The Barents sea region*, pp. 16. Oljedirektoratet, Stavanger.
- Glørstad-Clark, E., Birkeland, E., Nystuen, J., Faleide, J. and Midtkandal, I.** (2011) Triassic platform-margin deltas in the western Barents Sea. *Marine and Petroleum Geology*, **28**, 1294-1314.
- Heinrich, H.** (1988) Origin and Consequences of Cyclic Ice Rafting in the Northeast Atlantic Ocean During the Past 130,000 Years. *Quat. res*, **29**, 142-152.
- Johannessen, E.P. og Nøttvedt, A.** (2006) Norge omkranset av kystsletter og deltaer. Tidlig og mellomjura; 201-164 Ma. I: *Landet blir til. Norges geologi* (Eds I.B. Ramberg, I. Bryhni, A. Nøttvedt and K. Rangnes) 2. edn, pp. 358-385. Norsk Geologisk Forening Trondheim.
- Kochhann, M.V.L., Cagliari, J., Kochhann, K.G.D. and Franco, D.R.** (2020) Orbital and Millennial-Scale Cycles Paced Climate Variability During the Late Paleozoic Ice Age in the Southwestern Gondwana. *Geochemistry, geophysics, geosystems : G3*, **21**, n/a.
- Liu, C., Zhang, J.-F., Jiao, P. and Mischke, S.** (2016) The Holocene history of Lop Nur and its palaeoclimate implications. *Quaternary science reviews*, **148**, 163-175.
- Macquaker, J.H.S., Bentley, S.J. and Bohacs, K.M.** (2010) Wave-enhanced sediment-gravity flows and mud dispersal across continental shelves; reappraising sediment transport processes operating in ancient mudstone successions. *Geology (Boulder)*, **38**, 947-950.
- Marshall, N., Zeeden, C., Hilgen, F. and Krijgsman, W.** (2017) Milankovitch cycles in an equatorial delta from the Miocene of Borneo. *Earth and planetary science letters*, **472**, 229-240.
- Milana, J.P. and Lopez, S.** (1998) Solar cycles recorded in Carboniferous glacial marine rhythmites (Western Argentina): relationships between climate and sedimentary environment. *Palaeogeography, palaeoclimatology, palaeoecology*, **144**, 37-63.

- Mørk, M.B.E.** (1999) Compositional variations and provenance of Triassic sandstones from the Barents Shelf. *Journal of Sedimentary Research*, **69**, 690-710.
- Nichols, G.** (2009a) Deltas. In: *Sedimentology and stratigraphy* 2. edn, pp. 179-198. Wiley-Blackwell, Chichester.
- Nichols, G.** (2009b) Rivers and alluvial fans. In: *Sedimentology and stratigraphy* 2. edn, pp. 129-159. Wiley-Blackwell, Chichester.
- Nichols, G.** (2009c) Shallow marine carbonate and evaporite environments. In: *Sedimentology and stratigraphy* 2. edn, pp. 225-246. Wiley-Blackwell, Chichester.
- Nichols, G.** (2009d) Shallow sandy seas. In: *Sedimentology and stratigraphy* 2. edn, pp. 215-224. Wiley-Blackwell, Chichester.
- Nøttvedt, N. og Johannessen, E.P.** (2006) Grunnlaget for Norges oljerikdom. Seinjura, et øyhav vokser fram; 164-145 Ma. I: *Landet blir til. Norges geologi* (Eds I.B. Ramberg, I. Bryhni, A. Nøttvedt and K. Rangnes) 2. edn, pp. 386-421. Norsk Geologisk Forening, Trondheim.
- Olsen, H.** (1990) Astronomical forcing of meandering river behaviour: Milankovitch cycles in Devonian of East Greenland. *Palaeogeography, palaeoclimatology, palaeoecology*, **79**, 99-115.
- Schieber, L., Southard, J. and Thaisen, K.** (2007) Accretion of Mudstone Beds from Migrating Floccule Ripples. *Science*, **318**, 1760-1763.
- Schwarzacher, W.** (1993) *Cyclostratigraphy and the Milankovitch theory*. Elsevier, Amsterdam.
- Smelror, M., Basov, V.A. and Norges geologiske, u.k.** (2009) *Atlas : geological history of the Barents Sea*. Geological Survey of Norway, Trondheim.
- Steel, R.J., Maehle, S., Nilsen, H., Roe, S.L. and Spinnangr, A.** (1977) Coarsening-upward cycles in the alluvium of Hornelen Basin (Devonian) Norway; sedimentary response to tectonic events. *Geological Society of America bulletin*, **88**, 1124-1134.
- Tucker, M.E., Gallagher, J. and Leng, M.J.** (2009) Are beds in shelf carbonates millennial-scale cycles? An example from the mid-Carboniferous of northern England. *Sedimentary geology*, **214**, 19-34.
- Williams, G.E.** (1991) Milankovitch-band cyclicity in bedded halite deposits contemporaneous with Late Ordovician-Early Silurian glaciation, Canning Basin, Western Australia. *Earth and planetary science letters*, **103**, 143-155.
- Worsley, D.** (2008) The post-Caledonian development of Svalbard and the western Barents Sea. *Polar research*, **27**, 298-317.
- Yawar, Z. and Schieber, J.** (2017) On the origin of silt laminae in laminated shales. *Sedimentary geology*, **360**, 22-34.



